Atoms to applications and the future of electronics

A.F.J. Levi

Presented at Fermilab, 3.30pm on Wednesday, March 26, 2025

Global system innovation and integration challenges for electronics after transistor scaling ends

6 µm technology Intel 8080 8-bit processor in 1974 with 4,500 transistors in 20.1 mm² area and 2 MHz clock

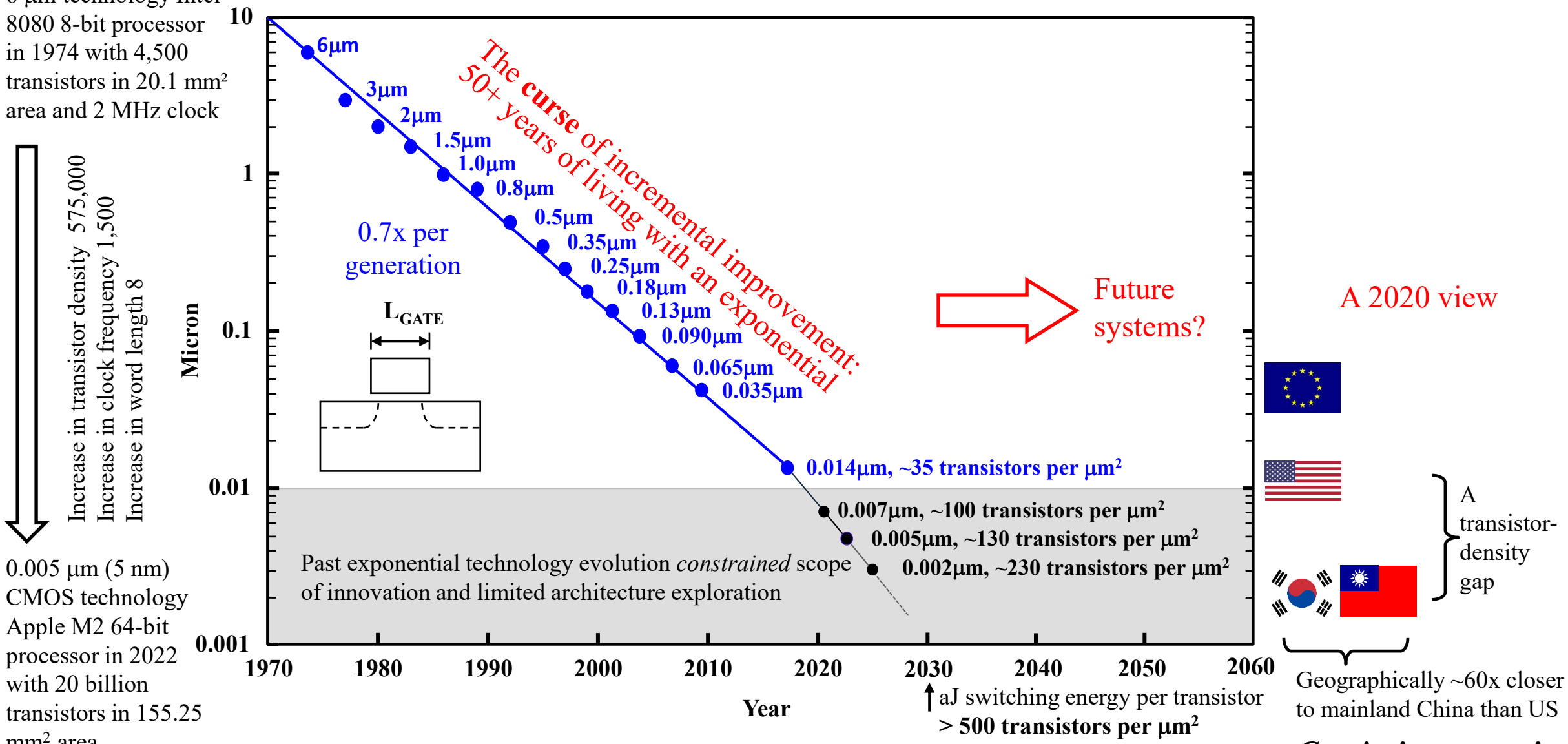

0.005 µm (5 nm) CMOS technology Apple M2 64-bit processor in 2022 with 20 billion transistors in 155.25 mm² area and 3 GHz clock

"Towards Quantum Engineering", A F J Levi, *Proceedings of the IEEE* **96**, 335 (2008)

***Gravity* in economics**

Gravity in circuit design …

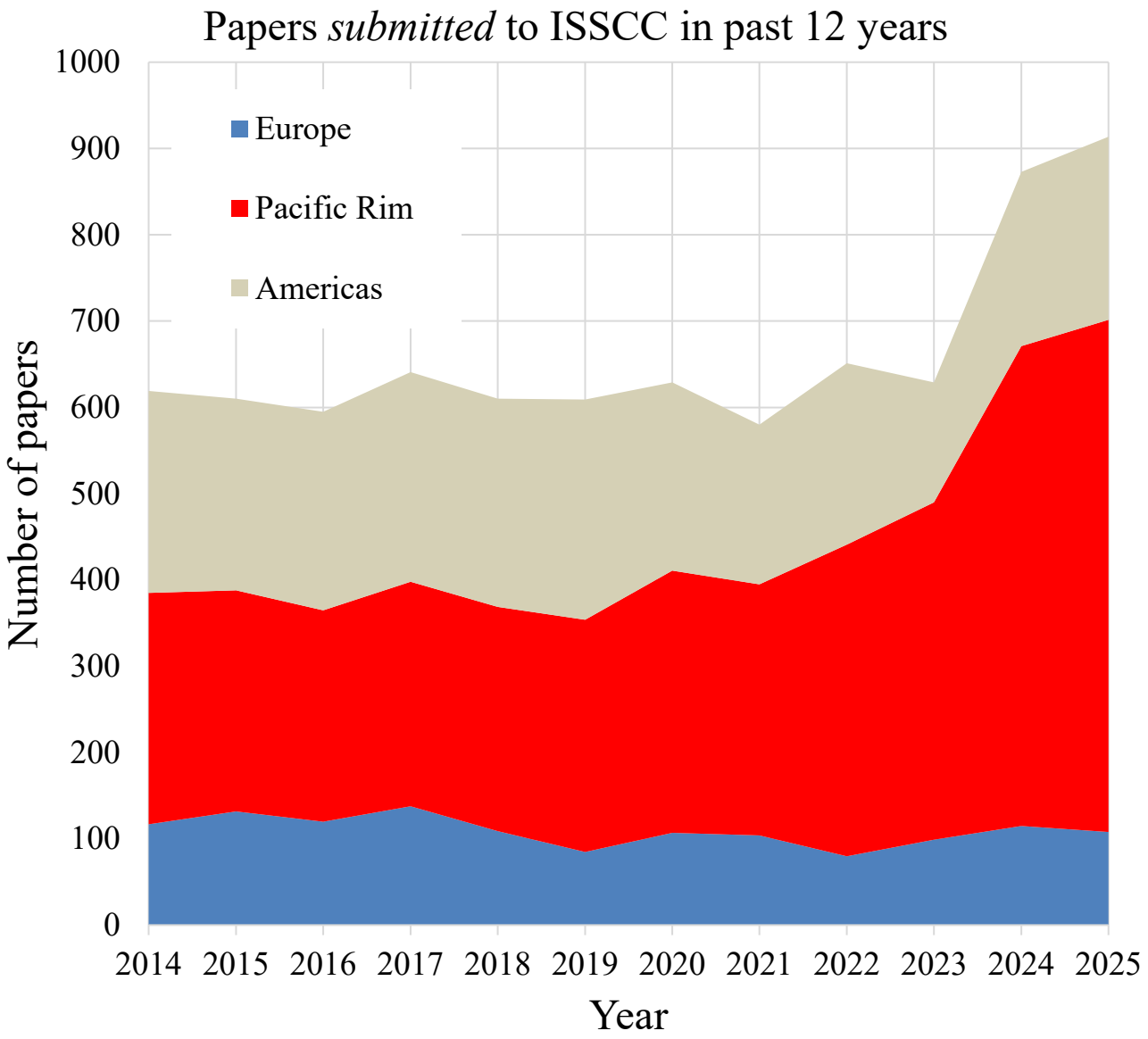

Americas

Pacific Rim

Europe

International Solid-State Circuits Conference (ISSCC)

ISSC 2025
27% overall acceptance rate

Accepted papers as a percentage of all papers at the conference

23% Americas

65% Pacific Rim, of which more than half from China

12% Europe

3D X-ray imaging of CMOS circuits at nm-scale

- The objective is to rapidly find out "*what's inside*" any integrated circuit
- Non-destructive lensless ptychographic coherent X-ray diffraction computational 3D-imaging of advanced-technology CMOS integrated circuits

Key contributors: Tomas Aidukas, Mirko Holler, Manuel Guizar-Sicairos, Michal Odstrcil, Elisabeth Müller, Ana Diaz, Gabriel Aeppli, and A. F. J. Levi

Publications: M. Holler et al., *Nature Electronics* **2**, 464 (2019)

A.F.J. Levi and G. Aeppli, spectrum.ieee.org/chip-x-ray (2022)

I. Kang et al., *Optica* **10**, 1000 (2023) – 16x speedup using ML

T. Aidukas et al., *Nature* **632**, 81 (2024) – 4 nm resolution

Recent progress: Compared to 2019: Optimization of hardware *and* algorithms gives10x increase in depth of field to 5µm using filtered backpropagation tomography, 4x improvement in resolution to 4 nm using burst ptychography to remove experimental instabilities, 16x speedup using ML

Future work: 50x brilliance *after* synchrotron upgrade in 4Q25, 100x flux with new channel-cut crystal monochromator X-ray optics in 4Q25, 3D reconstruction of integrated circuits with potential sub-nm resolution, speedup with new hardware and algorithms, speedup with ML and AI, integration with XRF for trace detection and multimodal imaging

USC

USC-designed digitizing matrix-multiplier chip for Machine Learning manufactured by Global Foundries in 2017 in 14 nm FinFET CMOS technology

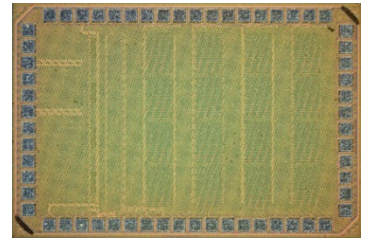

GlobalFoundries Inc.

Swiss Light Source (SLS) at PSI, ETH-Zurich

CSAXS 6 keV photons, 0.2 nm wavelength
2024 coherent photon flux at sample 7×10^8 s^{-1}

Non-destructive 3D X-ray imaging of integrated circuits at 4 nm resolution

- 3D X-ray imaging using coherent 6 keV (λ_0 = 0.207 nm) photons at the SLS synchrotron with ~200 nW absorbed in the sample
- 5 µm depth of field with filtered backpropagation
- Example: 3D X-ray image of metal interconnect (connectome) and transistors in AMD Ryzen 5 5600G Processor with TSMC 7 nm CMOS FinFET technology and ~100 digital transistors per µm^2 area, 57 nm gate pitch, 30 nm fin pitch, 6 nm fin width, 52 nm fin height
- Efficient image reconstruction via the use of prior information and ML

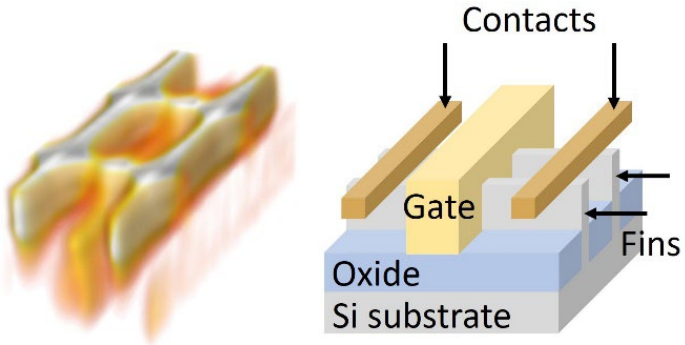

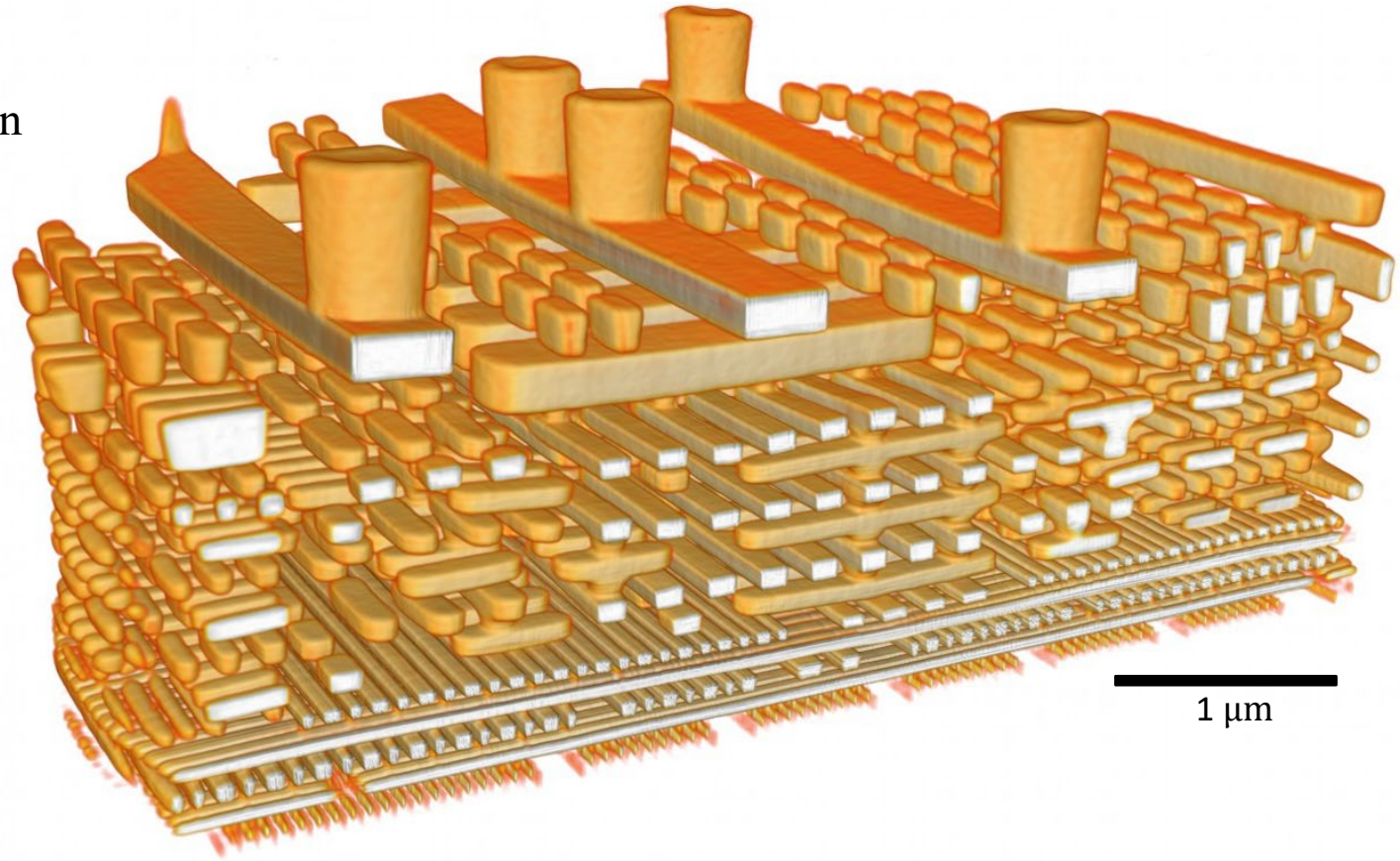

"High-performance 4-nm-resolution X-ray tomography using burst ptychography", T. Aidukas, N. W. Phillips, A. Diaz, E. Poghosyan, E. Müller, A. F. J. Levi, G. Aeppli, M. Guizar-Sicairos and M. Holler, *Nature* **632**, 82-88 (2024).

Beyond the exponential increase in the number of transistors per unit area

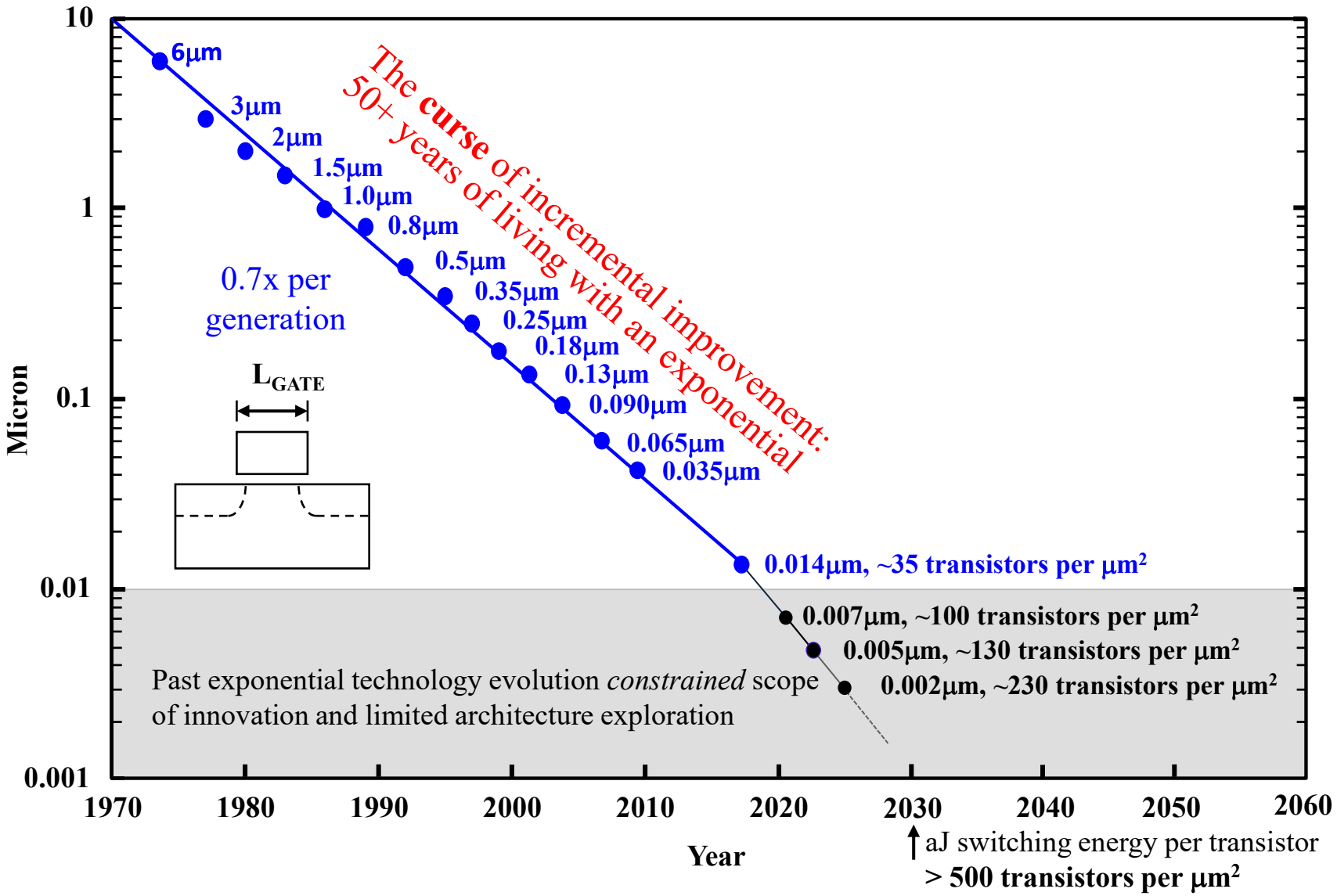

"Towards Quantum Engineering", A F J Levi, *Proceedings of the IEEE* **96**, 335 (2008)

Small increases in hardware provide access to an *exponentially vast* cyberspace

Exponential leverage of classical hardware resources:

- Single clock cycle:
- 8-bit bus has address space $2^8 = 256 = 2.5 \times 10^2$
- 64-bit bus address space is $2^{64} = 1.8 \times 10^{19}$
- Efficient double-precision FP calculations
- Specialized accelerators, FPU, ALU, GPU, …

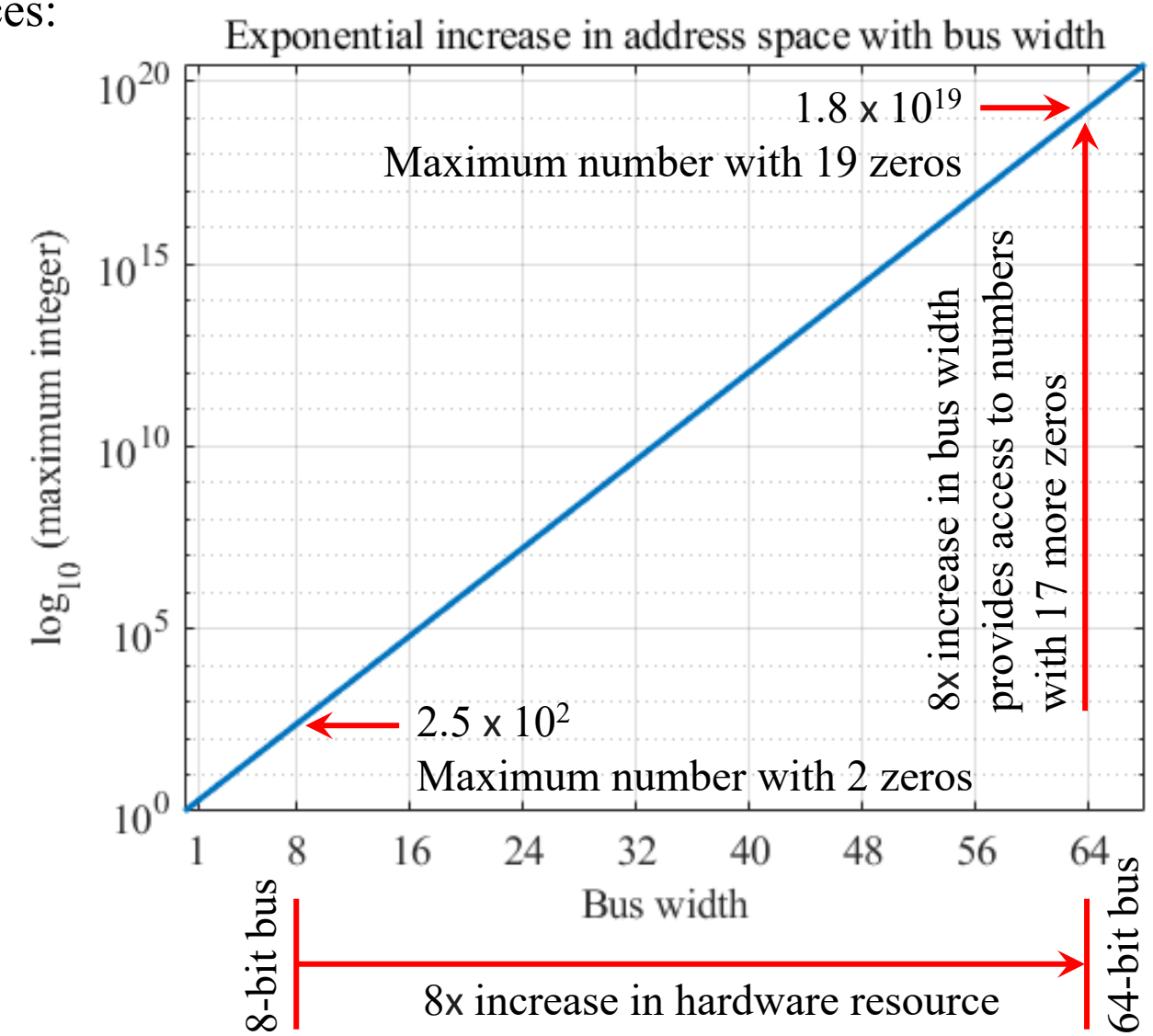

The vastness of cyberspace

- 8-bit versus 64-bit address space
- $2^8 = 256 = 2.5 \times 10^2$
- $2^{64} = 1.8 \times 10^{19}$

Photon round-trip time to measure the height of 256 one-dollar bills

$\tau_{RT} = 186$ ps

The vastness of cyberspace

- 8-bit versus 64-bit address space
- $2^8 = 256 = 2.5 \times 10^2$
- $2^{64} = 1.8 \times 10^{19}$

Photon round-trip time to measure the height of 256 one-dollar bills
τ_{RT} = 186 ps

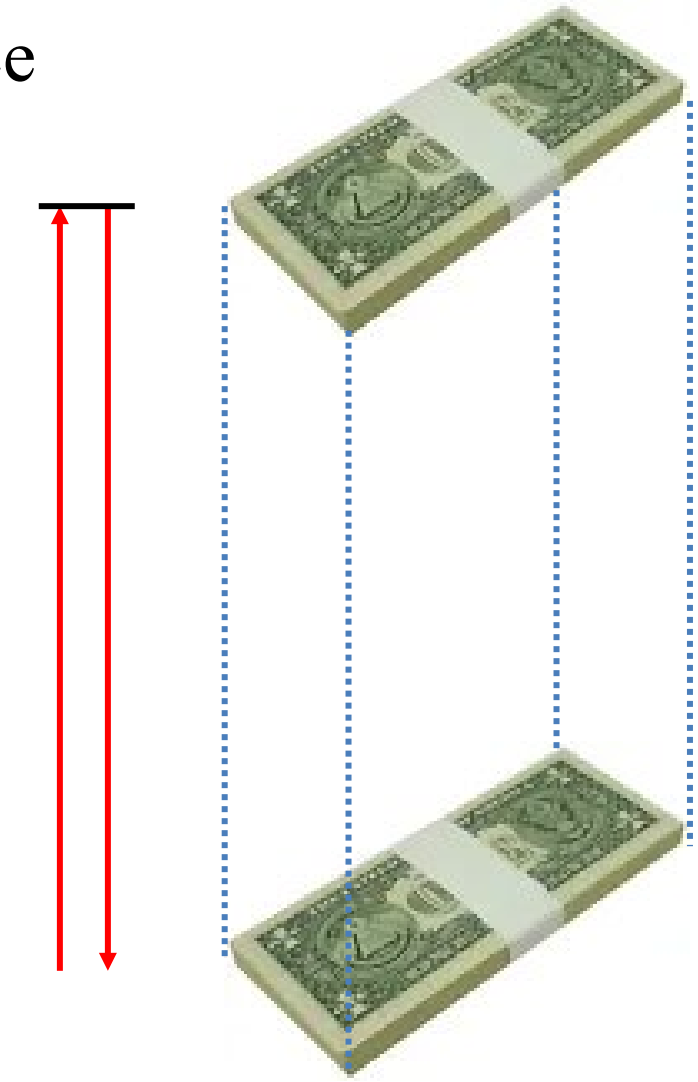

Photon round-trip time to measure the height of 2×10^{19} one-dollar bills
$\tau_{RT} = 7.3 \times 10^6$ seconds = 168 days = 5.6 months

The vastness of cyberspace

- 8-bit versus 64-bit address space
- $2^8 = 256 = 2.5 \times 10^2$
- $2^{64} = 1.8 \times 10^{19}$

Photon round-trip time to measure the height of 256 one-dollar bills
τ_{RT} = 186 ps

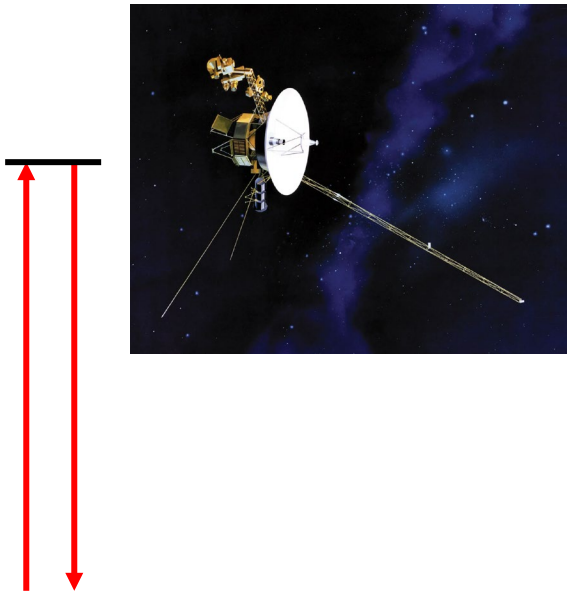

Photon round-trip time to Voyager 1 spacecraft launched in 1977 and now 24B km from Earth
τ_{RT} = 44 hours = 1.8 days

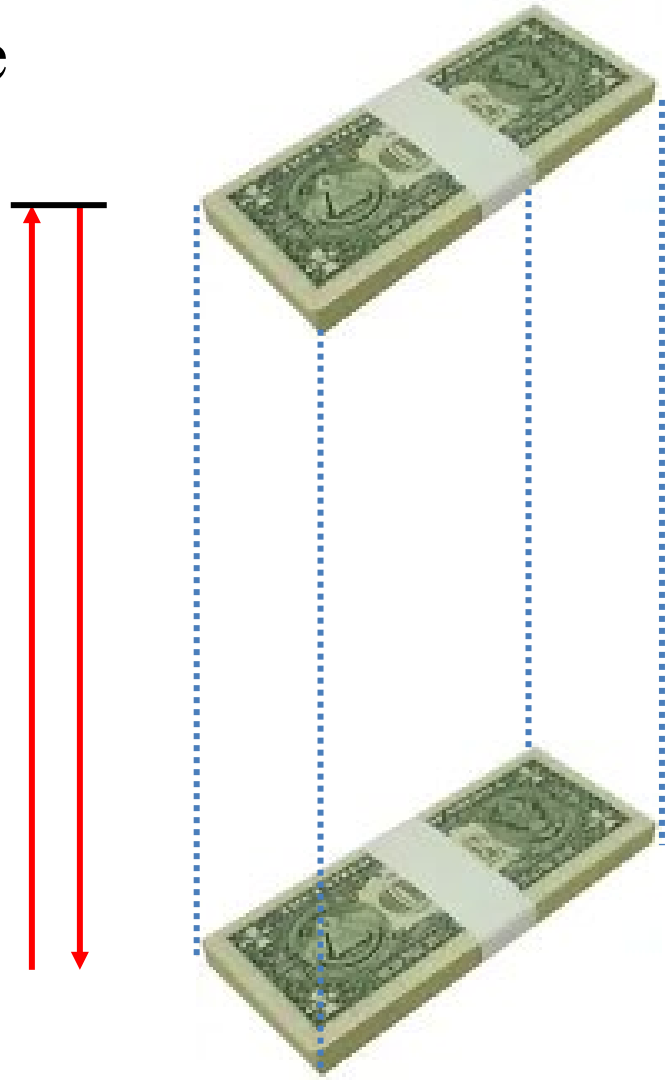

Photon round-trip time to measure the height of 2×10^{19} one-dollar bills
τ_{RT} = 168 days = 5.6 months

Vast cyberspace →  search engine

Nano-precision fabrication provides access to an *exponentially vast design space*

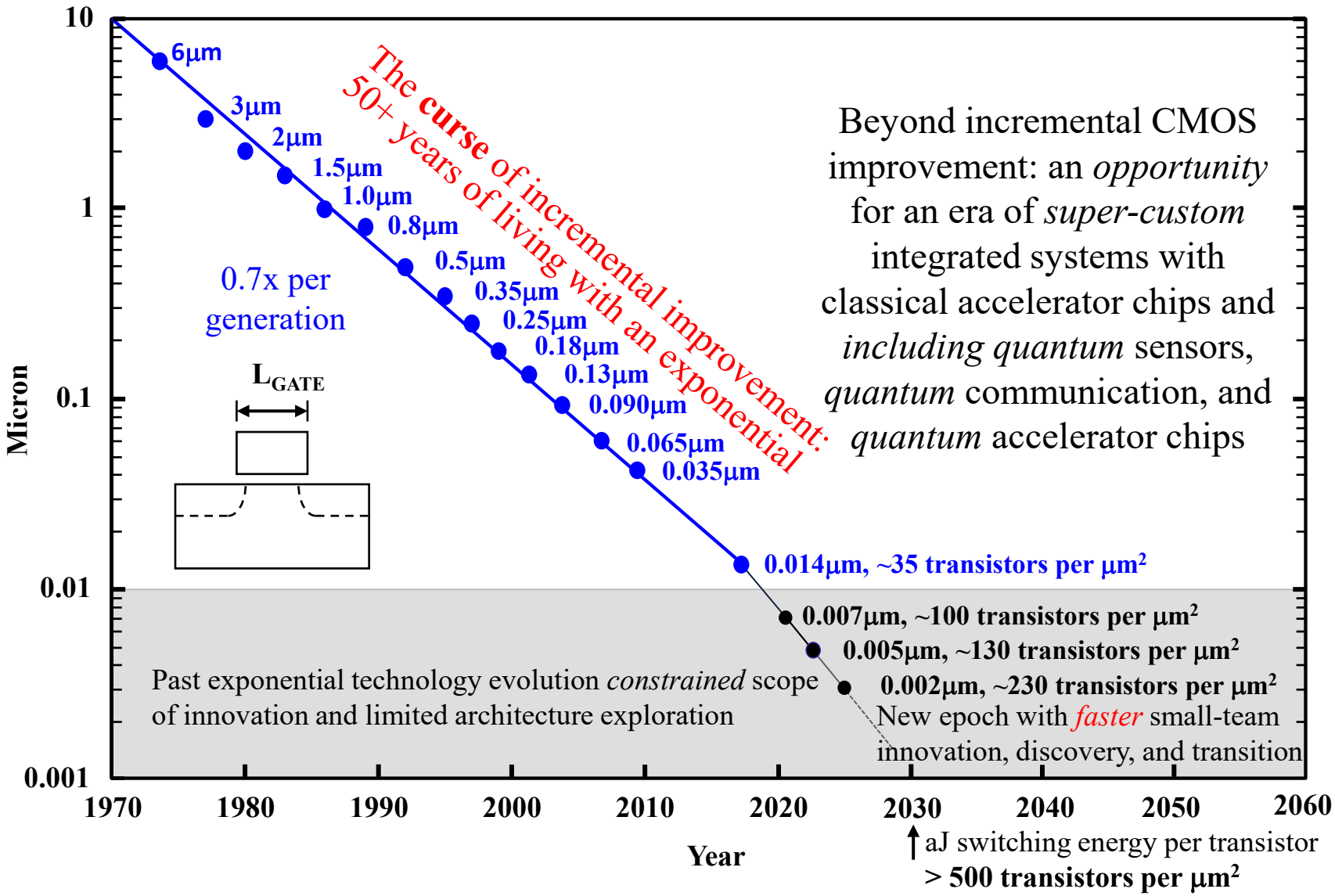

"Towards Quantum Engineering", A F J Levi, *Proceedings of the IEEE* **96**, 335 (2008)

Search in an exponentially vast design space

Exponential leverage of classical hardware resources:

- 64-bit bus address space, $2^{64} = 1.8 \times 10^{19}$
- Efficient double-precision FP calculations
- Specialized accelerators, FPU, ALU, GPU, …

An opportunity to use design automation and large computational resources to search for new, often nonintuitive, optimal quantum electronic component materials, geometry, and system functionality

The existence of a massive search space in which to find optimal device function

Solutions are often characterized by broken symmetry geometries and unanticipated combinations of materials

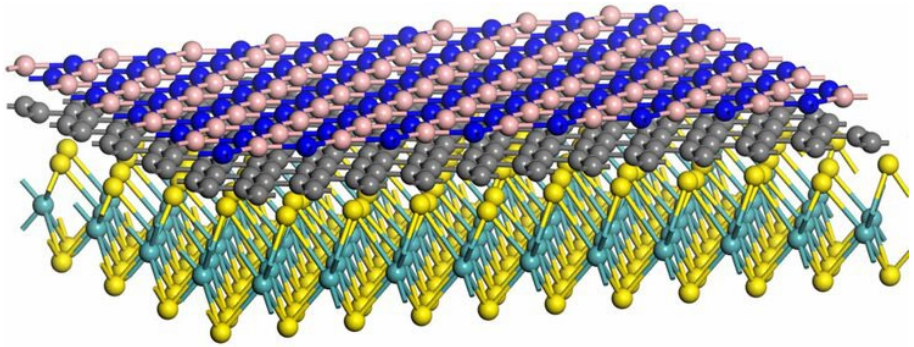

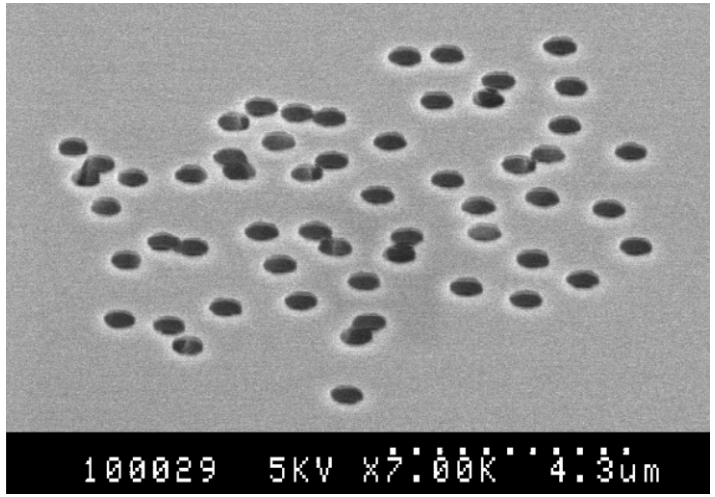

Vast quantum engineering design space

→ new **Quantum** search engine

(an opportunity for those with access to large computing resources?)

Atoms to applications

Quantum engineering: Atom position and function

Quantum search engine at the component level:

- Materials, geometry, and forward physical model
  - Identify atom configurations that deliver the desired device function *and* system function
  - Identify non-equilibrium or nonthermal pathways for both synthesis *and* function

Quantum engineering: Broken symmetry to control density of electron states

Motivation

- Electron transitions (scattering) determined by the golden rule (the first term in the Born series)
  - Use the position of atoms to control the density of electron states, $N(E)$
- Example: Forward physical model (an *abstraction*) is *long-range* tight binding using s-orbitals with hopping integral interaction strength, $t_{i,j}$, parameterized by power law, α
  - Periodic boundary conditions
  - Full matrix
- In this example, optimization minimizes $\mathcal{L}^{\gamma}$ (γ=2) distance measure between simulated and objective density of states

$$\frac{1}{\tau_n} = \frac{2\pi}{\hbar} |W_{mn}|^2 N(E) \delta (E_m - E_n)$$

$$\hat{H}_{\hat{c}^\dagger \hat{c}} = -\sum_{i<j} t_{i,j} (\hat{c}_i^\dagger \hat{c}_j + \hat{c}_i \hat{c}_j^\dagger)$$

$$t_{i,j} = t_{\text{hop}} / |\mathbf{r}_i - \mathbf{r}_j|^{\alpha}$$

$$C_{\text{cost}} = \sum_j |N_{\text{sim},j} - N_{\text{obj},j}|^2$$

Quantum engineering: Broken symmetry to control density of electron states

Quantum engineering: Broken symmetry to control density of electron states

Typical heuristics

- Non-convex landscape with many local minima
- The optimization algorithm provides a *single-point solution*
  - *No understanding*. The optimization algorithm *does not explain the physics* or why the solution works
- Degeneracy from symmetries
  - Example: rotational symmetry
- Dilute limit has hierarchy of symmetric primitive building blocks that contribute to the objective density of states, $N(E)$
  - Dimers for symmetric $N(E)$
  - Trimers and larger molecular configurations can add asymmetry to $N(E)$

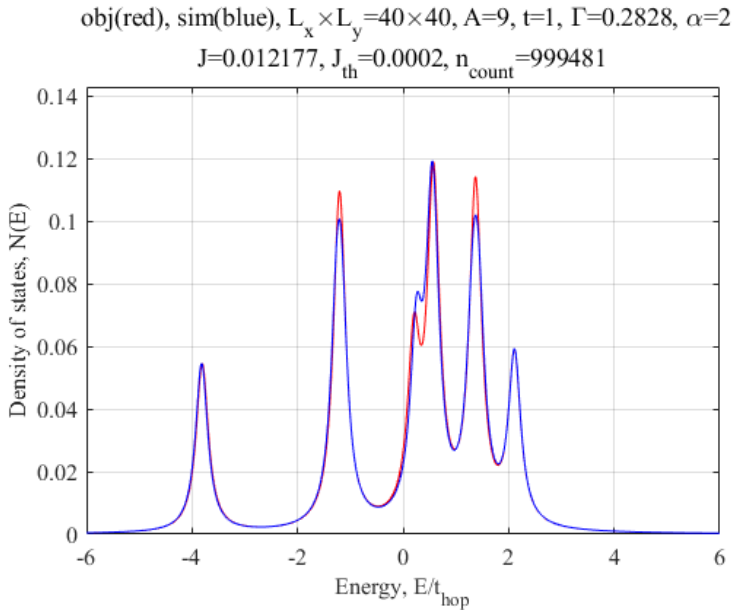

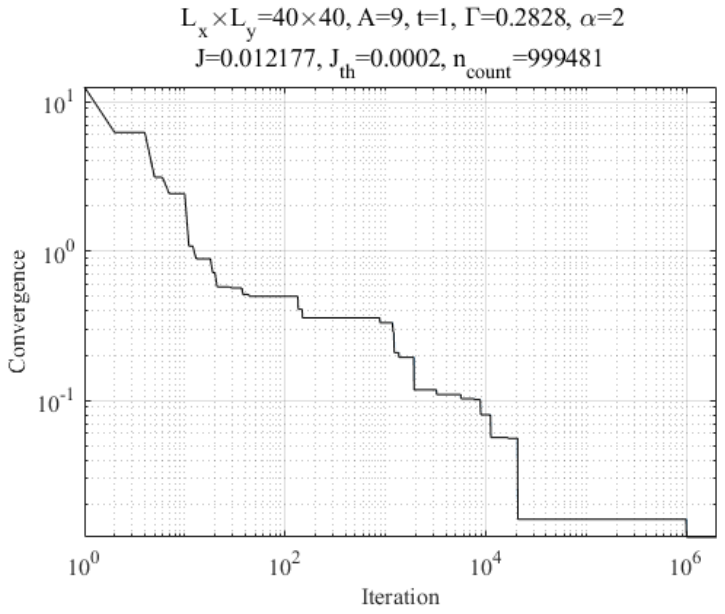

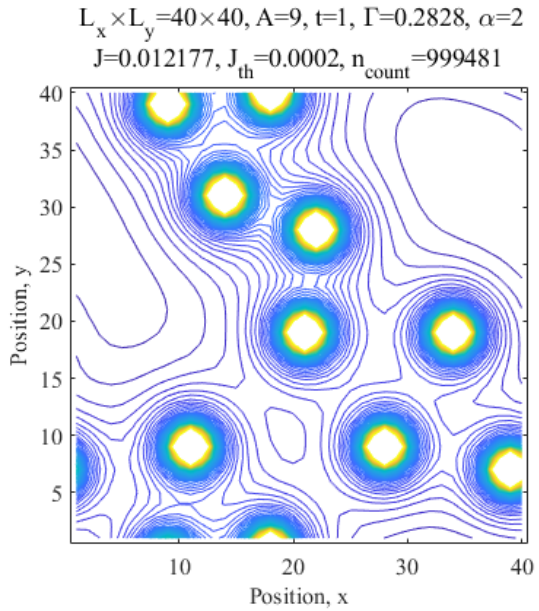

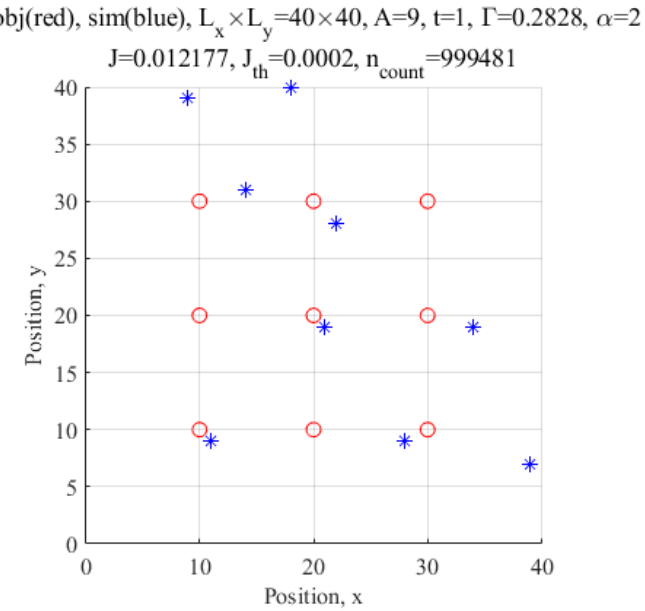

Expanding electronic component design space using quantum engineering of multiple crystalline atomic layers for function

hBN

Graphene

MoS_2

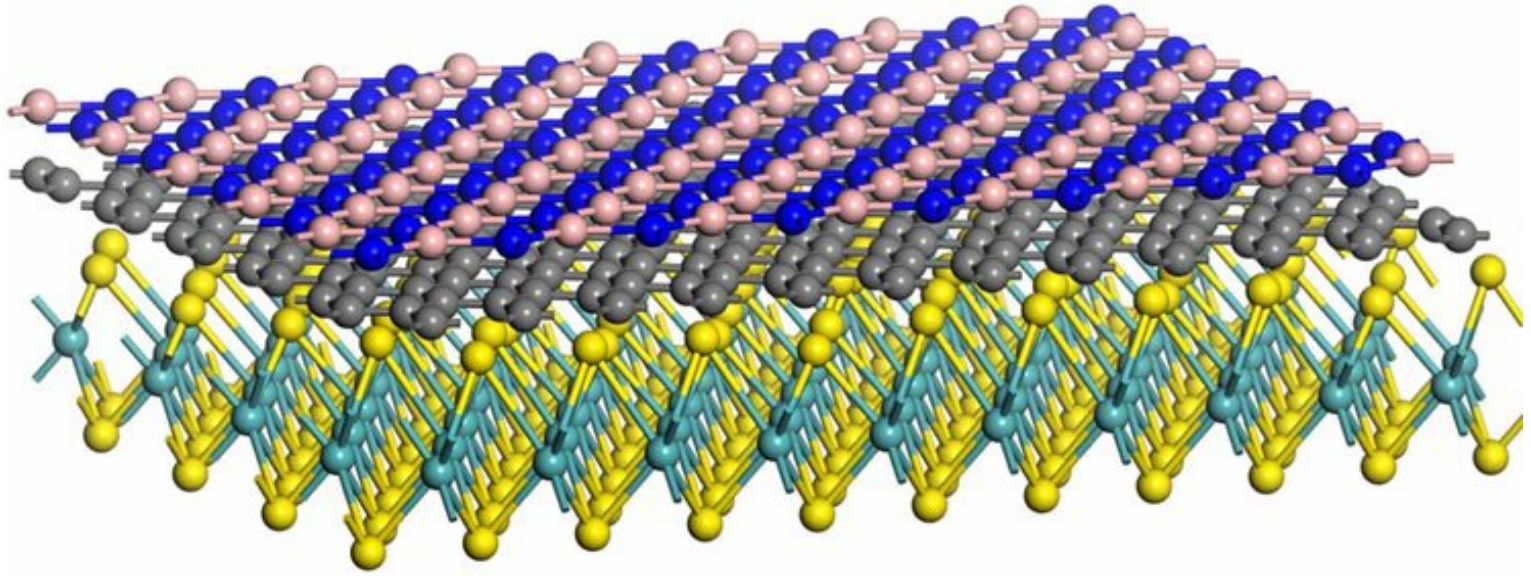

Example materials systems featuring atomic-layer precision:

- Stacked and twisted vdW heterostructures
- Broken-symmetry single-crystal MBE compound semiconductors and other layered materials

Quantum engineering and electron transport: Non-intuitive design

Motivation

- What is the current-voltage characteristic of this semiconductor diode conduction band potential profile?
- $Al_xIn_yGa_{1-x-y}As$ n-i-n diode with -0.15 eV $\leq U_j \leq$ 0.3 eV and lattice constant L = 0.5653 nm
- 16 layers, each 1.131 nm thick
- n_0 = 1.5 x 10^{18} cm^{-3}, effective electron mass m^* = 0.07 x m_0

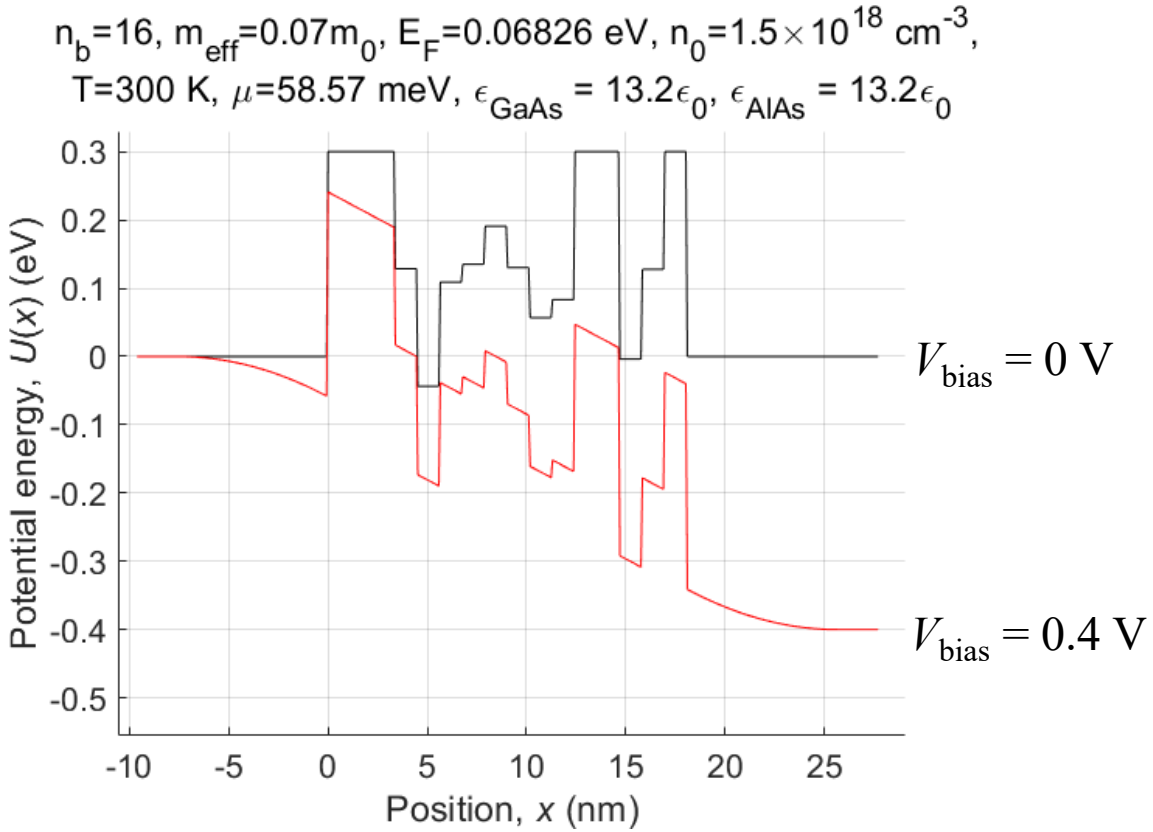

Quantum engineering and electron transport: Non-intuitive design

Motivation

- What is the current-voltage characteristic of this semiconductor diode conduction band potential profile?
- Solution: Linear
  - Could you have guessed that? A *totally different* approach to creating the precise linear transfer function of a "resistor"
  - The optimization algorithm provides *a single-point solution*. There is *no understanding*. The optimization algorithm *does not explain the physics*, why the solution is *robust*, and *why the solution works so well*

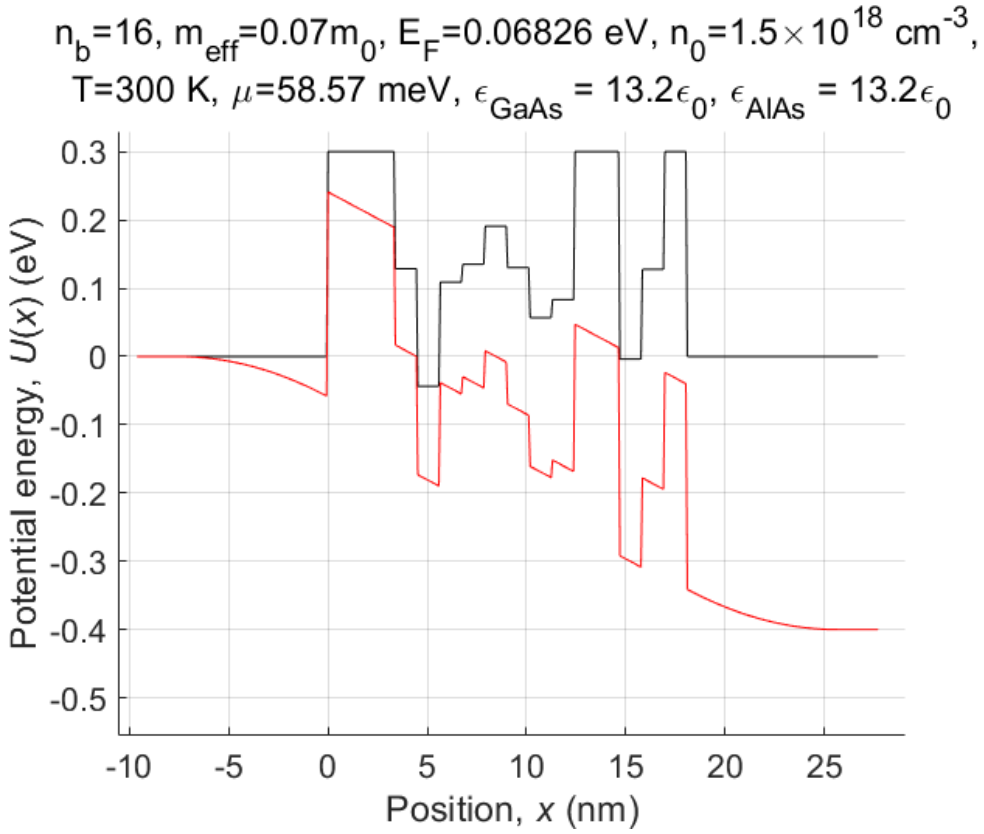

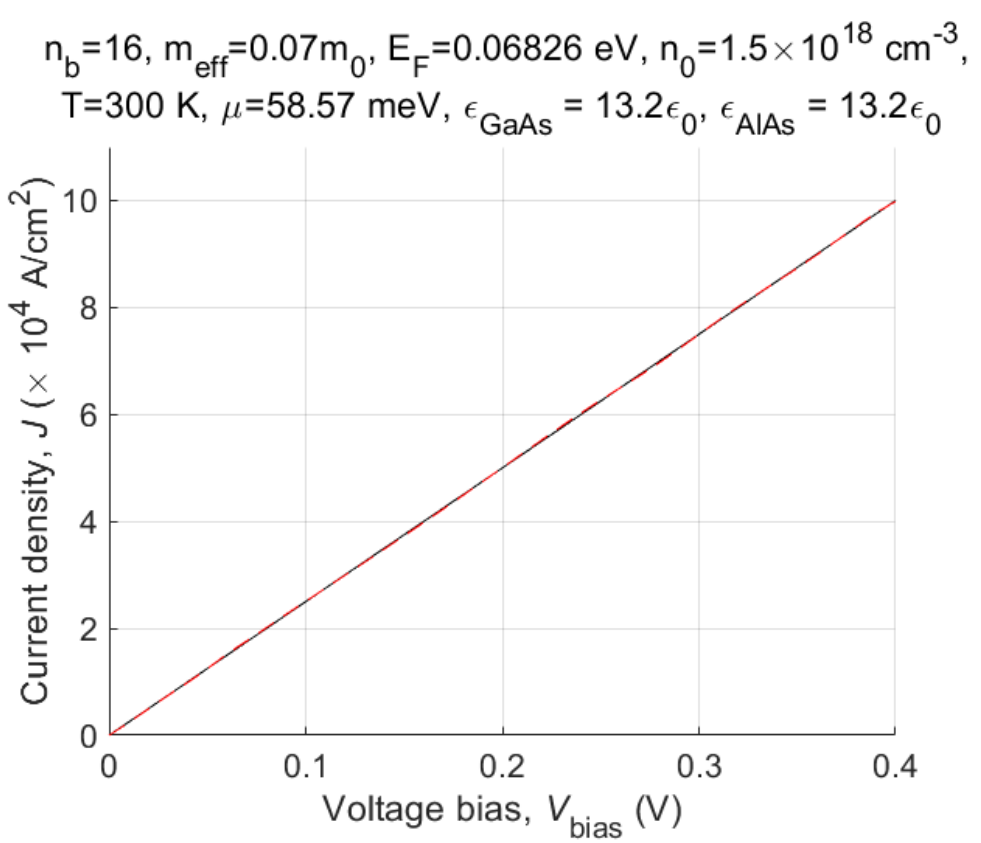

Quantum engineering and electron transport: Non-intuitive design

Motivation

- What is the current-voltage characteristic of this semiconductor diode conduction band potential profile?
- $Al_xIn_yGa_{1-x-y}As$ n-i-n diode with -0.15 eV $\leq U_j \leq$ 0.3 eV and lattice constant L = 0.5653 nm
- 32 layers, each 1.131 nm thick
- n_0 = 1.0 x 10^{18} cm^{-3}, effective electron mass m^* = 0.07 x m_0

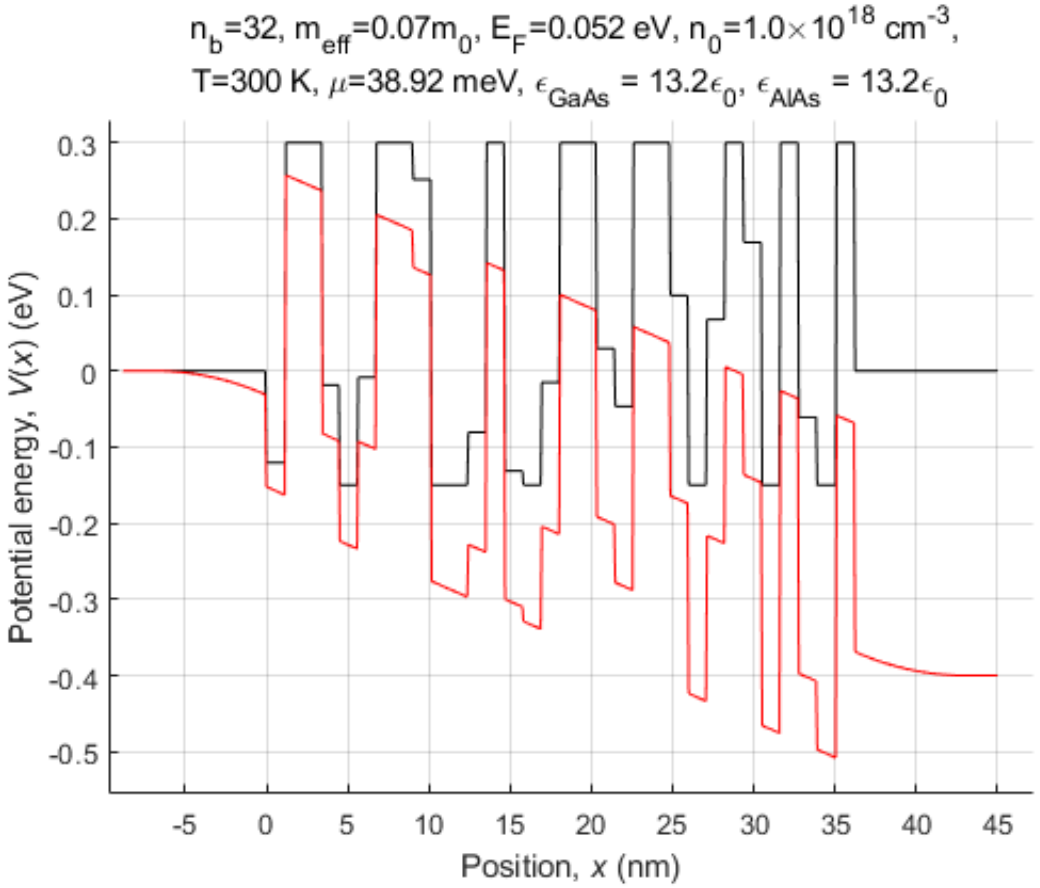

Quantum engineering and electron transport: Non-intuitive design

Motivation

- What is the current-voltage characteristic of this semiconductor diode conduction band potential profile?
- Solution: Sinusoidal objective
  - Could you have guessed that?

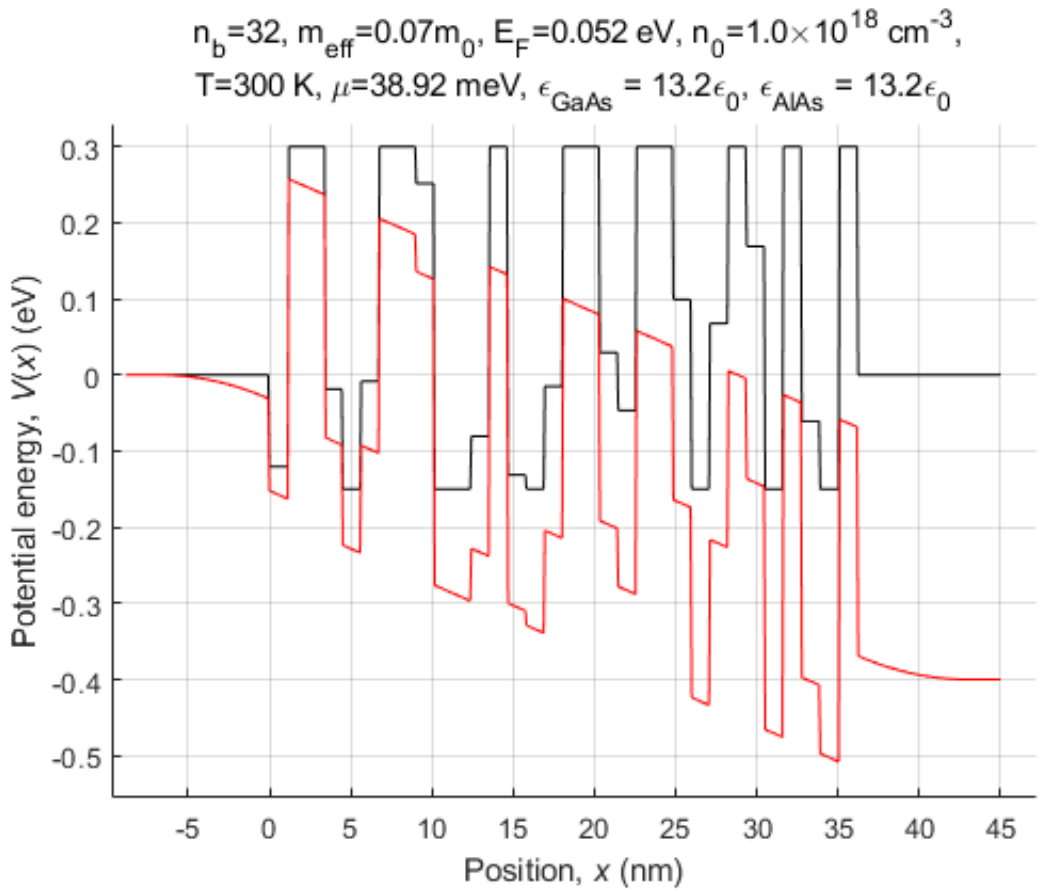

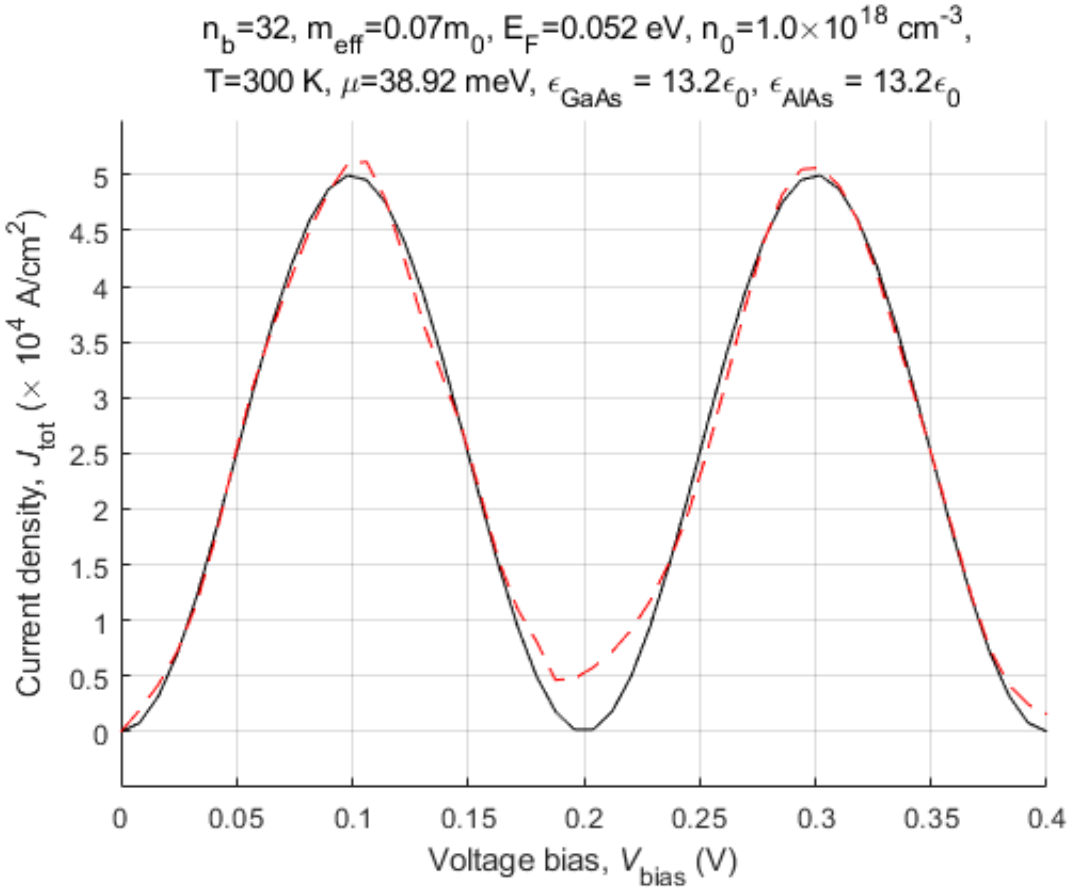

Quantum engineering and electron transport: Nonequilibrium electron transistor

MBE-grown semiconductor layers

- The objective is to find the materials and geometry for a single-crystal unipolar nonequilibrium (ballistic) electron transistor with vertical transport that operates at room temperature
- Non-symmetric conduction band potential profile
- What is the current-voltage characteristic of this semiconductor conduction band potential profile?

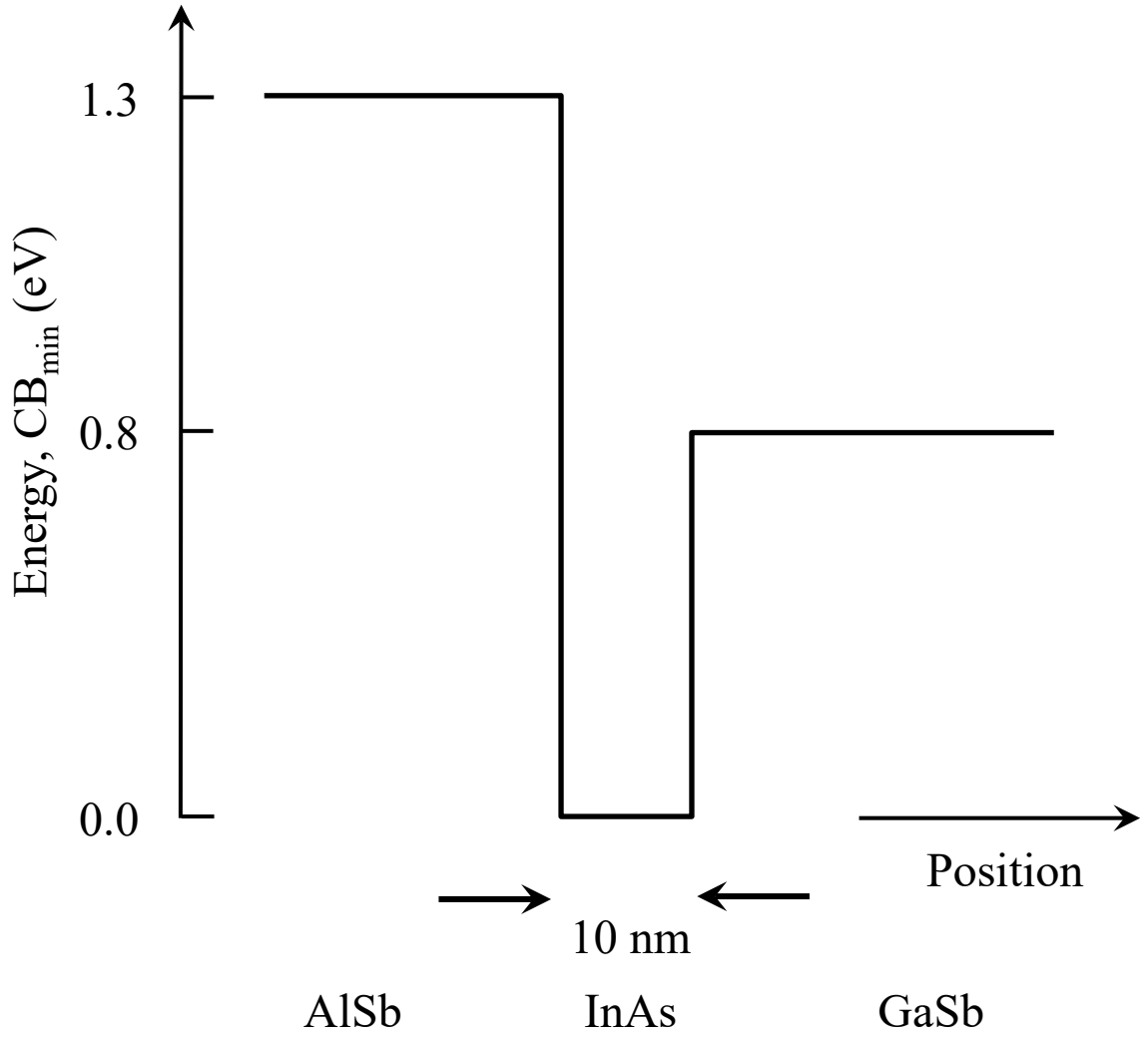

Quantum engineering and electron transport: Nonequilibrium electron transistor

- Room temperature operation, $T = 300$ K
- Common-emitter current gain, $\beta = 10$
- Why does this combination of materials and geometry work so well?

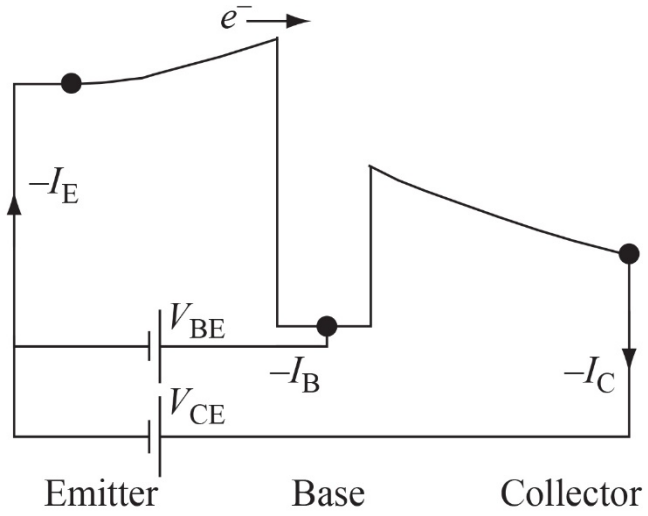

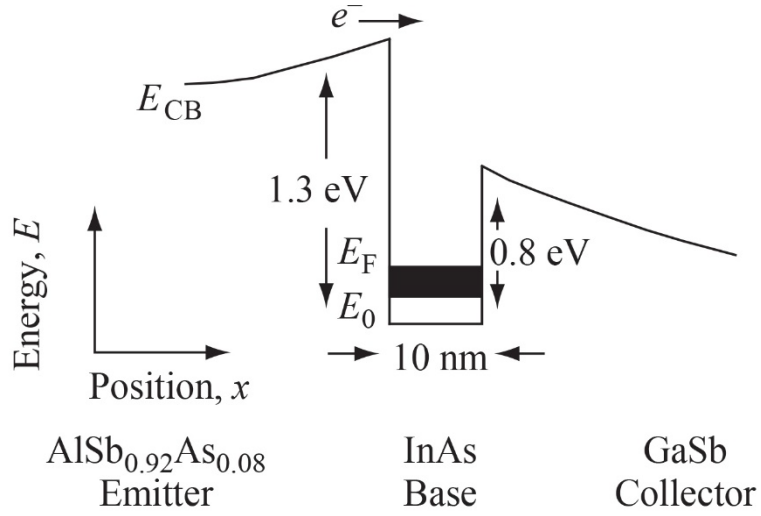

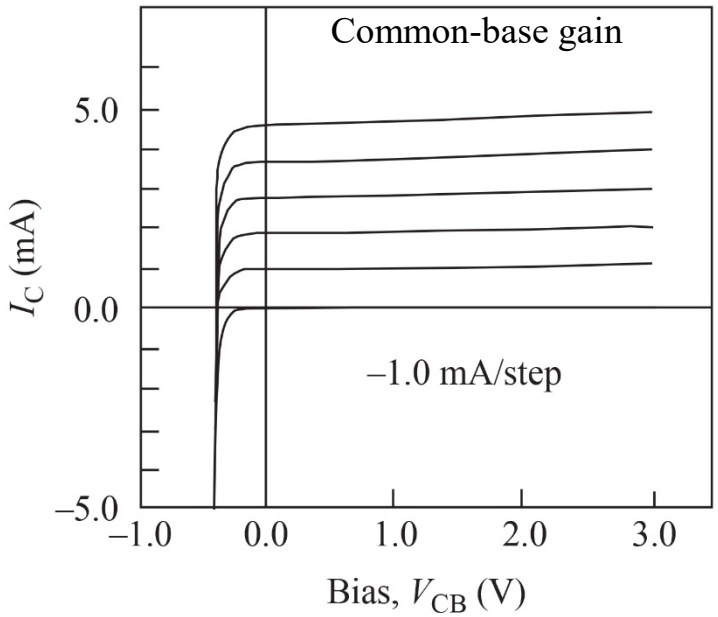

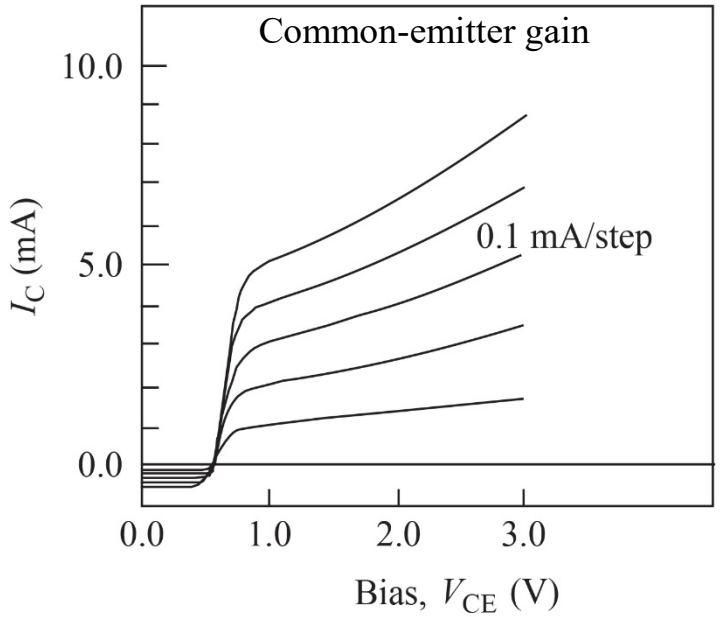

"Room Temperature Operation of Hot Electron Transistors", A. F. J. Levi and T. H. Chiu, *Appl. Phys. Lett.* **51**, 984-986 (1987).

Quantum engineering and electron transport: Nonequilibrium electron transistor

- Nonequilibrium electron spectroscopy using tunnel current injection
- The physics of electron transmission and impedance matching (use of bulk band structure as a guide to help describe electron transport in nm-scale geometries)
  - Group velocity, $\upsilon_g = \partial\omega/\partial k$
  - Character of atomic orbitals
- Reliable quantitative prediction of many-body nonequilibrium electron scattering in any realistic nano-scale geometry remains an outstanding challenge for the community
  - Accurate DFT and nonequilibrium electron transport in 40 x 50 x 325 nm^3 volume containing 32.5M atoms

"Electron transport in an AlSb/InAs/GaSb tunnel emitter hot electron transistor", T. H. Chiu and A. F. J. Levi, *Appl. Phys. Lett.* **55**, 1891-1893 (1989).

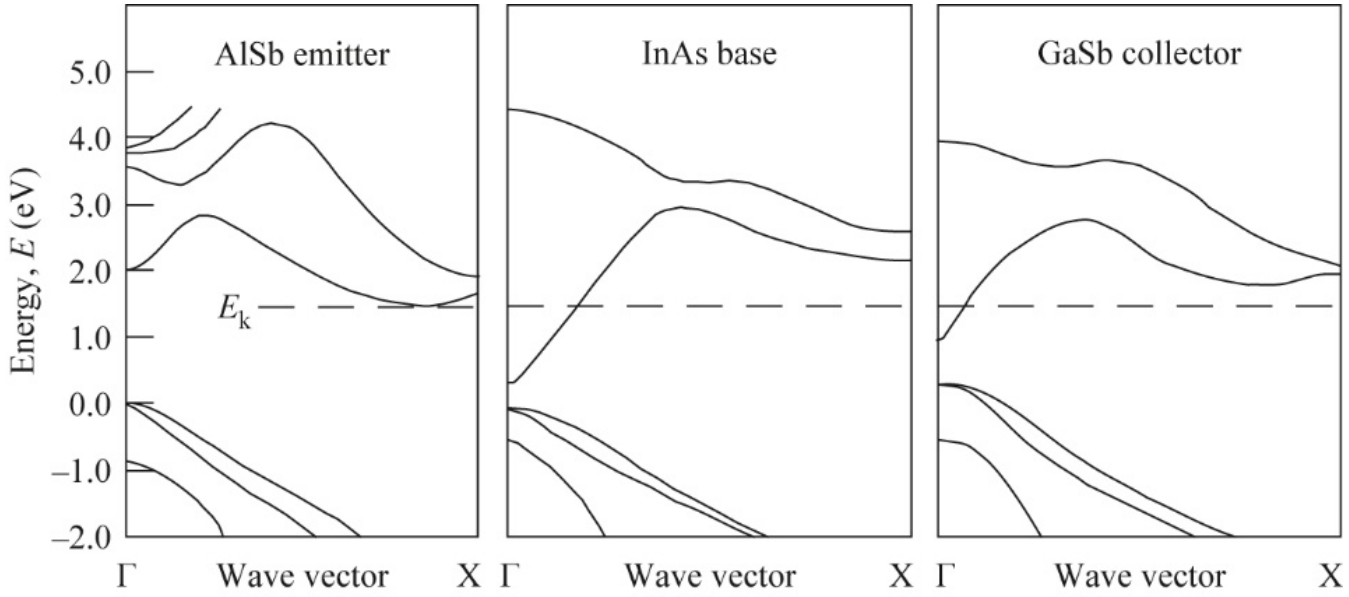

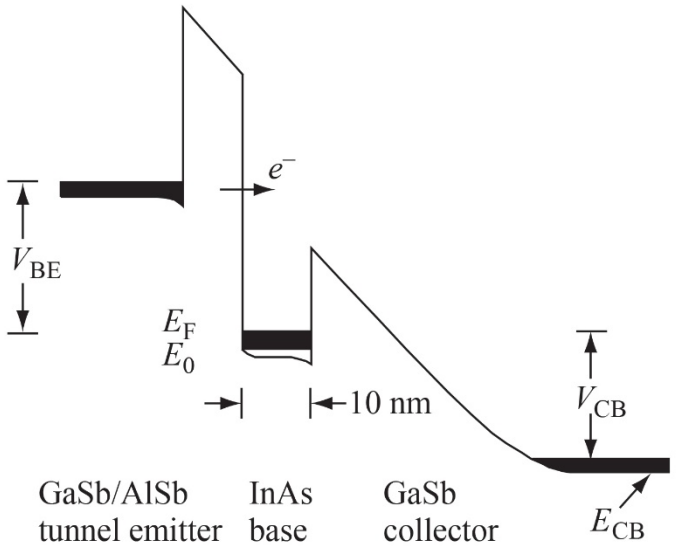

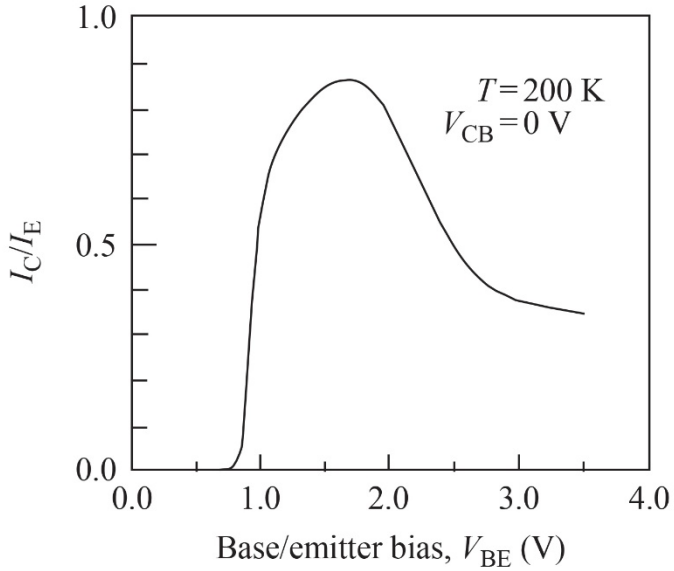

Complex band structure as a degree of freedom for design

Complex band structure

- Textbook example of *complex band structure* in a 1D Kronig-Penney model
- Propagating states have pure real k and group velocity $\upsilon_g = d\omega/dk$
- States with complex k violate translational symmetry in *bulk* crystal and are not proper solutions to Schrödinger's equation in a bulk crystal. However, states with complex k *are* useful for estimating spatial decay at interfaces and defects in nanoscale geometries
- Example: $V_0 = 2$ eV, $L = 1$ nm, $L_b = 0.5$ nm, $L_w = 0.5$ nm

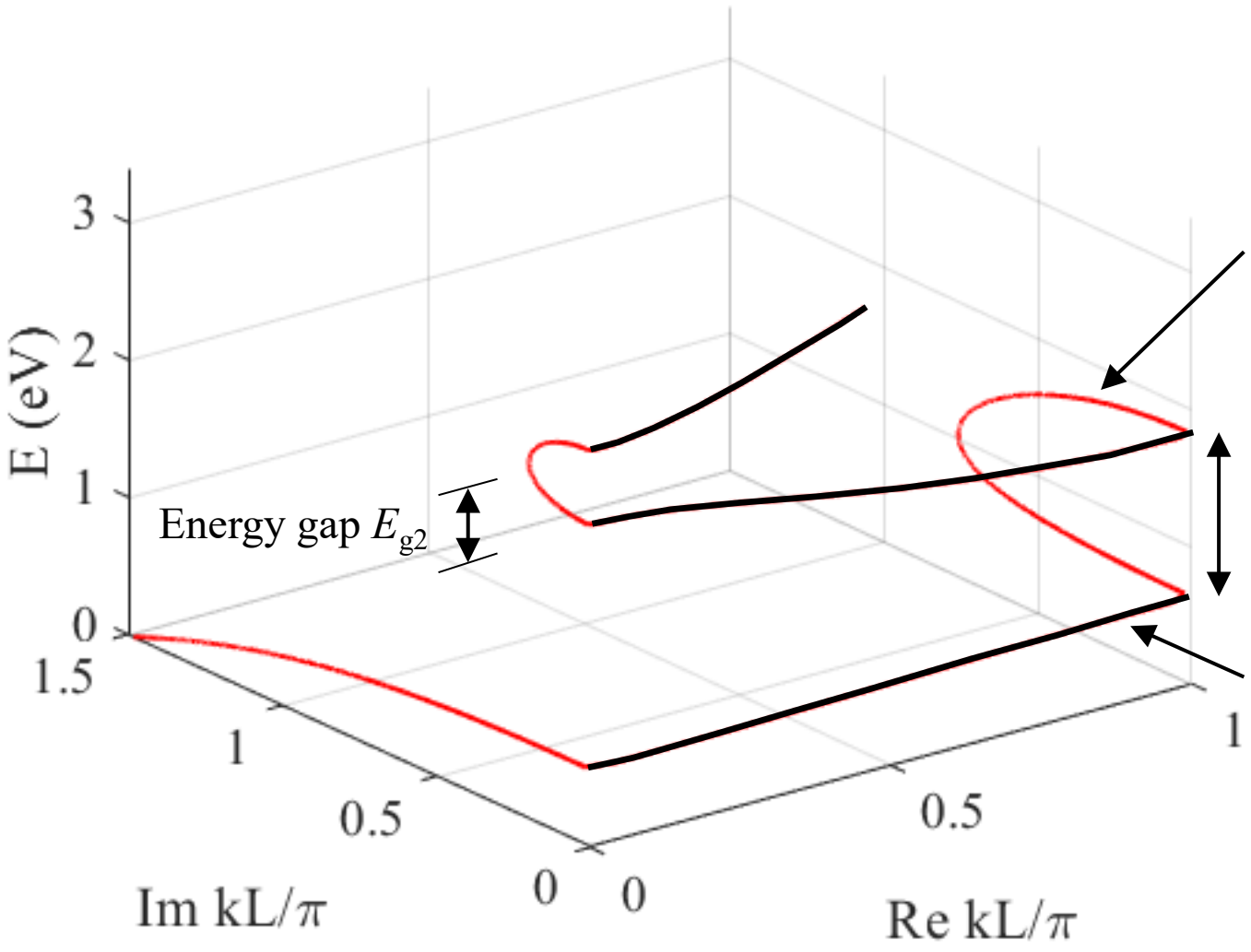

Real-space nearest-neighbor single-electron hopping on a 1D lattice

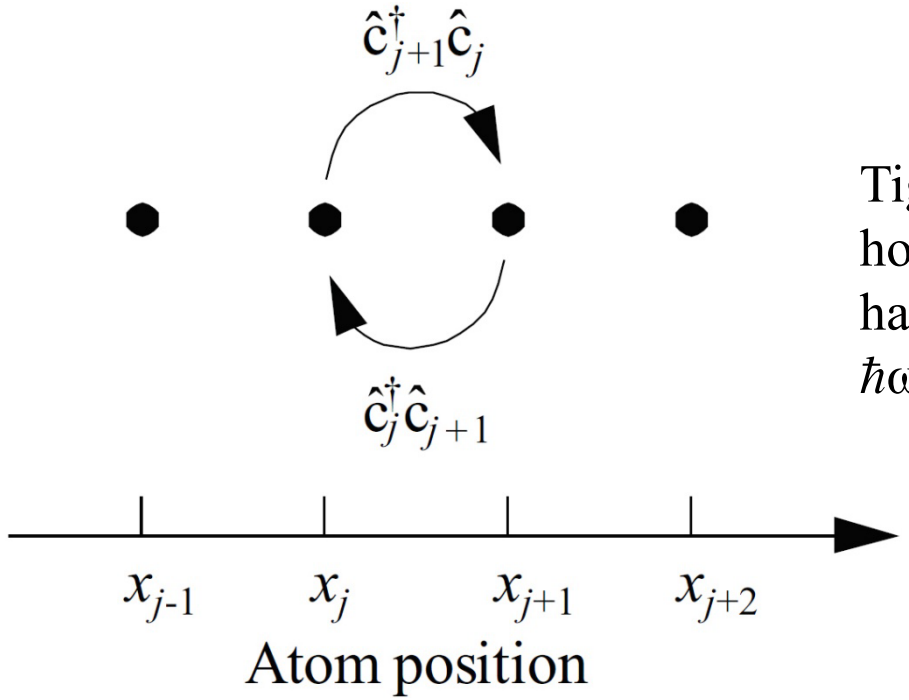

Tight-binding nearest-neighbor hopping energy t_h for s-orbitals has propagating k-state dispersion $\hbar\omega = -2\, t_h \cos(kL)$

$$H = T + V$$

$$= -t_h \sum_{j=1}^{N} \left(c_j^\dagger c_{j+1} + c_{j+1}^\dagger c_j \right) + \sum_{j \in \mathcal{J}} U_j c_j^\dagger c_j$$

Nearest-neighbor tight-binding dispersion in electrode and tunnel barrier

- (a) Propagating electron state (dot) of energy E_0 in the real nearest-neighbor tight-binding s-orbital cosine band of the electrode (black curve)
- (b) Cosine band shifted up in energy relative to (a) to form a potential barrier of energy V_B. An electron of energy E_0 incident on the potential barrier may be viewed as tunneling via the imaginary k-state (dot) in the *normal* imaginary dispersion in the band structure (red dashed curve with *negative slope and curvature*)

Tight-binding nearest-neighbor hopping energy t_h for s-orbitals propagating k-state dispersion
$\hbar\omega = 2\ t_h\ (1 - \cos(kL))$

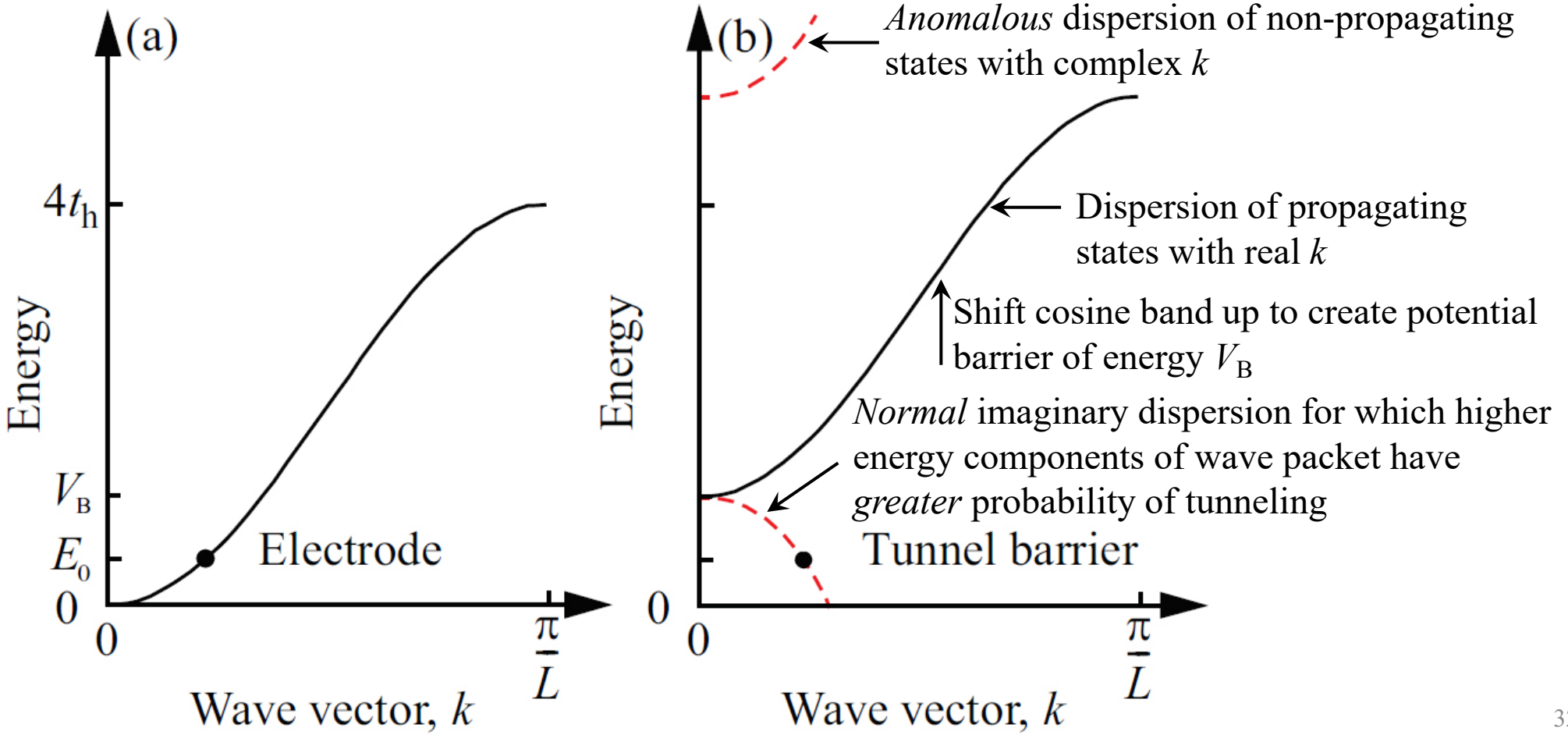

High-pass k-space filter in a tunnel barrier

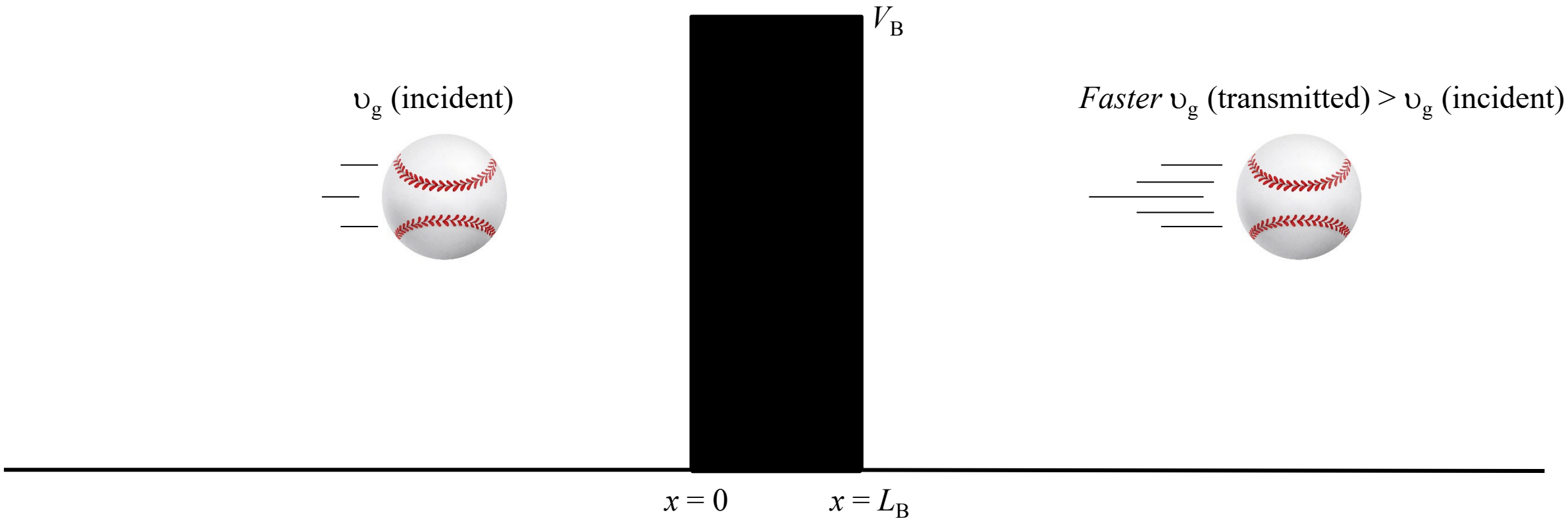

No tunnel barrier

υ_g (incident)

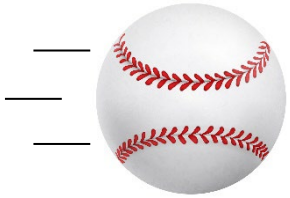

υ_g (transmitted) = υ_g (incident)

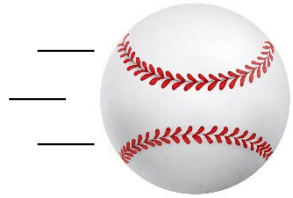

Electrode

Electrode

Low-pass k-space filter in a tunnel barrier

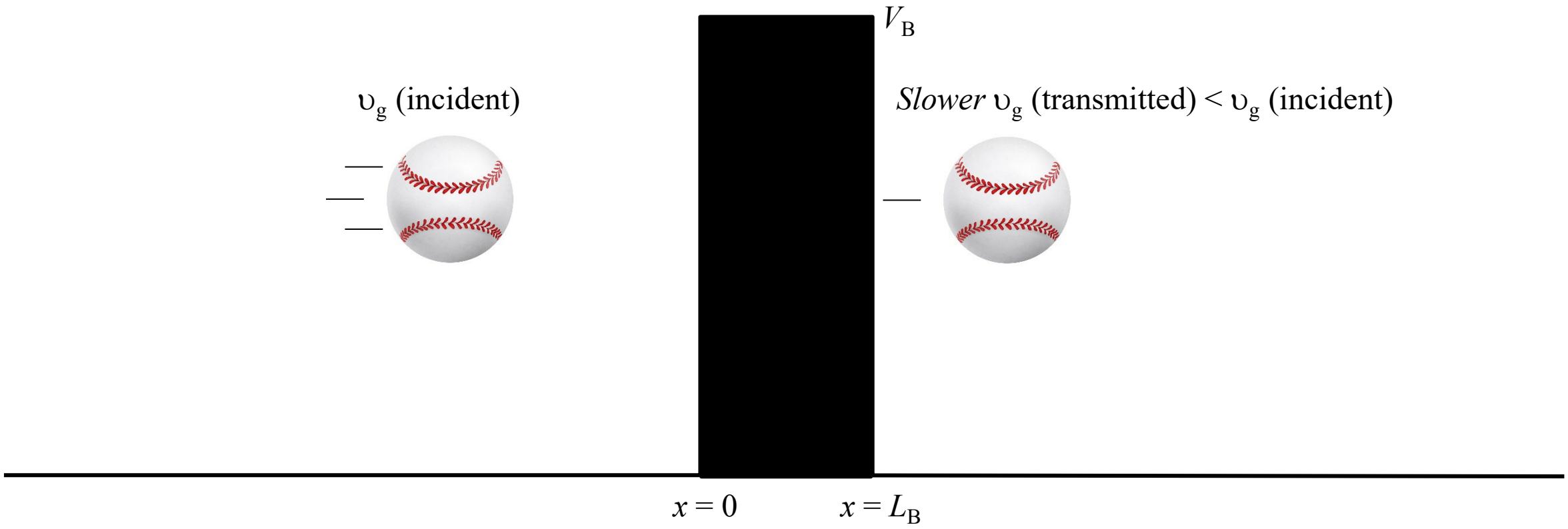

Complex dispersion and a double barrier resonant tunnel diode

- Increase peak-to-valley current ratio from PVR = 5 for device with normal complex dispersion (negative slope Im(dω/dk)) to PVR = 45 with anomalous complex dispersion (positive slope Im(dω/dk)) in the second barrier

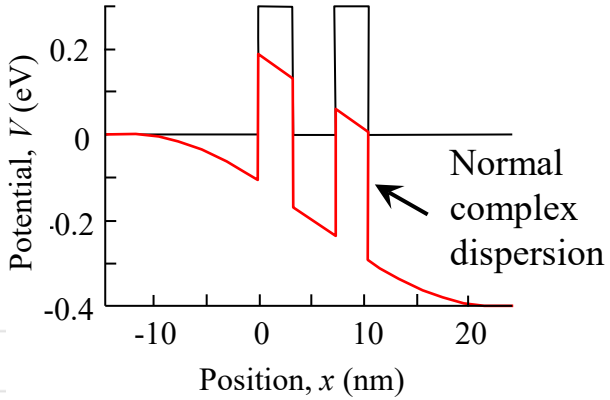

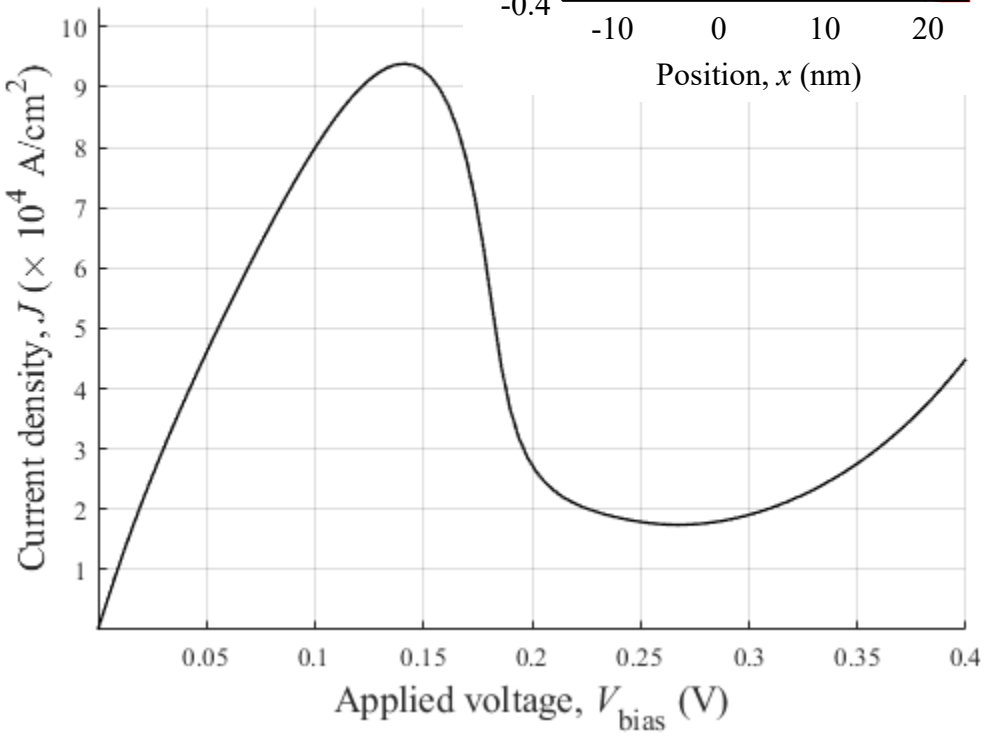

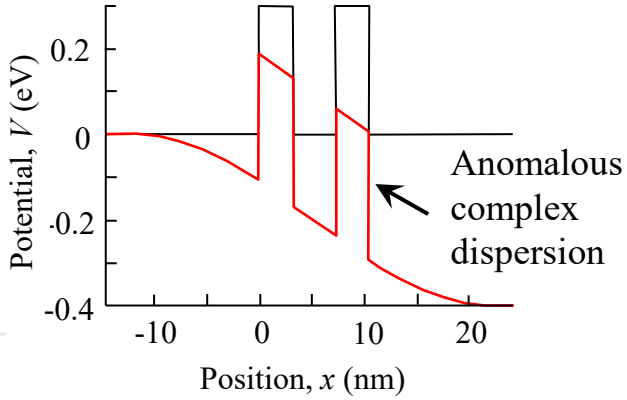

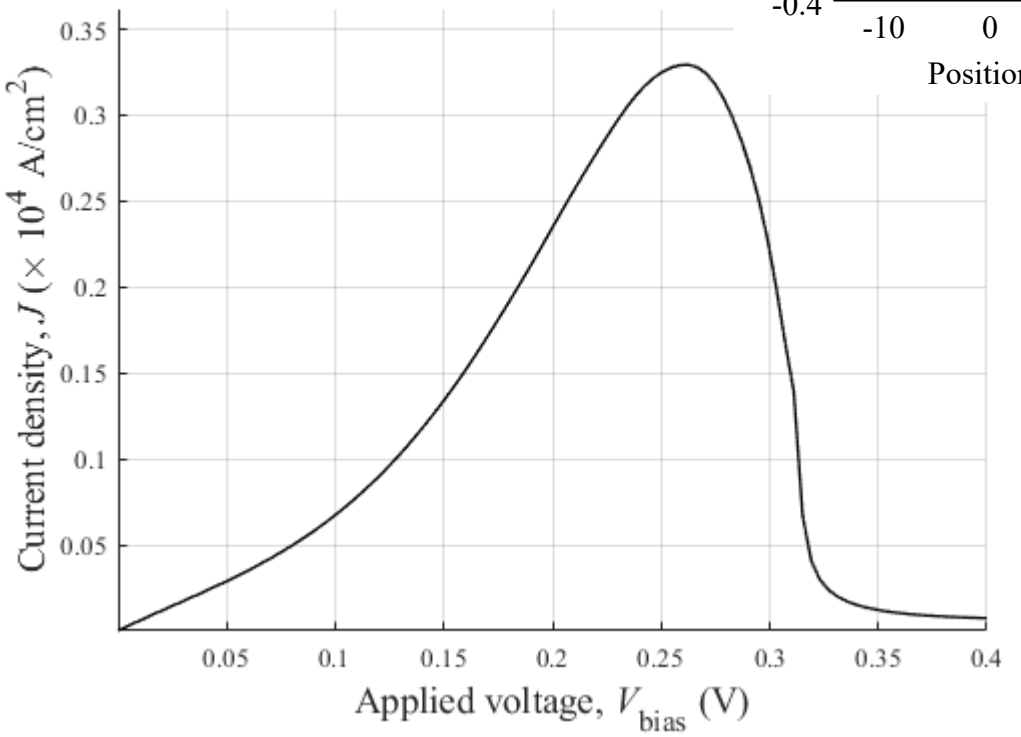

Complex dispersion with next-nearest neighbor

- Number of layers (N_b) and next nearest neighbor interaction ($t_2 = 0.5\ t_1$) are resources that enable an optimal solution

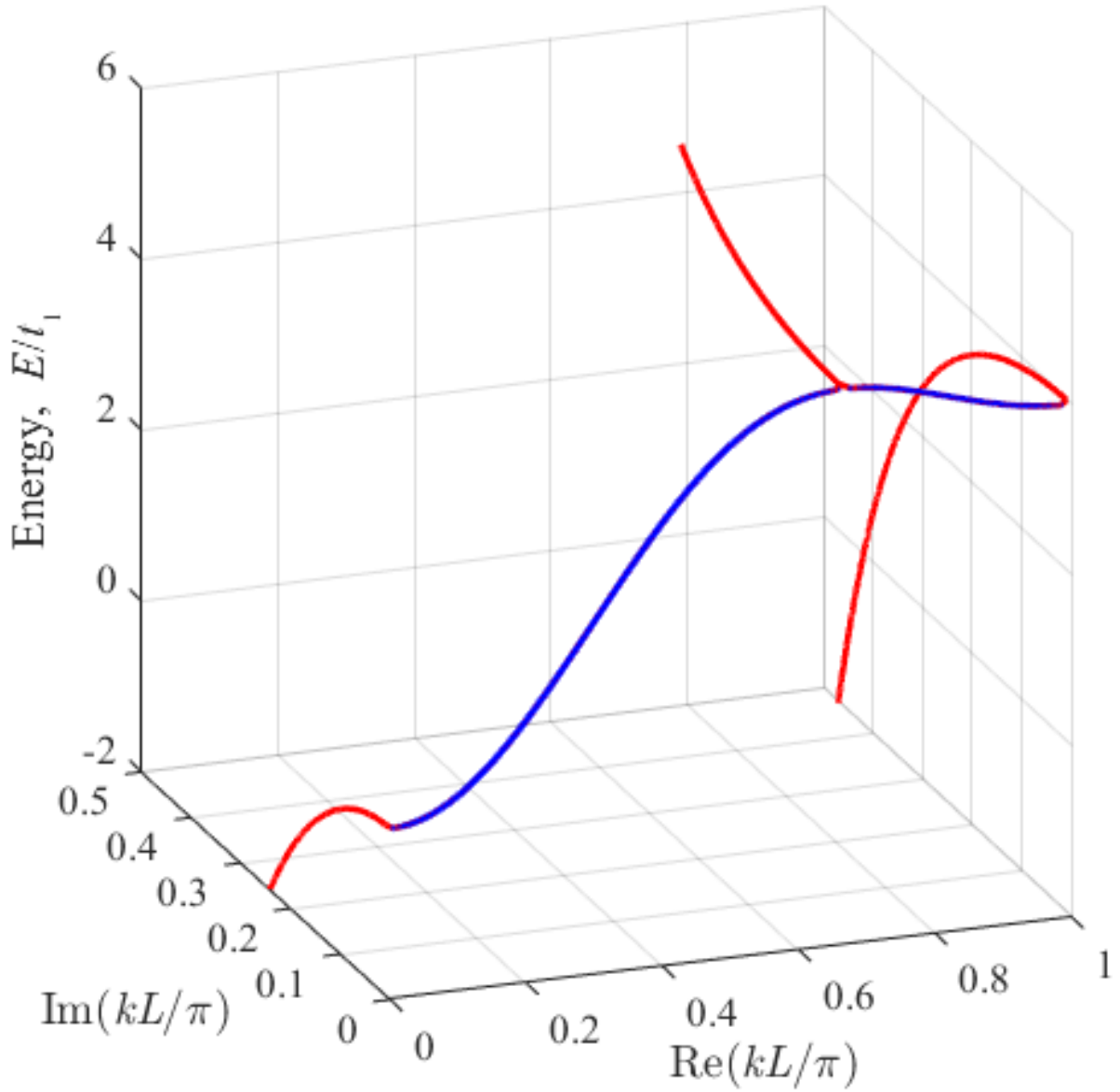

Complex dispersion and the N_b=8-layer diode

- Number of layers (N_b) and next nearest neighbor interaction ($t_2 = 0.5\ t_1$) are resources
- Example sigmoid current-voltage objective (red dash)
- Do *not* require tunneling to create RTD current-voltage characteristics!

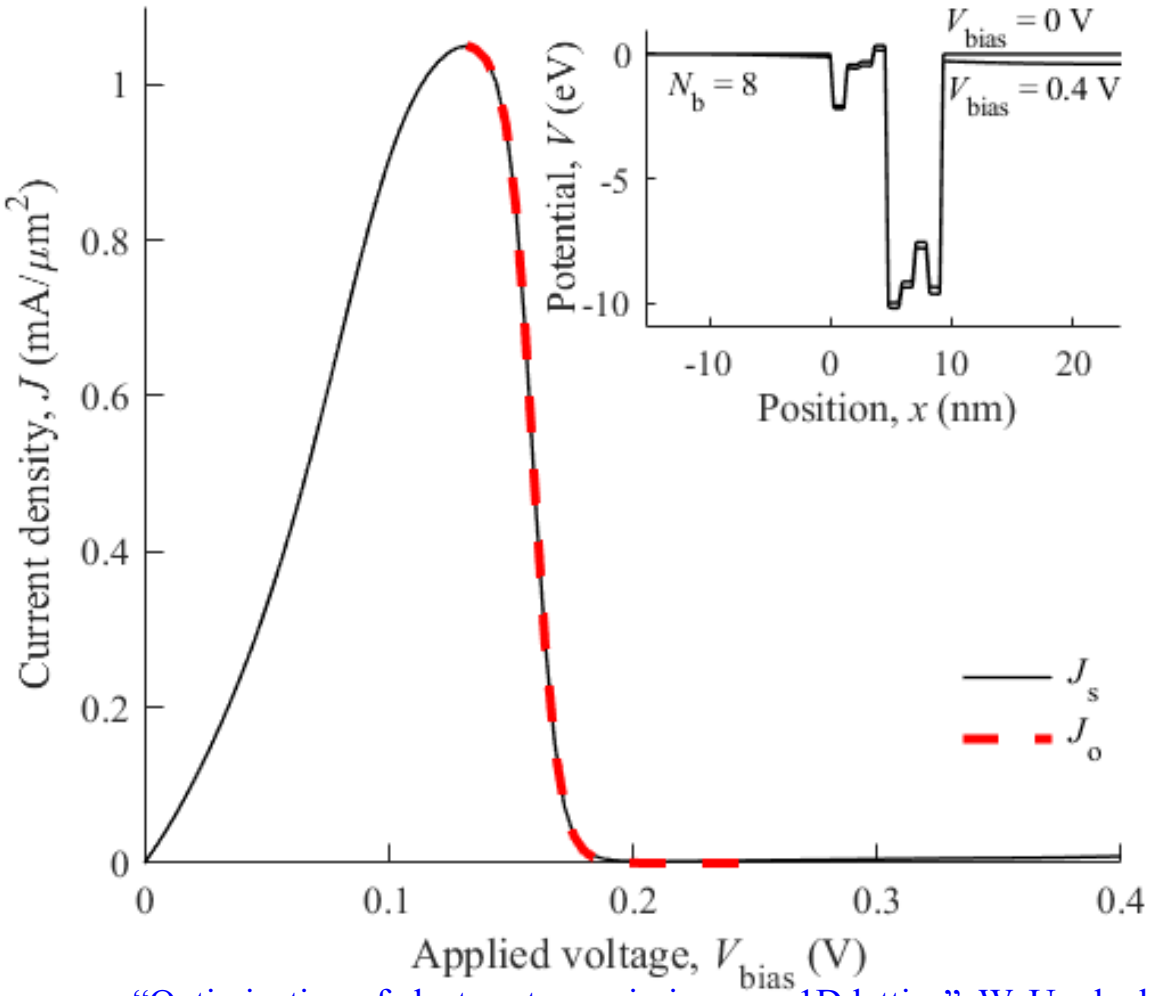

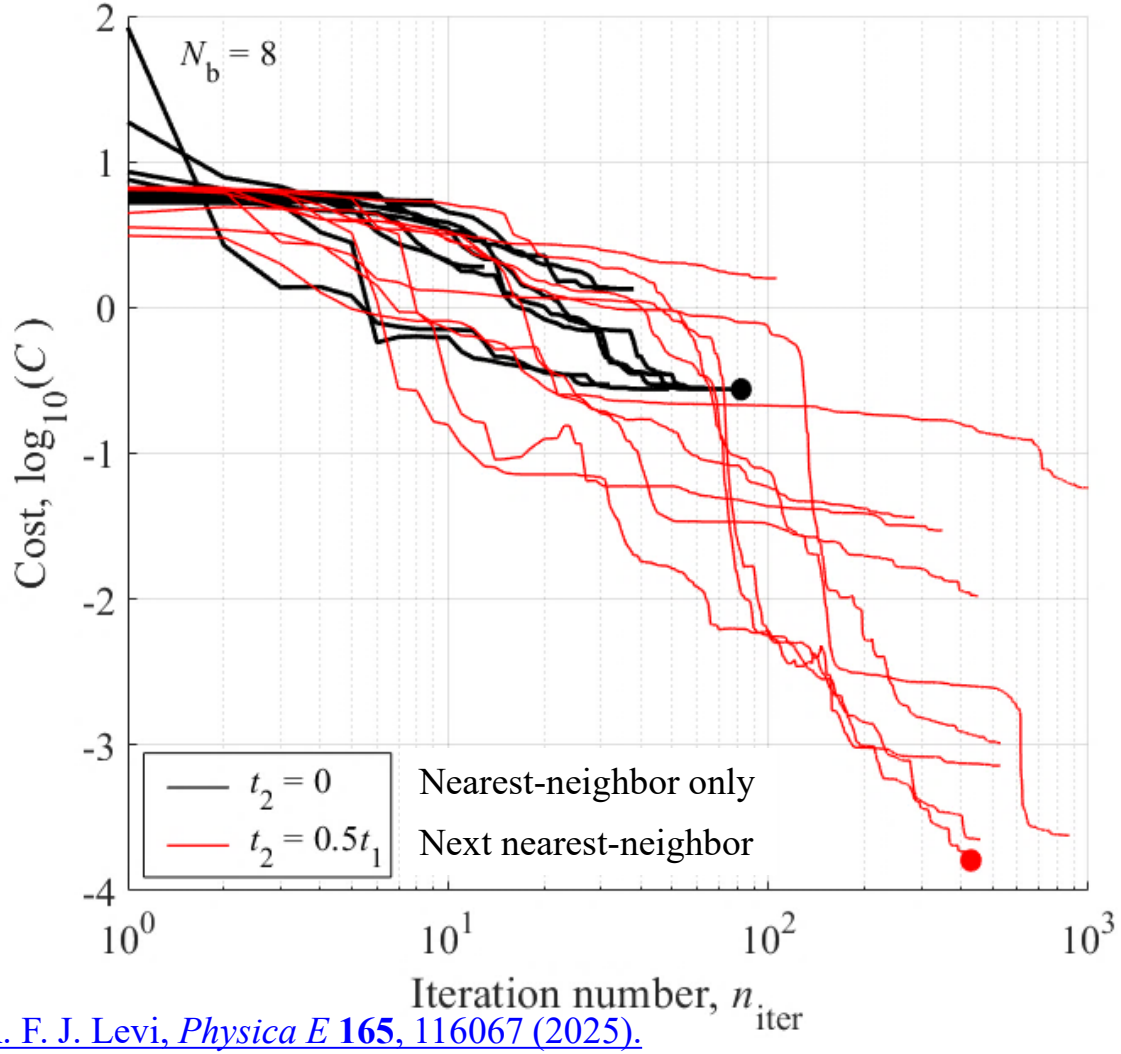

"Optimization of electron transmission on a 1D lattice", W. Unglaub and A. F. J. Levi, *Physica E* **165**, 116067 (2025).

Vast quantum engineering design space

→ new **Quantum** search engine

(an opportunity for those with access to large computing resources?)

Quantum engineering: Controlling photons

Application of high-Q microdisk electrooptic resonators that enhance light-matter interaction in an RF-cavity

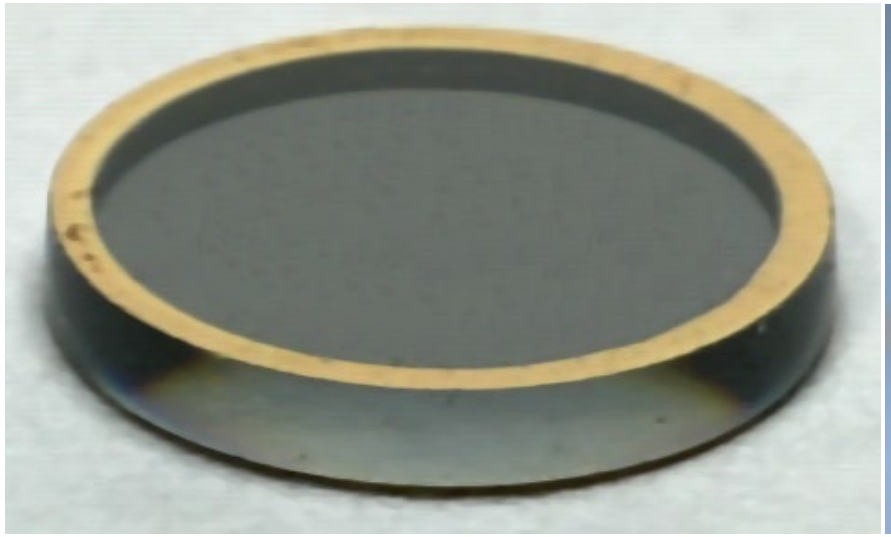

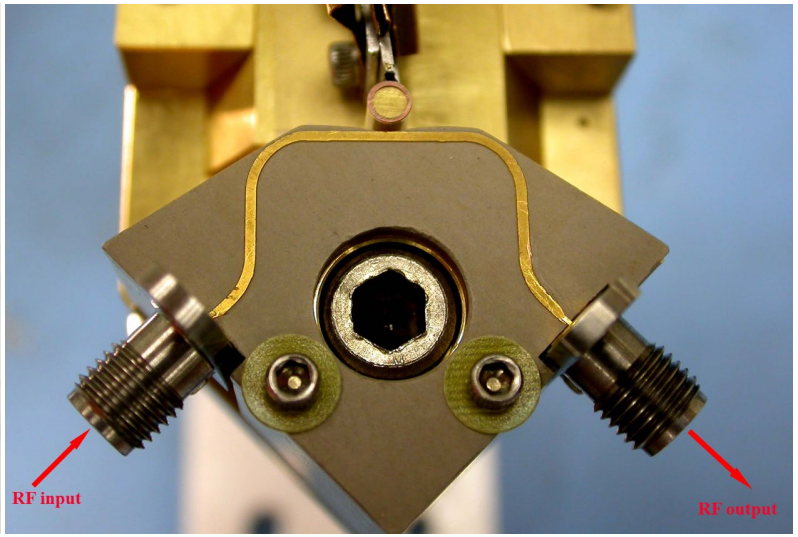

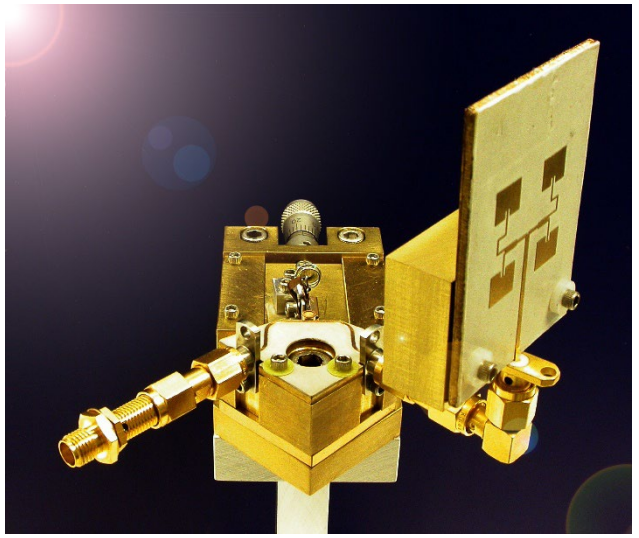

- Initial microdisk electrooptic modulator z-cut $LiNbO_3$, R = 5.8 mm, d = 0.74 mm, measured optical $Q = 4 \times 10^6$
  - Demonstration of classical mm-wave and 14.6 GHz (λ_0 = 20.7 mm) receiver by up-conversion of RF to laser light at 200 THz (λ_0 = 1500 nm), optical filtering, and direct optical detection of baseband
  - Simultaneous optical and RF resonance in a cavity. Unloaded RF $Q \sim 260$
- Future application of high-Q microdisk electrooptic resonators to quantum transduction and entangling microwaves with laser light
  - Recent realization by the Johannes Fink group: "Entangling microwaves with light", R. Sahu, L. Qiu, W. Hease, G. Arnold, Y. Minoguchi, P. Rabl, and J. M. Fink, *Science* **380**, 718 (2023)

"Microphotonic components for a *mm*-wave receiver", D.A.Cohen and A.F.J. Levi, *Solid-State Electronics* **45**, 495-505 (2001).
"Ring resonator-based photonic microwave receiver modulator with picowatt sensitivity", M. Hossein-Zadeh and A. F. J. Levi, *IET Optoelectron.* **5**, 36-39 (2011).

Optimal design of dielectric structures

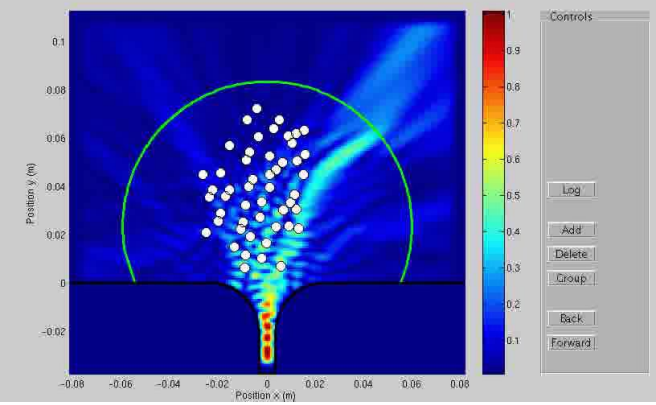

Leverage and explore expanded exponentially large design space:

- Non-intuitive broken-symmetry robust optimal design
  - *Non-intuitive* because of broken symmetry in a very large design space
  - *Not* an inverse problem because unknown if the solution exists
  - ML-assisted search
- Optimal design of mm-wave passive and active metal-dielectric structures that exploit the near-field
- Optimal design of aperiodic nano-photonic structures
- Optimal design of semiconductor light-matter interaction
- Optimal coherent control of light in a resonator
- Optimal coherent quantum control of single photons

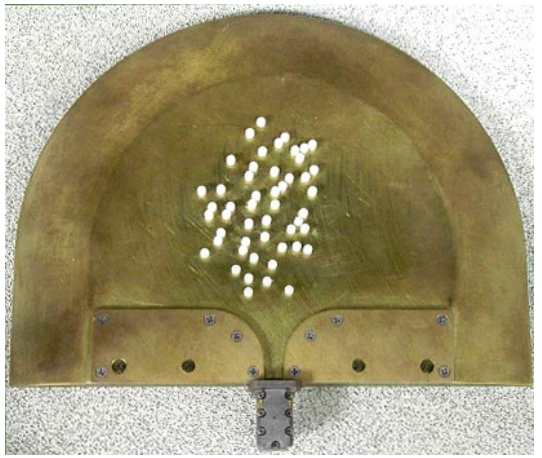

37.5 GHz

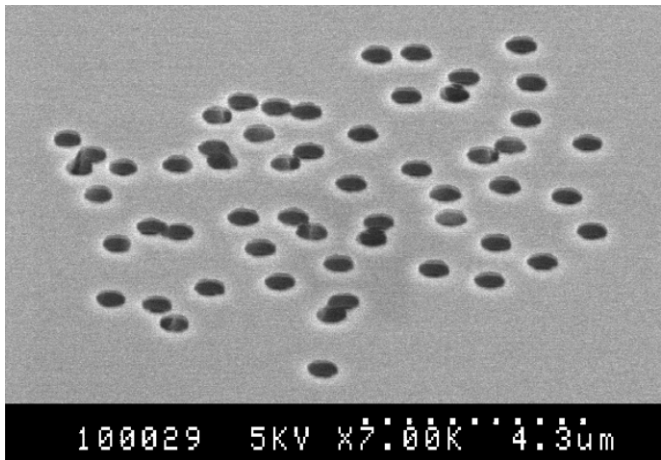

200 THz

"Optimization of aperiodic dielectric structures", P. Seliger, M. Mahvash, C. Wang and A. F. J. Levi, *J. Appl. Phys*. **100**, 034310 (2006).
"Coherent control of non-Markovian photon resonator dynamics", A. F. J. Levi, L. Campos Venuti, T. Albash and S. Haas, *Phys. Rev. A* **90**, 022119 (2014).
Optimal Device Design, A. F. J. Levi and S. Haas eds. Cambridge University Press, 2010. ISBN 0521780144

Example: Experiments performed using a 37.5 GHz (λ_0 = 8 mm) RF source

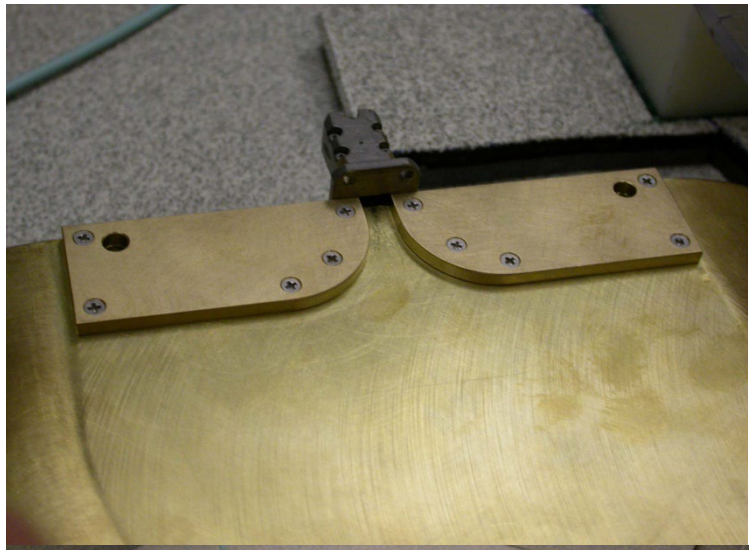

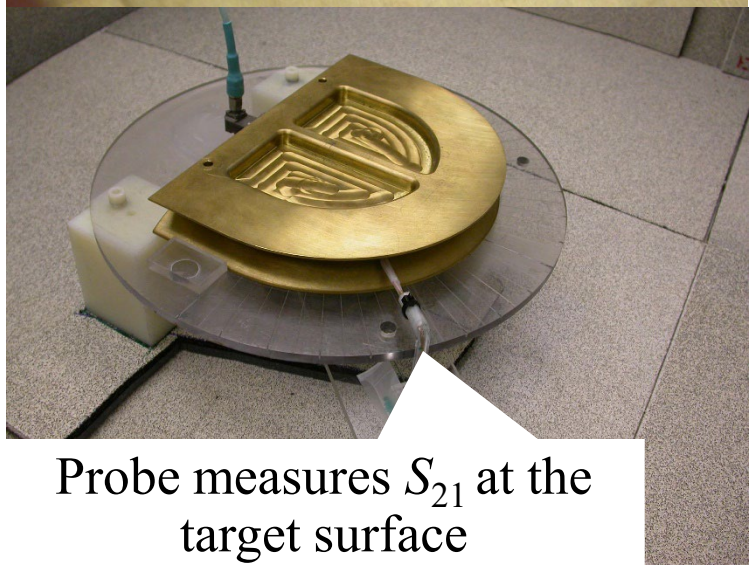

Probe measures S_{21} at the target surface

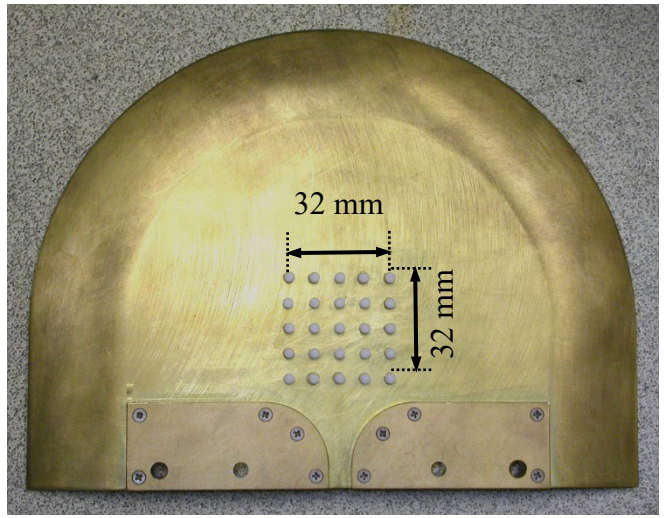

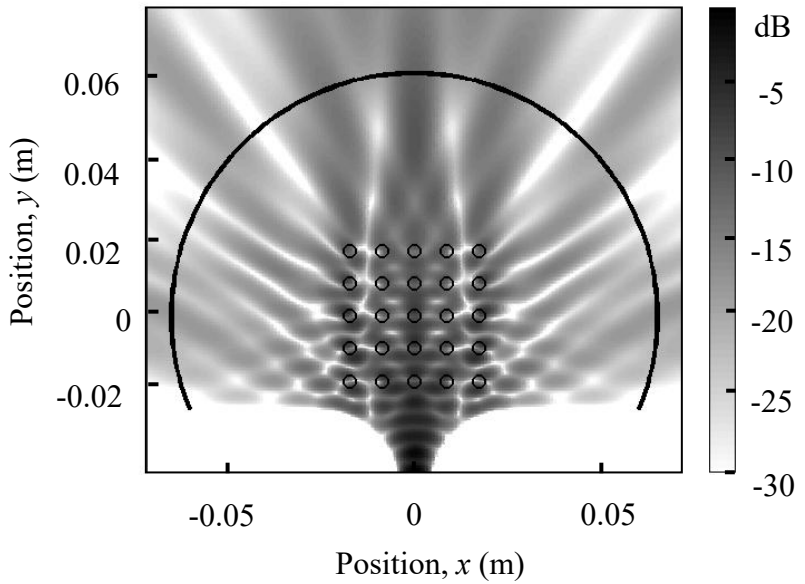

Finite-sized period structure has limited functionality

50 teflon cylinder configuration in a slab waveguide to focus 37.5 GHz RF power into a uniform top hat distribution between 30 and 60 degrees

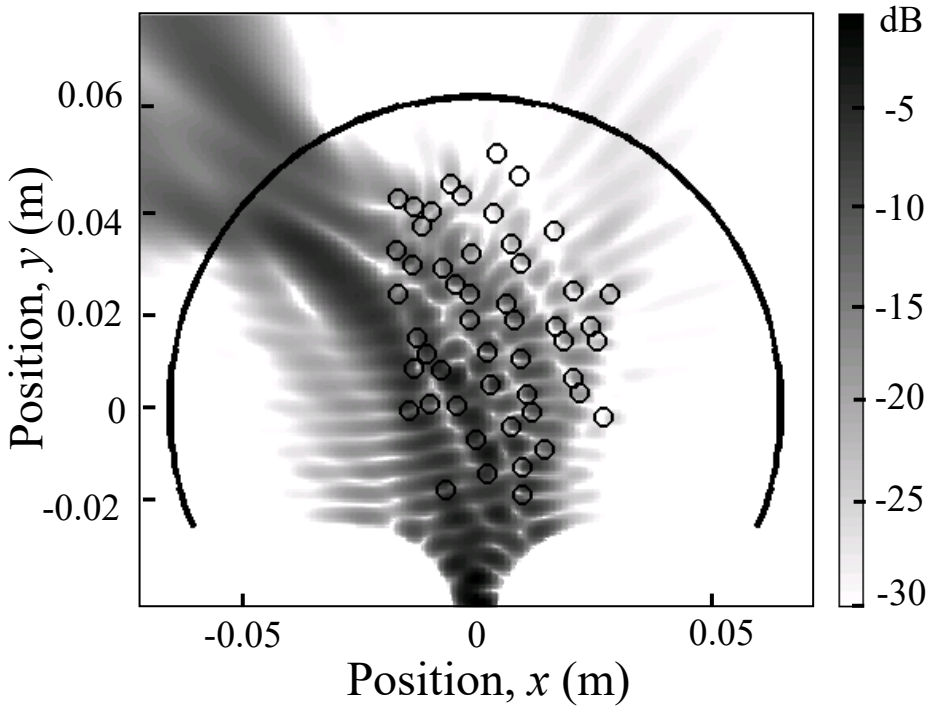

- Optimized configuration for 50 teflon cylinders found by machine search is aperiodic and non-intuitive
  – Cylinder diameter is 3.175 mm, relative permittivity $\varepsilon_r = 2.05$, RF source of frequency 37.5 GHz ($\lambda_0 = 8$ mm)
- Finite Difference (FD) frequency-domain solver with efficient local gradient optimization

$$\nabla \times (\mu^{-1}) \cdot \nabla \times \mathbf{E} - \omega^2 \varepsilon_0 \varepsilon_r \mathbf{E} = 0$$

Comparison of measured and modeled power profile for optimized position

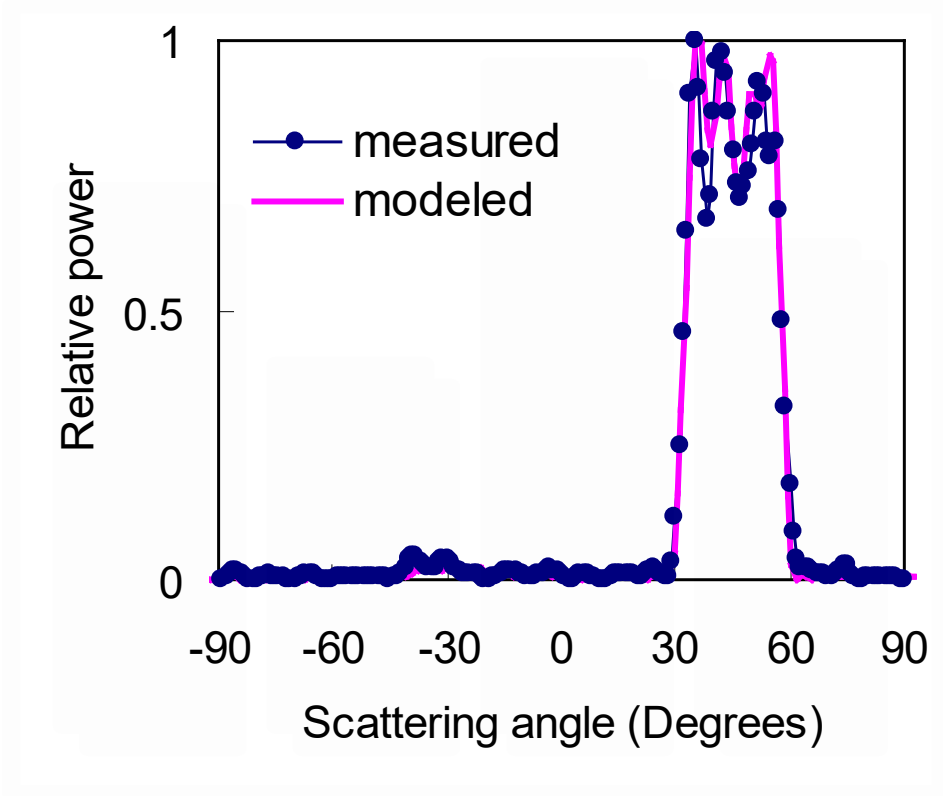

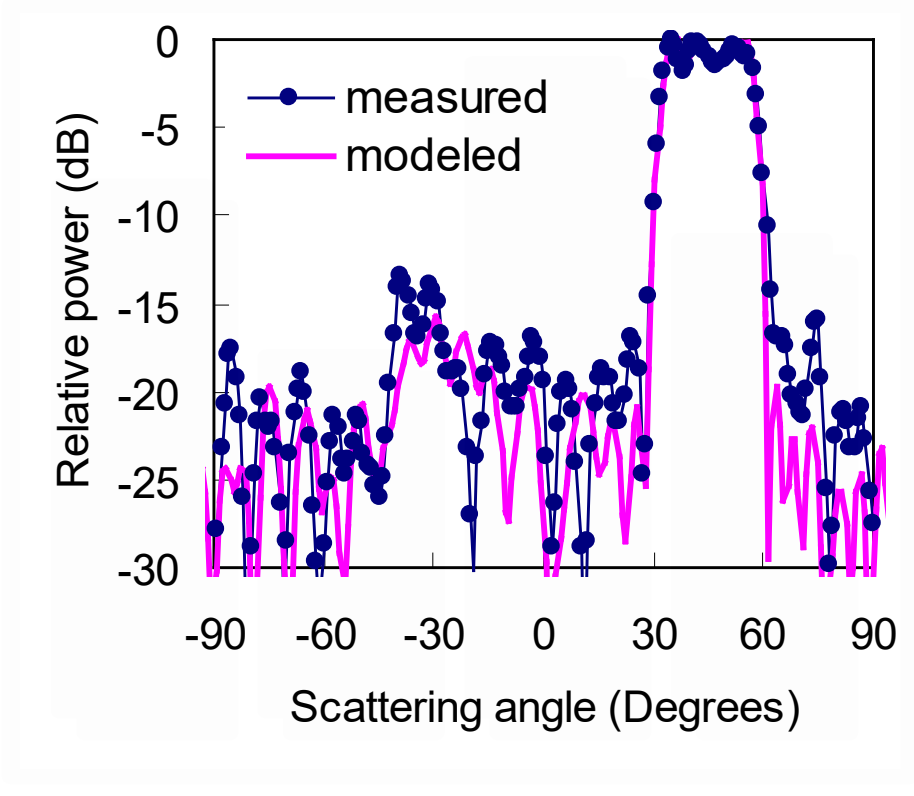

- Model predicts 95.37% of 37.5 GHz RF power focused between 30 and 60 degrees, and 1.45 dB top hat ripple
- Measurements show 92.7% of power focused and 3.5 dB top hat ripple

Coherent control of photons

- Coherent
  - Keep track of field amplitude, phase, and maintain precise timing within a characteristic length or time scale
- Control
  - Methods to modify the behavior of a system with one or more inputs
- Photon
  - A wavelike particle of energy that produces a click on a detector
- … and, there may be additional opportunities with *quantum* aspects of photons
  - Quantum
    - No accepted measure of "quantumness"
    - Classical analogies often exist (e.g., the coherent oscillator state) except for:
      - Wave-particle duality
      - Identical indistinguishable particles
      - Linearity and superposition of particle states
      - Entanglement of particles
- Motivation: Demonstrate a path to *intuitive* control of transient photon dynamics (in quantum systems)
  - Open-loop control with control field generator

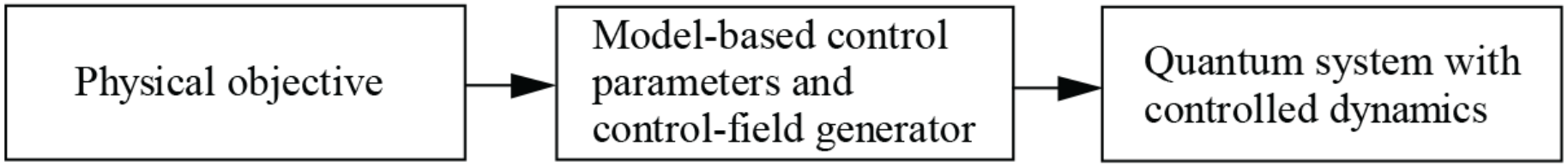

Uncontrolled short single-photon pulse and cavity ring-down

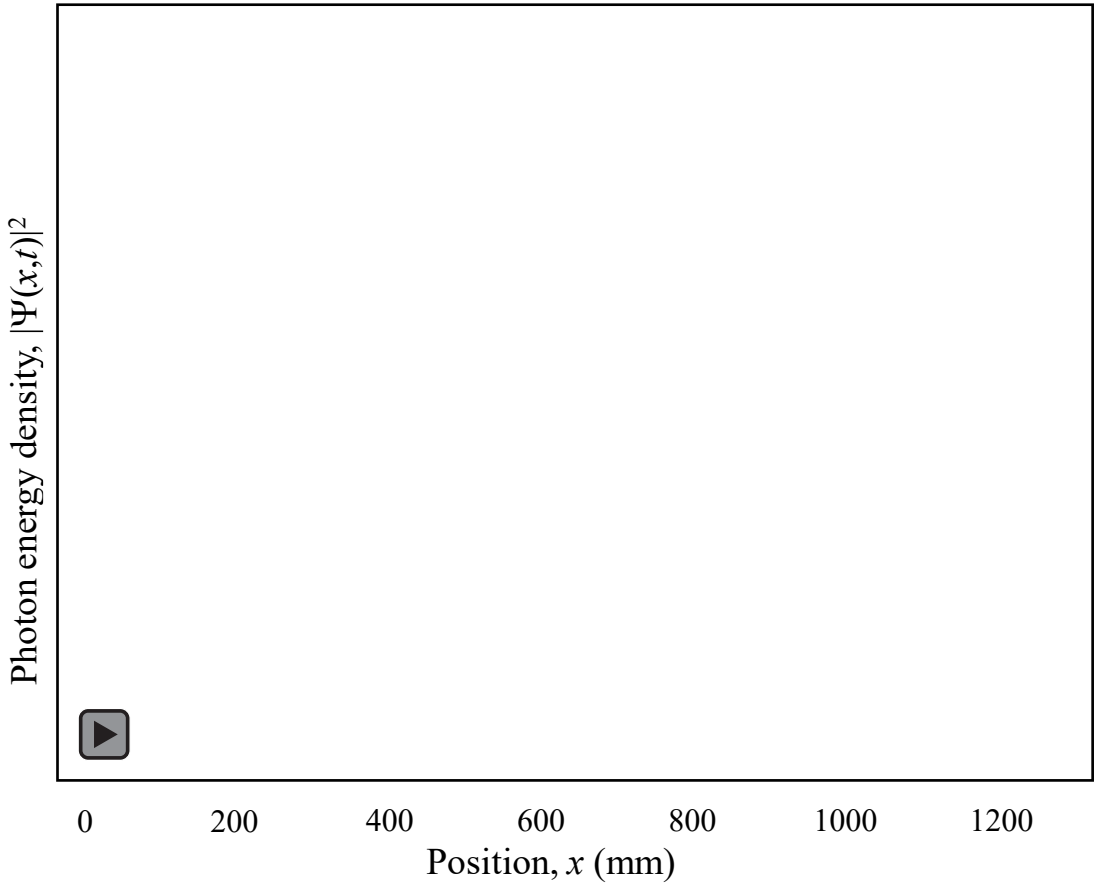

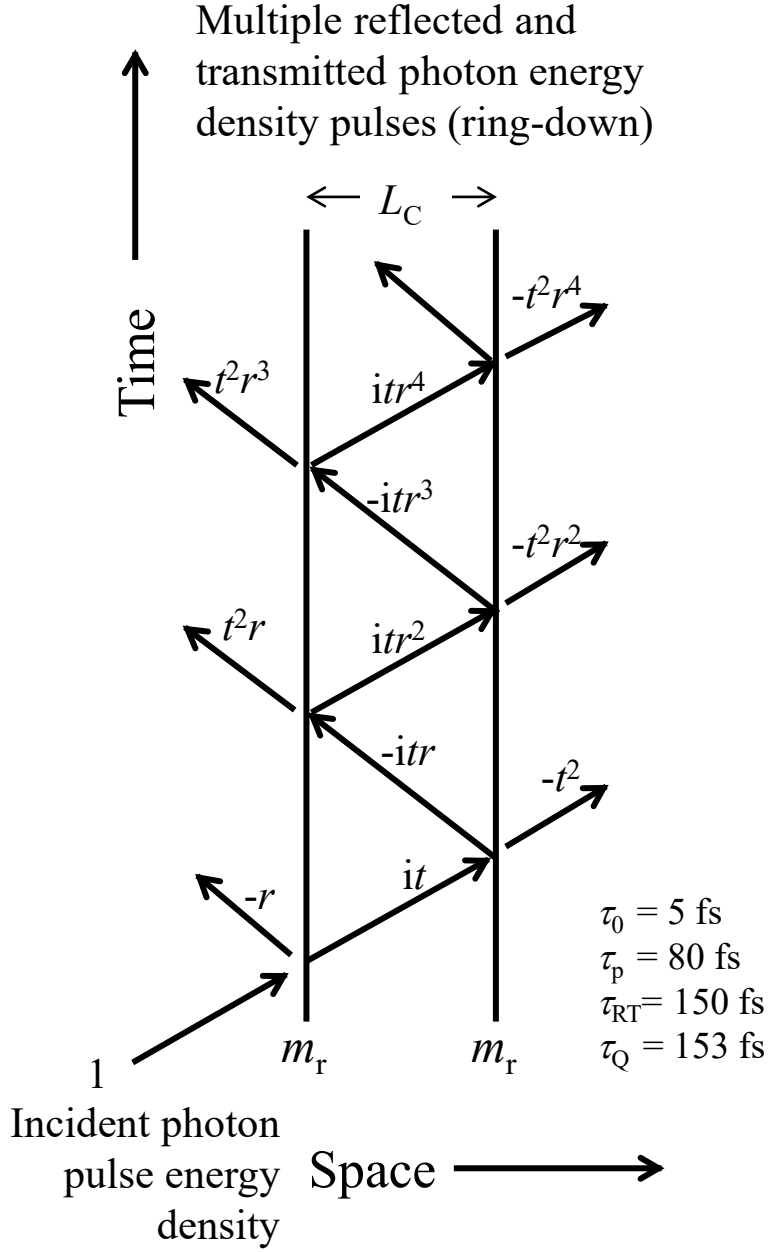

- Identical lossless dielectric mirrors m_r with complex field reflectivity r and transmission t
- π phase shift on reflection of the incident field
- Resonant photon field *in* resonator is geometric series $(1 + re^{i\phi} + r^2e^{i2\phi} + r^3e^{i3\phi} + \ldots) = 1/(1 - re^{i\phi})$ where phase per round-trip is $2\phi = 2\pi\omega/\Delta\omega$ and spacing between resonances is $\Delta\omega = \pi c/L_C n_r$

Uncontrolled single-photon cavity ring-down

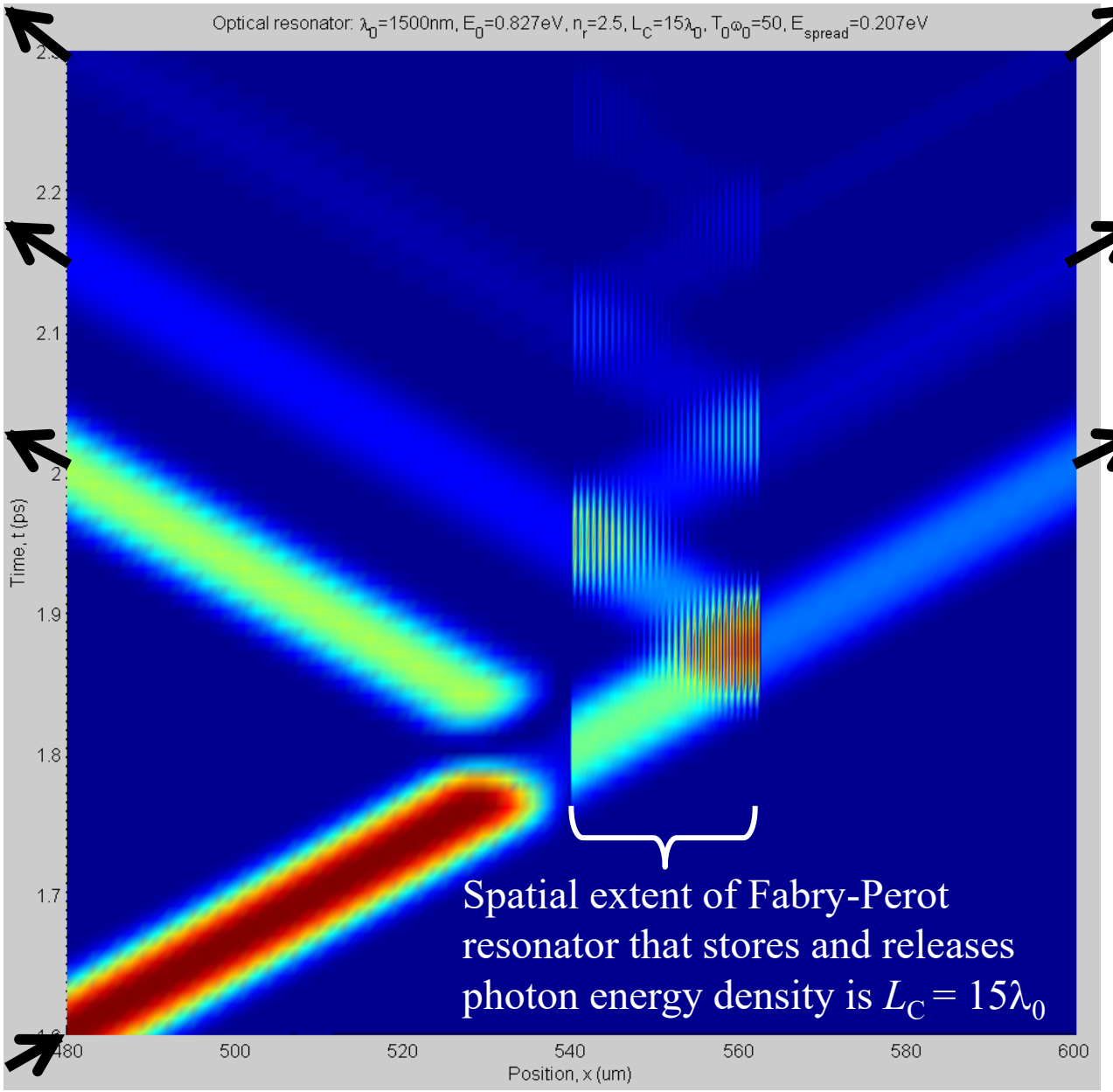

Multiple reflected photon energy density pulses (ring-down)

Multiple transmitted photon energy density pulses (ring-down)

Time

Incident photon pulse energy density

Spatial extent of Fabry-Perot resonator that stores and releases photon energy density is $L_C = 15\lambda_0$

Space

τ_0 = 5 fs
τ_p = 80 fs
τ_{RT}= 150 fs
τ_Q = 153 fs

Coherent control of *transient dynamics*

- Zero-energy ground-state is a *guaranteed* control point
- Question: How do you *stop* a bell ringing ?
  - The “ringing bell” could be *excitations* of a molecule, a crystal, a device, …

Coherent control of *transient dynamics*

- Question: How do you *stop* a bell ringing ?
- Answer: You hit it ! (… in a *very* controlled and precise way)

Control field generator System

Controlled single-photon zero cavity ring-down

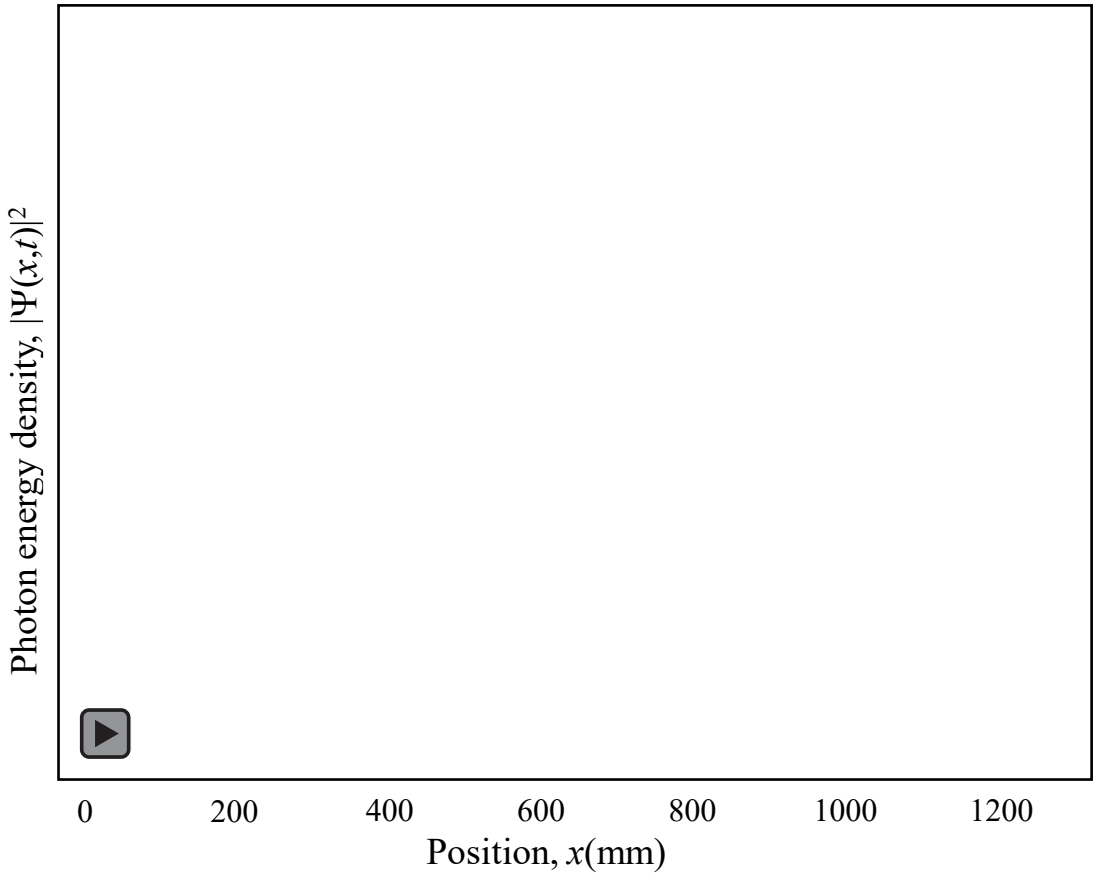

- Identical lossless dielectric mirrors m_r with field reflectivity r and field transmission t
- Control pulse with optimal amplitude and phase shift to eliminate photon energy density in resonator
- Formal control methods replaced by *intuitive* ray-tracing of *resonant* part of photon field

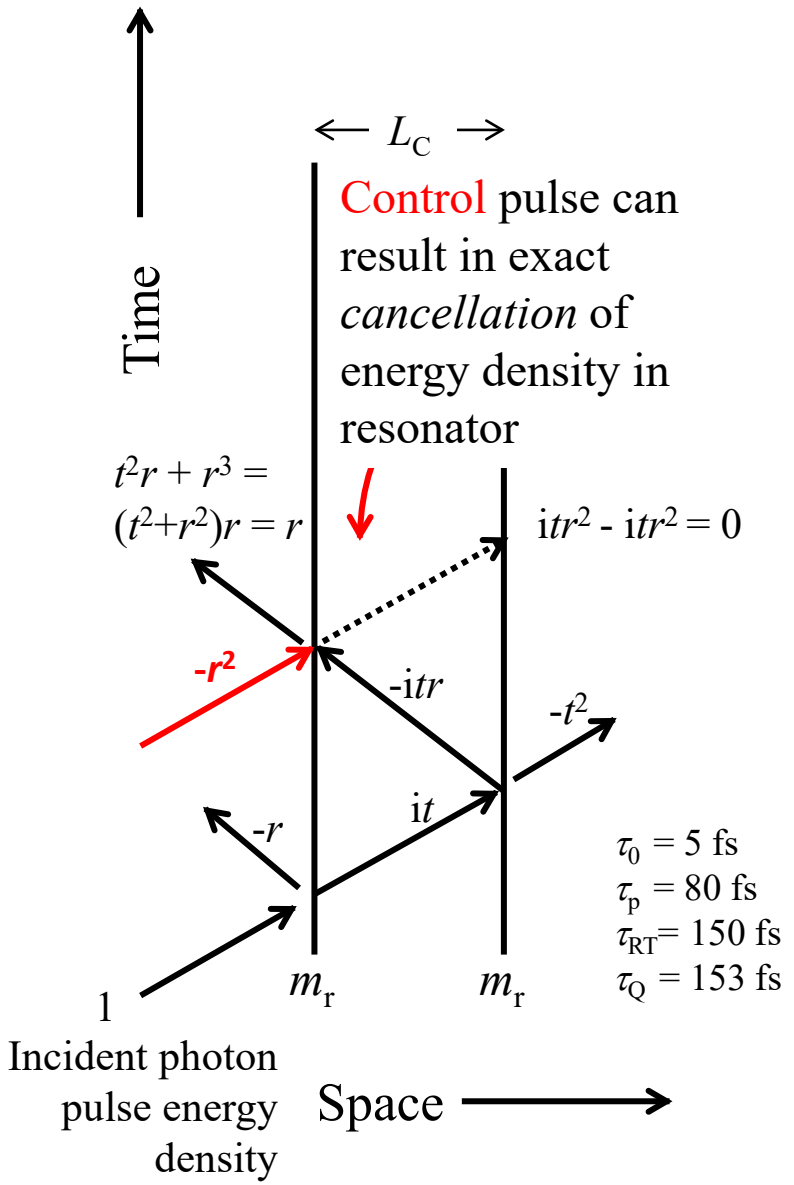

Controlled single-photon zero cavity ring-down

Dual reflected photon pulse energy density

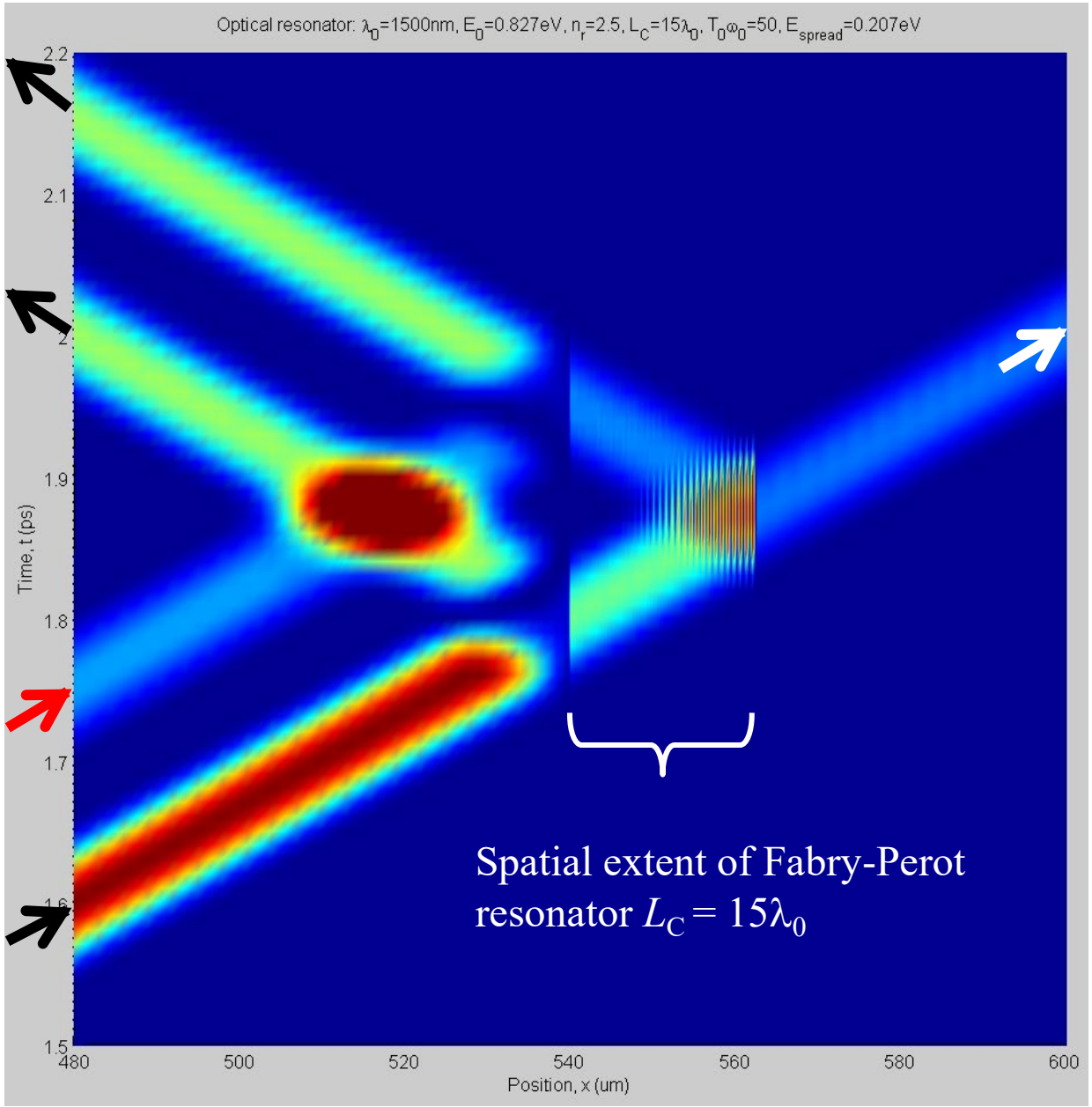

Time

Incident control photon pulse and lead pulse energy density

Spatial extent of Fabry-Perot resonator $L_C = 15\lambda_0$

Space

Transmitted single-photon pulse energy density (cancellation of ring-down)

τ_0 = 5 fs
τ_p = 80 fs
τ_{RT}= 150 fs
τ_Q = 153 fs

Experimental validation using Fabry-Perot resonator in waveguide

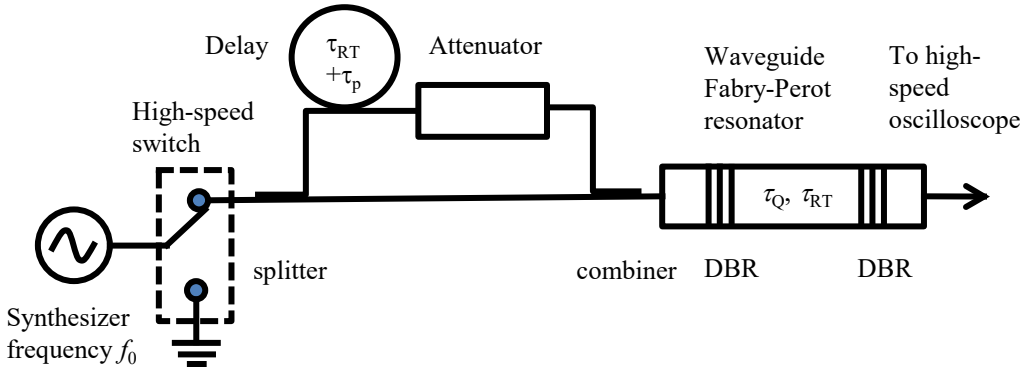

f_0 = 8 GHz, τ_{Coh} = 1 s, τ_0 = 125 ps, τ_p = 7 ns, τ_{RT} = 13.7 ns, τ_Q = 12.5 ns

No control pulse

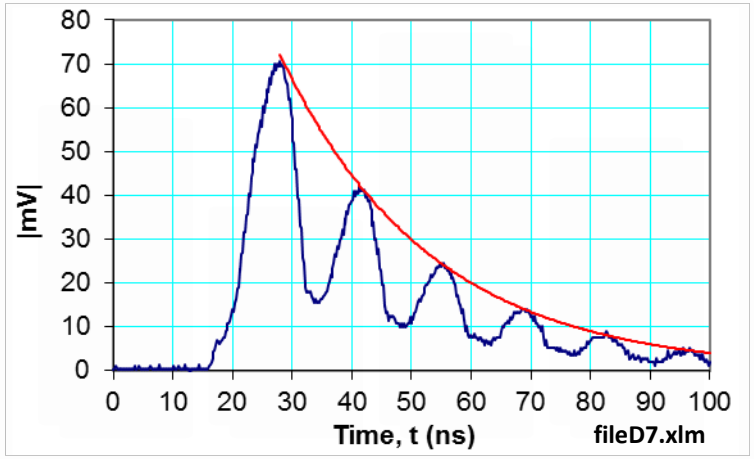

With single control pulse

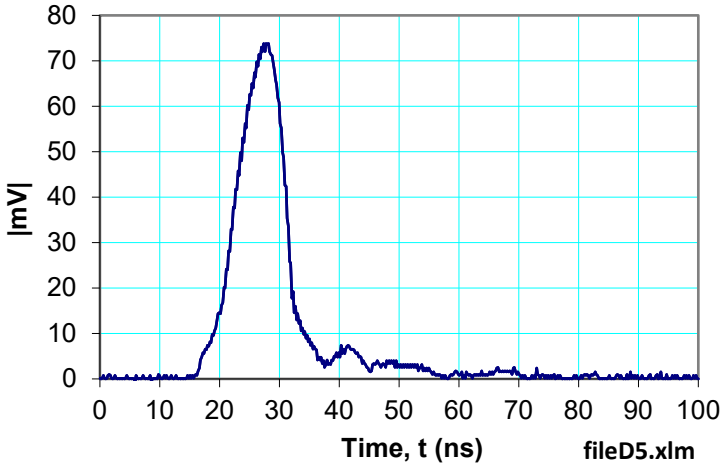

- Coherent control of resonator *short* output pulse using single *short* control pulse
- Short electromagnetic pulse of width τ_p = 10 ns < τ_{RT}, τ_Q
- Round-trip time in resonator τ_{RT} = 13.7 ns
- Resonator Q = 633 corresponds to τ_Q = 12.5 ns (red curve)
- Measured transmitted electromagnetic signal in time-domain |mV| into 50 Ω

Coherent control of single-photon resonator output pulse using one backward control pulse

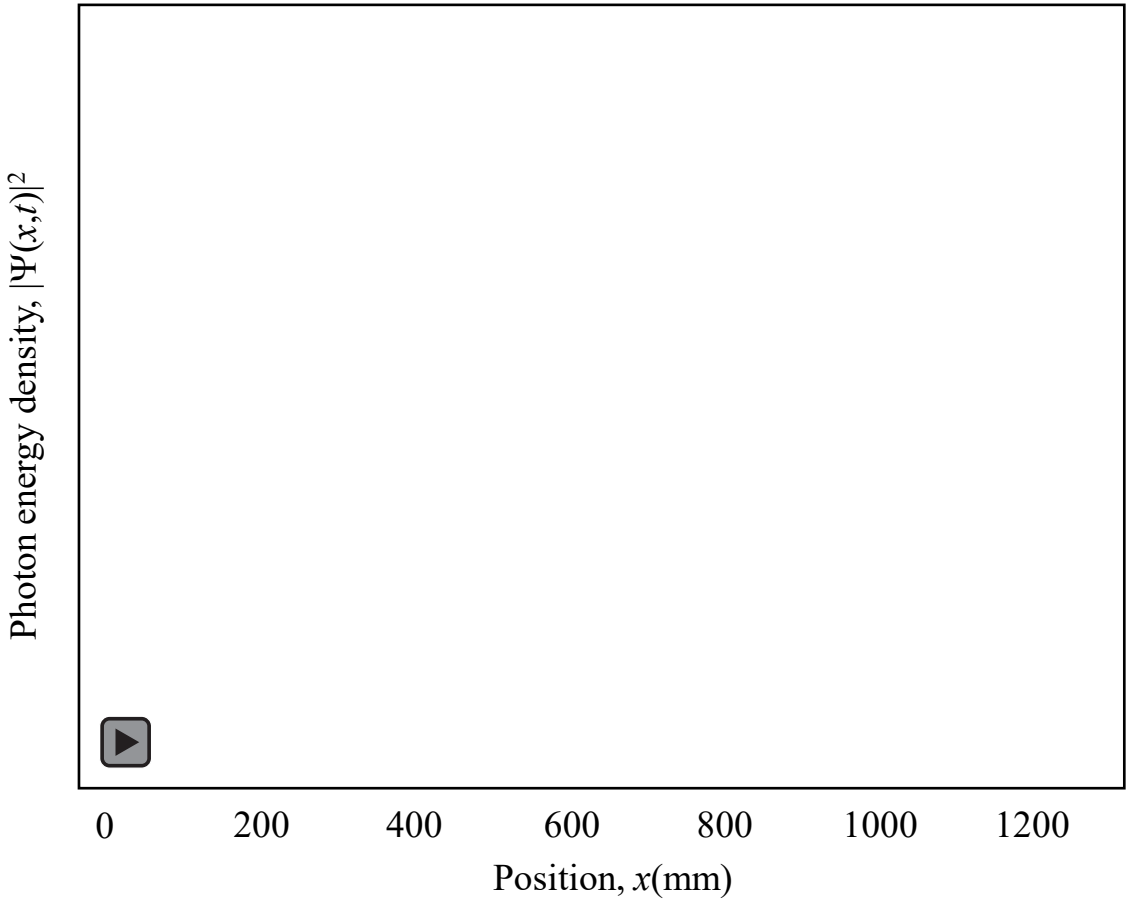

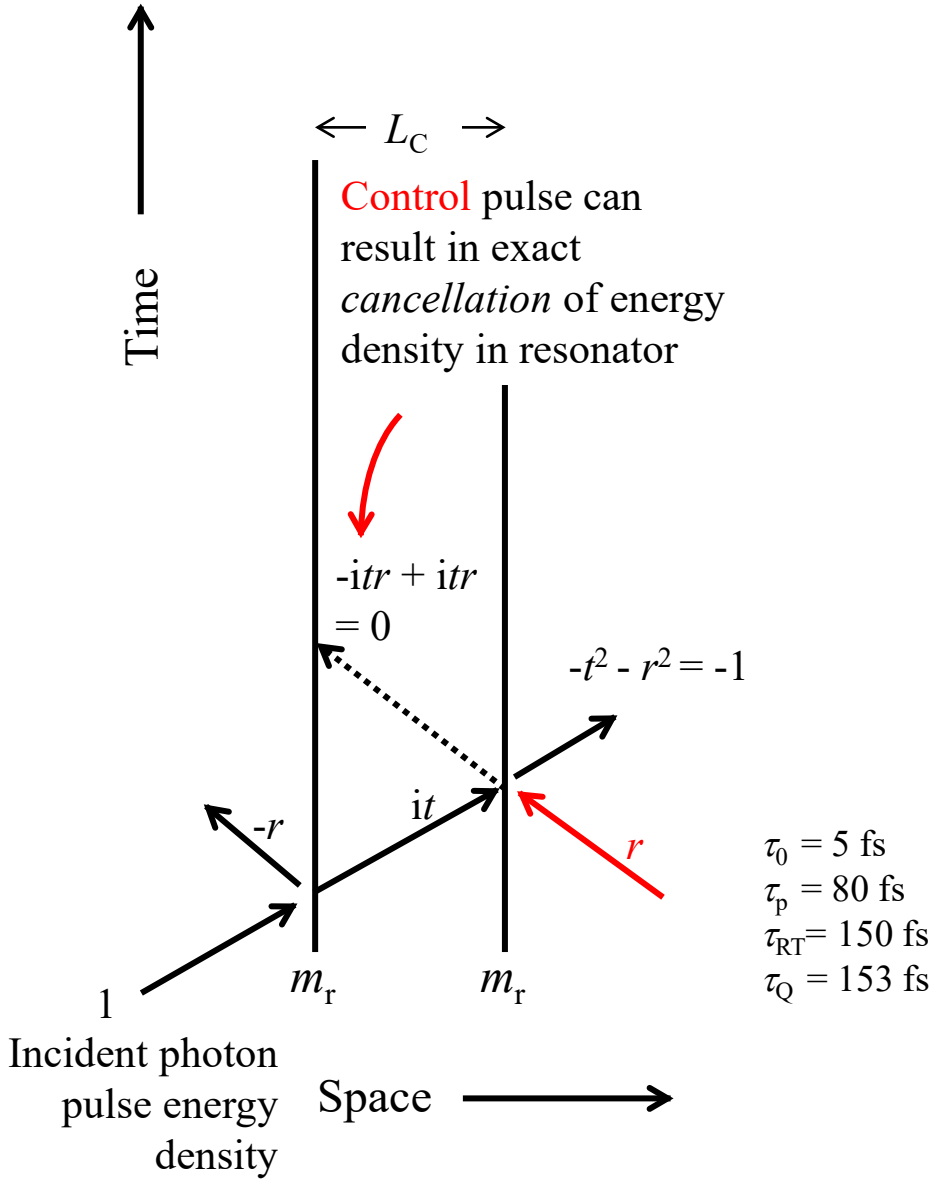

- Lead pulse and *one* backward propagating control pulse incident on resonator
- Single pulse transmitted and single pulse reflected with *no* ring-down

Coherent control of single-photon resonator output pulse using one backward control pulse

Single reflected photon pulse energy density

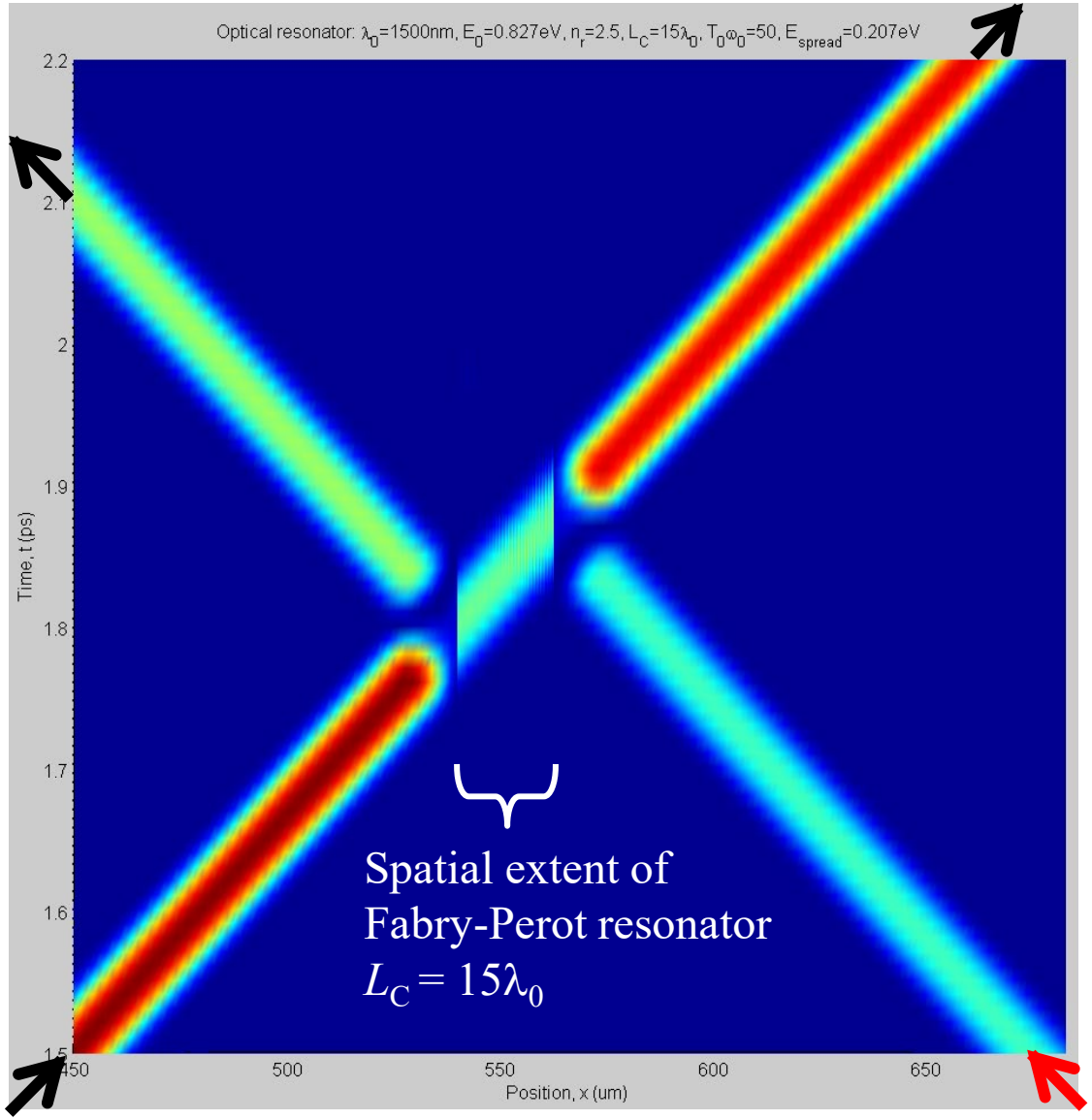

Time

Space

Transmitted photon energy density as single pulse

τ_0 = 5 fs
τ_p = 80 fs
τ_{RT}= 150 fs
τ_Q = 153 fs

Incident lead photon pulse energy density

Backward propagating control pulse

Geometric series using coherent control pulses to *confine* photon energy density in resonator

Useful relations: $t^2 + r^2 = 1$, $t^2/r^2 = 1/r^2 - 1$

$$\sum_{n=0}^{N-1} ax^n = a\,\frac{1-x^N}{1-x}$$

$$x = \frac{e^{i\phi}}{r}$$

$$a = t$$

$$\phi = \pi\omega / \Delta\omega$$

$$\Delta\omega = \pi c / L_C n_r$$

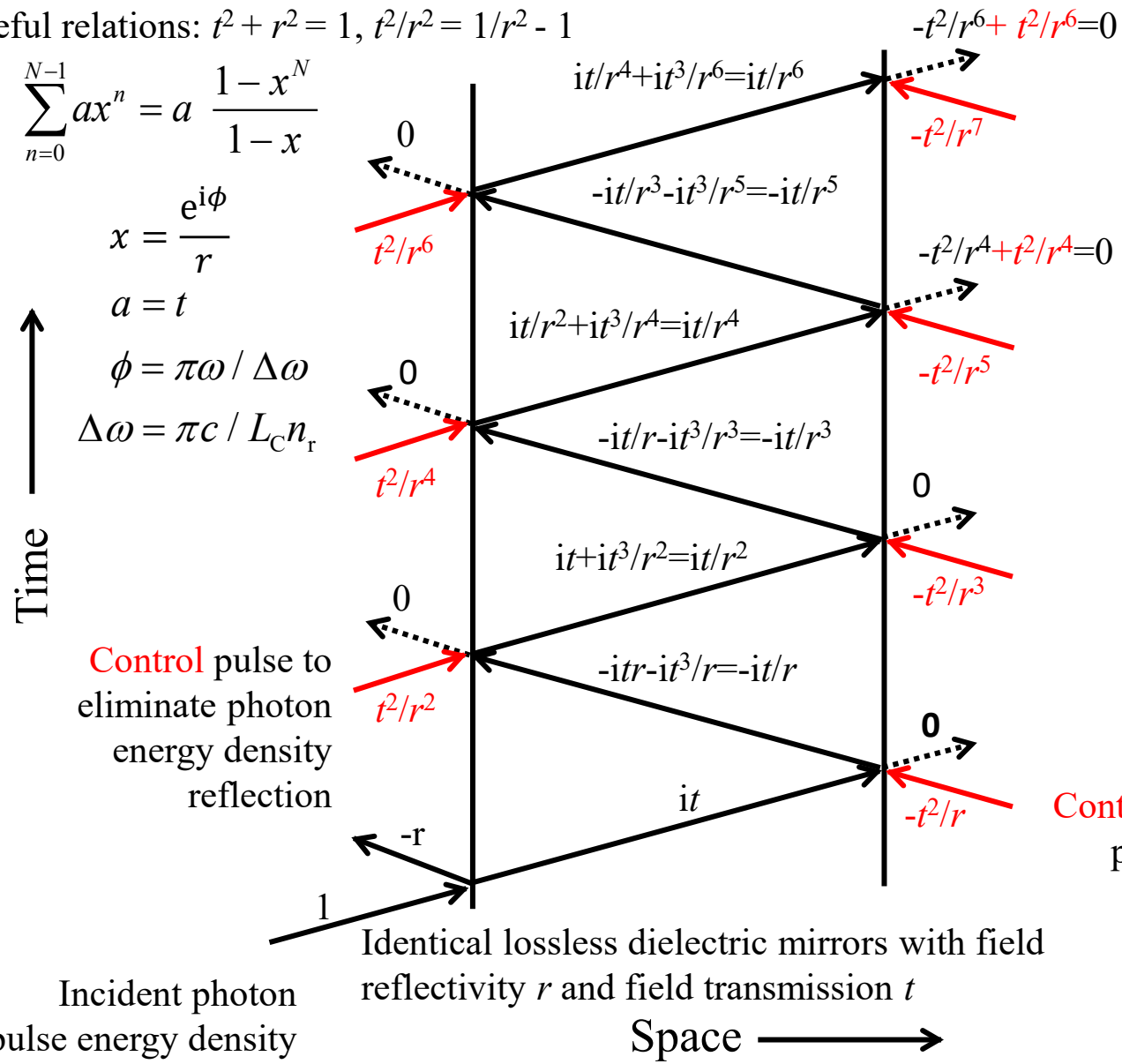

Control pulse to eliminate photon energy density reflection

Control pulse to eliminate photon energy density reflection

Identical lossless dielectric mirrors with field reflectivity r and field transmission t

Incident photon pulse energy density

Photon field *in* resonator is geometric series in $e^{i\phi}/r$ that sums to the N-1 value as $t(1+e^{i\phi}/r+e^{i2\phi}/r^2+e^{i3\phi}/r^3+\ldots)= t(1-(e^{i\phi}/r)^N)/(1-(e^{i\phi}/r))$ where phase per round-trip is $2\phi=2\pi\omega/\Delta\omega$ and spacing between resonances is $\Delta\omega=\pi c/L_C n_r$. The series does not converge because $r<1$ and so $|e^{i\phi}/r| >1$.

τ_0 = 5 fs
τ_p = 80 fs
τ_{RT} = 150 fs
τ_Q = 153 fs

Summary: Coherent control of single-photon energy density in a resonator

- Photonic resonator with lossless dielectric mirrors driven by phase-coherent source is open system coupled to continuum that evolves with unitary dynamics
  - Photon wave function, $\Psi(x,t)$, describes single-photon energy density, $U(x,t)=|\Psi(x,t)|^2$
  - Multiple resonator round-trip times, τ_{RT}, required to build-up steady-state behavior
  - Steady-state behavior evolves exponentially during characteristic resonator time, τ_Q
- *Transient behavior* controlled by incident waveform
  - Non-Markovian dynamics because of mirror reflections and energy stored in resonator
  - Can eliminate *all* energy density in resonator in less than one round-trip time, τ_{RT}
  - Can control *exact* number of identical transmitted and reflected pulses at multiples of round-trip time, τ_{RT}
  - Can use control to pass long pulses, $\tau_P > \tau_{RT}$, through resonator
  - Control of transient behavior is also control of Markovianity (and hence information flow)
    - Non-Markovianity may be viewed as resource for quantum information processing
- Natural time scales are $\{\tau_0,\ \tau_{RT},\ \tau_Q\} < \tau_{Coh}$
  - Resource for manipulation of single-photon quantum states
  - Use waveform as sensor probe of resonant structures (inverse problem)

Transient transmission and reflection of 2-photon Fock state at a Fabry-Perot resonator

- The input state is $|2,0\rangle_{in}$, i.e. 2 photons incident from the left
- The photons are prepared as rectangular wave packets
- The central frequency is on resonance with the Fabry-Perot resonator
- The spatial width of the wave packet $|\psi(x_1, x_2)|$ is much larger than that of the resonator

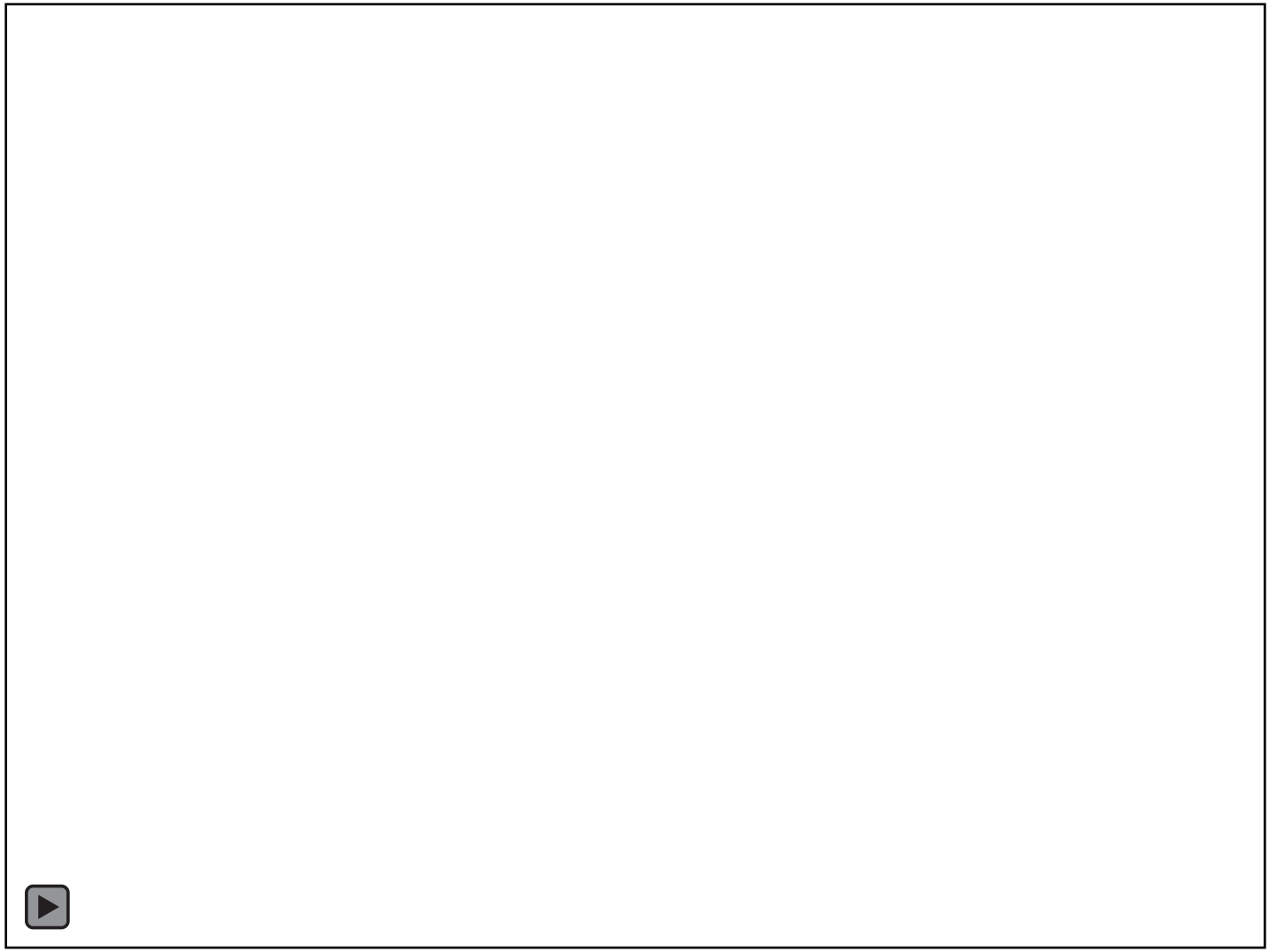

Why are “decoherence-free subspaces” fragile?

- Example: Su–Schrieffer–Heeger (SSH) model of polyacetylene $[C_2H_2]_{n=4}$
  - $N = N_{atom} = 8$ in a 1D chain with alternating *nearest-neighbor* hopping integral t_1 and t_2 and onsite potential $V = 0$
  - Fix hopping integral $t_1 = 1$ and sweep t_2

Polyacetylene

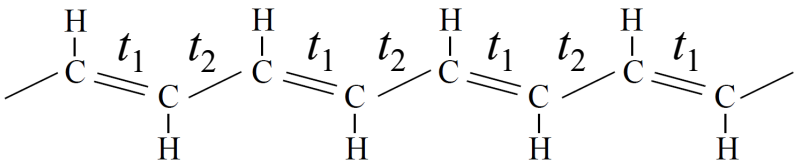

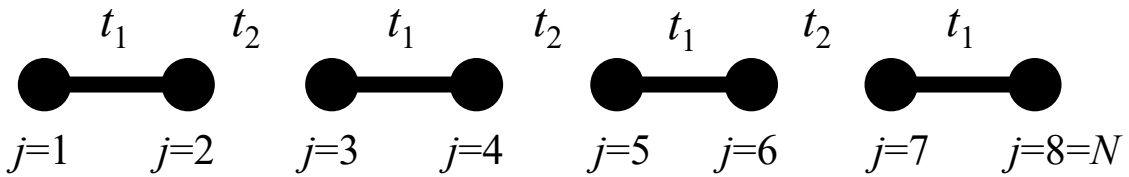

$t_2 = 0$, isolated dimers

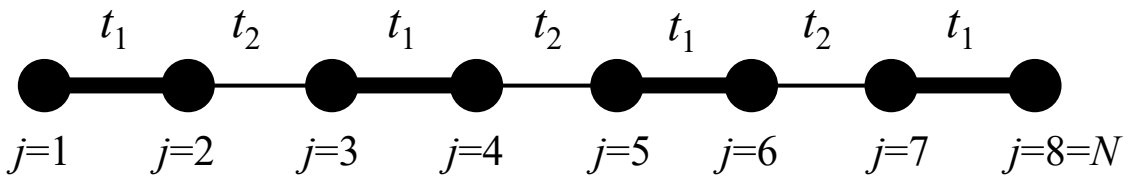

$t_2 < t_1$, bulk states only

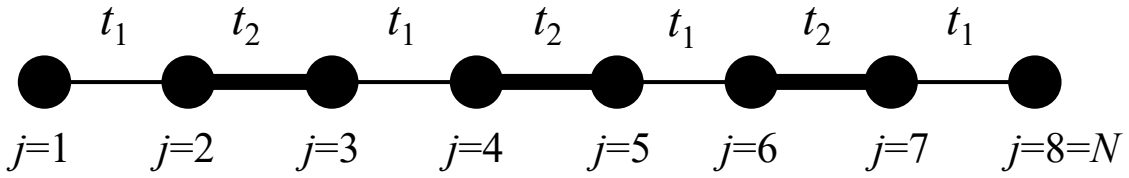

$t_2 > t_1$, bulk and isolated atom surface states as $N \to \infty$

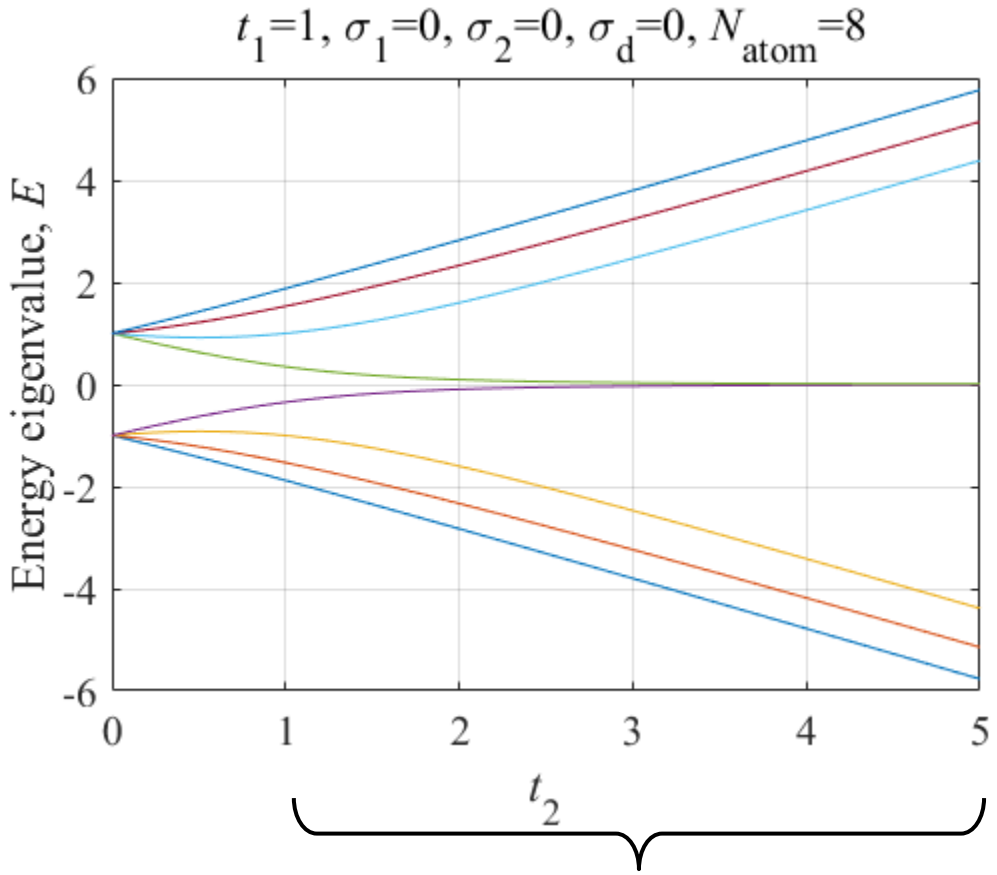

$t_2 > t_1$, bulk and isolated atom surface states as $N \to \infty$

Gaussian noise in hopping t introduces noise in eigenenergy and DOS. However, noise is *suppressed* for protected edge (surface) states ($t_2 > t_1$)

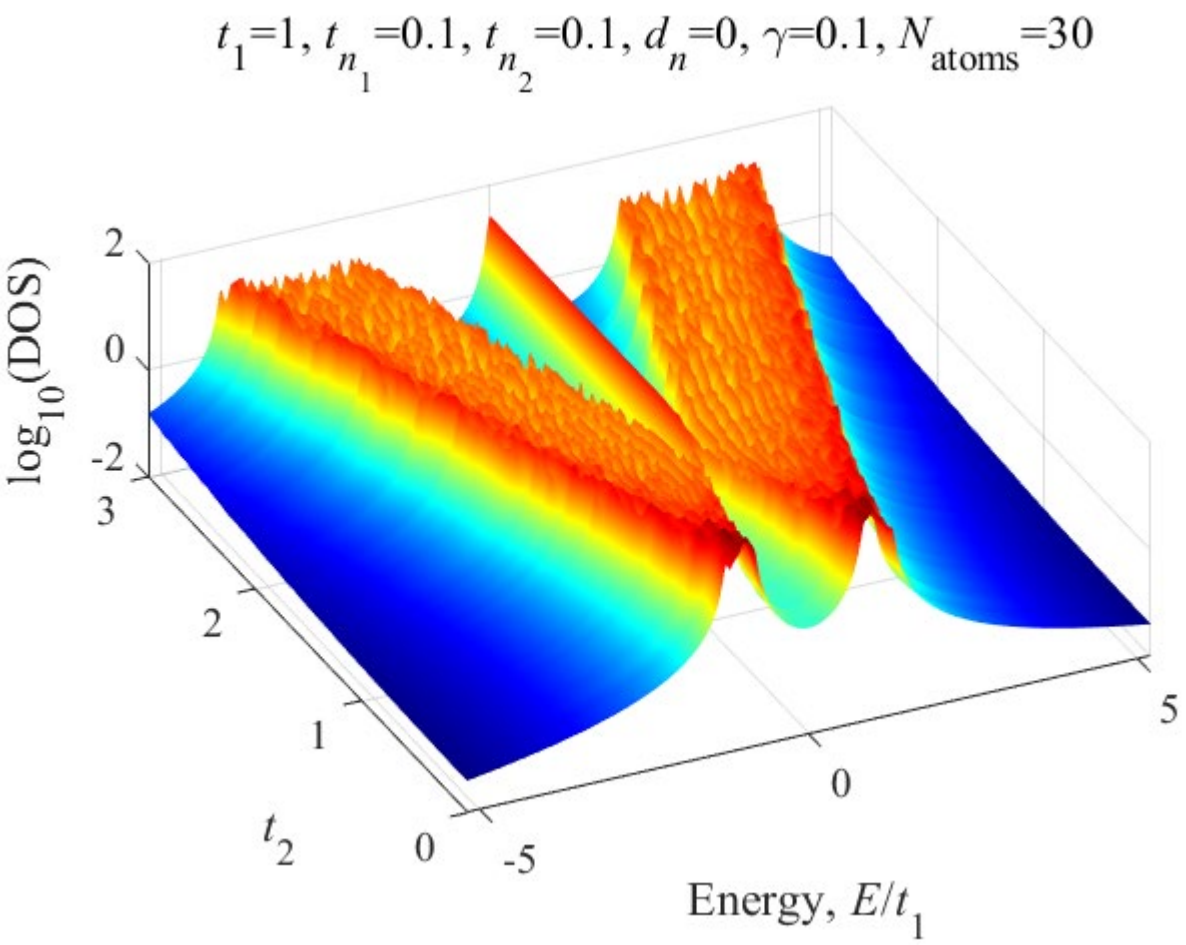

The edge-state protection is *removed* when on-site noise is introduced in the bulk and/or at the edges

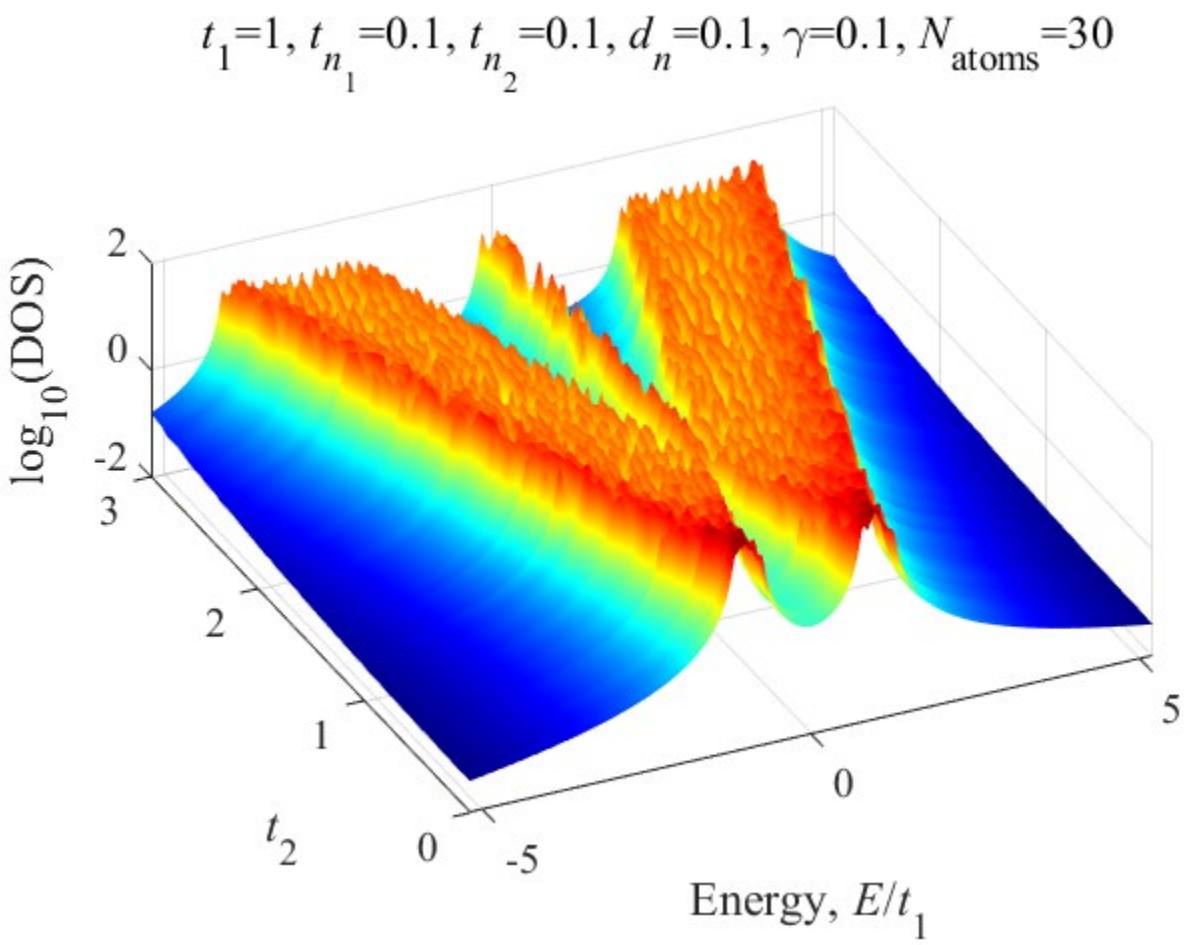

Next-next-nearest-neighbor hopping retains particle-antiparticle (PA) symmetry of energy eigenvalues

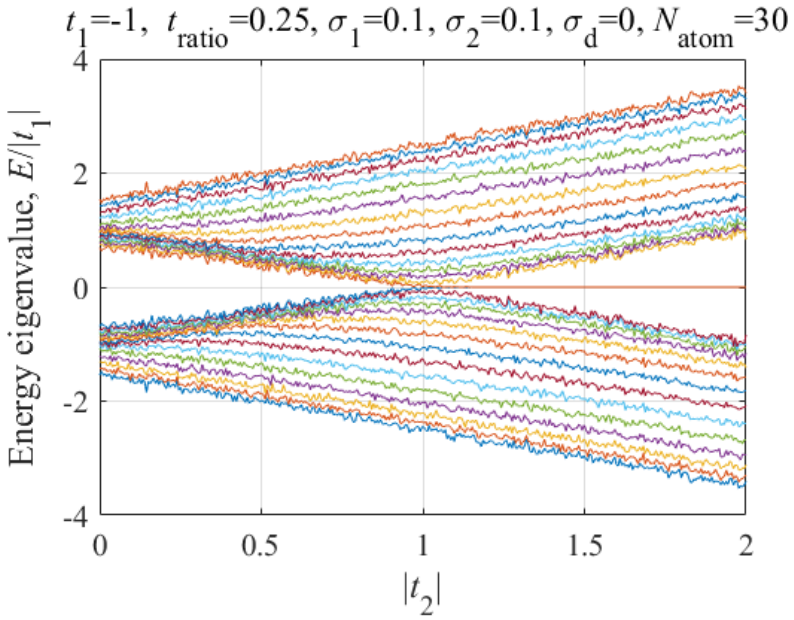

Next-next-nearest-neighbor interaction retains PA symmetry in energy eigenvalues and retains protection from noise.

$t_A = t_{ratio} t_1$

$t_B = t_{ratio} t_1$

$\delta_A = \text{noise}_1 t_A$

$\delta_B = \text{noise}_2 t_A$

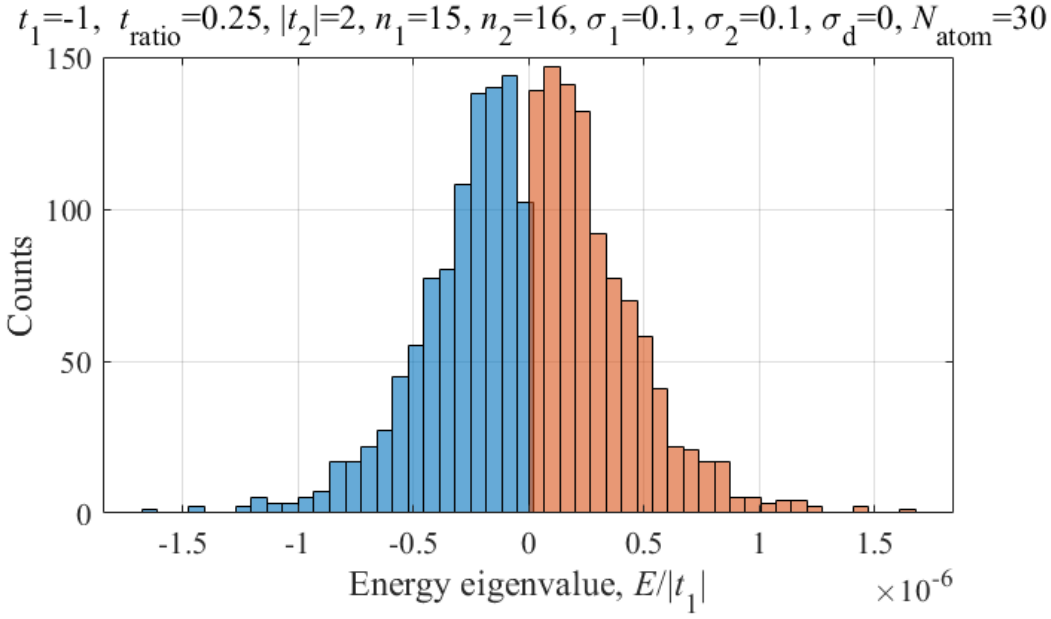

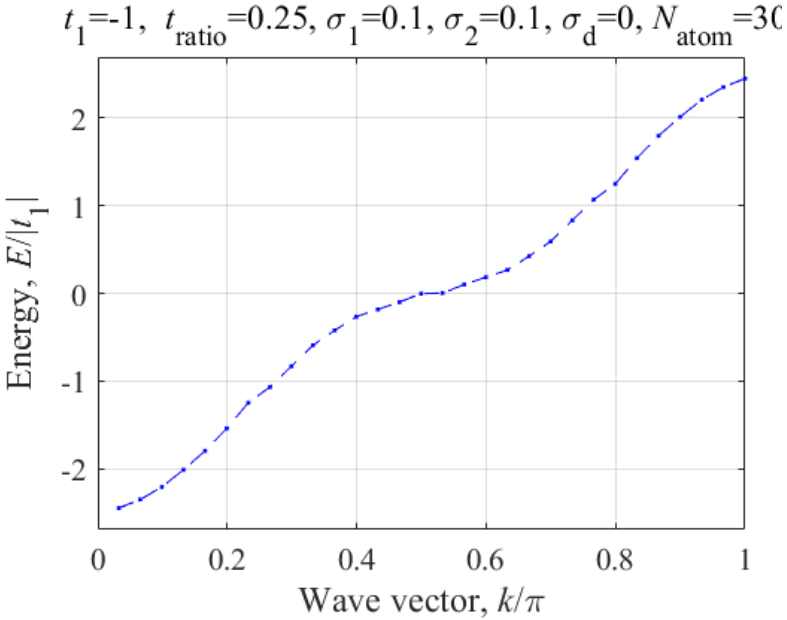

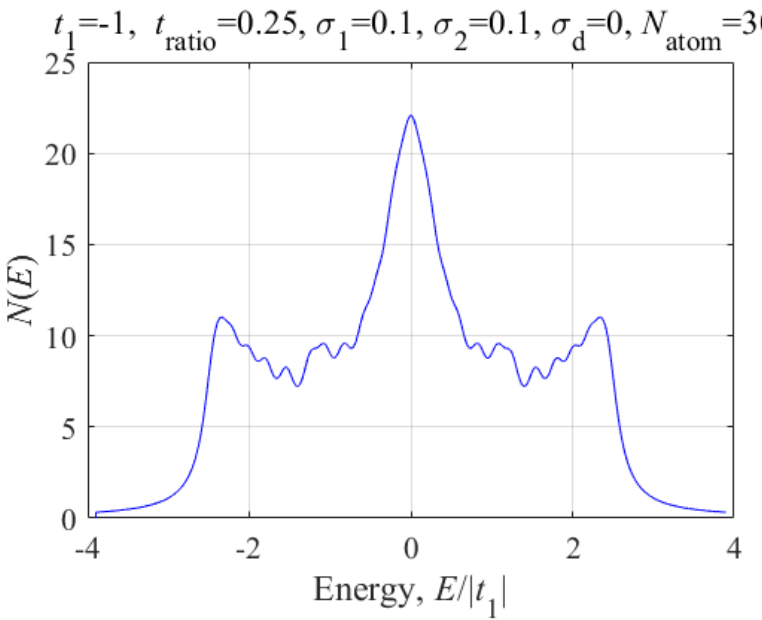

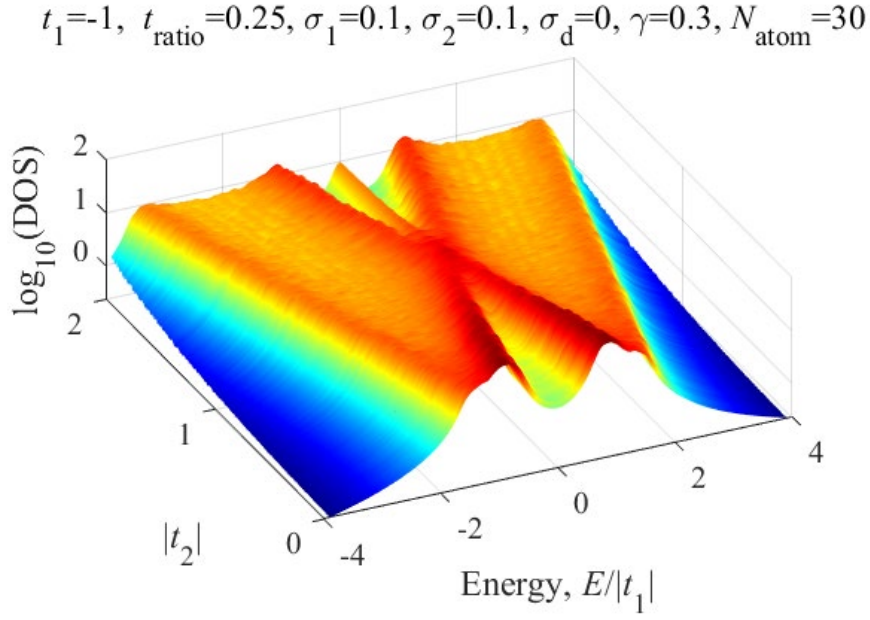

Two Hermitian sub-systems H_1 and H_2 coupled by H_{12} while retaining particle-antiparticle (PA) symmetry protection

$$H_1 + H_2 + H_{12} =$$

$$\begin{pmatrix}
a & t_1 & 0 & t_A & 0 & 0 & 0 & 0 & 0 & 0 & 0 & 0 & 0 & 0 & 0 & 0 \\
t_1 & a & t_2 & 0 & t_B & 0 & 0 & 0 & 0 & 0 & 0 & 0 & 0 & 0 & 0 & 0 \\
0 & t_2 & a & t_1 & 0 & t_A & 0 & 0 & 0 & 0 & 0 & 0 & 0 & 0 & 0 & 0 \\
t_A & 0 & t_1 & a & t_2 & 0 & t_B & 0 & 0 & 0 & 0 & 0 & 0 & 0 & 0 & 0 \\
0 & t_B & 0 & t_2 & a & t_1 & 0 & t_A & 0 & 0 & 0 & 0 & 0 & 0 & 0 & 0 \\
0 & 0 & t_A & 0 & t_1 & a & t_2 & 0 & \boldsymbol{t_B} & 0 & 0 & 0 & 0 & 0 & 0 & 0 \\
0 & 0 & 0 & t_B & 0 & t_2 & a & t_1 & 0 & \boldsymbol{t_A} & 0 & 0 & 0 & 0 & 0 & 0 \\
0 & 0 & 0 & 0 & t_A & 0 & t_1 & a & \boldsymbol{t_2} & 0 & \boldsymbol{t_B} & 0 & 0 & 0 & 0 & 0 \\
0 & 0 & 0 & 0 & 0 & \boldsymbol{t_B} & 0 & \boldsymbol{t_2} & V & t_1 & 0 & t_A & 0 & 0 & 0 & 0 \\
0 & 0 & 0 & 0 & 0 & 0 & \boldsymbol{t_A} & 0 & t_1 & V & t_2 & 0 & t_B & 0 & 0 & 0 \\
0 & 0 & 0 & 0 & 0 & 0 & 0 & \boldsymbol{t_B} & 0 & t_2 & V & t_1 & 0 & t_A & 0 & 0 \\
0 & 0 & 0 & 0 & 0 & 0 & 0 & 0 & t_A & 0 & t_1 & V & t_2 & 0 & t_B & 0 \\
0 & 0 & 0 & 0 & 0 & 0 & 0 & 0 & 0 & t_B & 0 & t_2 & V & t_1 & 0 & t_A \\
0 & 0 & 0 & 0 & 0 & 0 & 0 & 0 & 0 & 0 & t_A & 0 & t_1 & V & t_2 & 0 \\
0 & 0 & 0 & 0 & 0 & 0 & 0 & 0 & 0 & 0 & 0 & t_B & 0 & t_2 & V & t_1 \\
0 & 0 & 0 & 0 & 0 & 0 & 0 & 0 & 0 & 0 & 0 & 0 & t_A & 0 & t_1 & V
\end{pmatrix}$$

Next-next nearest-neighbor
Zero next nearest-neighbor term
Nearest-neighbor
On-site diagonal

Retain particle-antiparticle (PA) symmetry and include next-next-nearest-neighbor terms in both sub-systems H_1 and H_2
On-site potential, each element $V = a$. Require no dependence of t on a.
Nearest and next-next-nearest neighbor coupling determines non-zero off-diagonal H_{12} matrix elements

There is a lot to learn and get right …

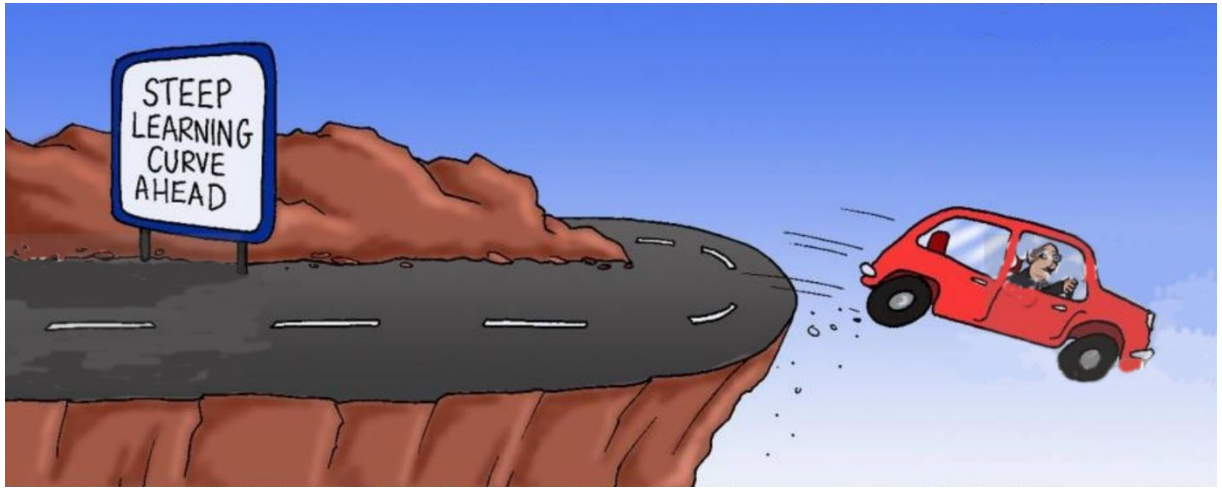

END

Nearest-neighbor tight-binding dispersion in electrode and tunnel barrier

- (a) Propagating electron state (dot) of energy E_0 in the real nearest-neighbor tight-binding s-orbital cosine band of the electrode (black curve)
- (b) Cosine band shifted up in energy relative to (a) to form a potential barrier of energy V_B. An electron of energy E_0 incident on the potential barrier may be viewed as tunneling via the imaginary k-state (dot) in the *normal* imaginary dispersion in the band structure (red dashed curve with *negative slope and curvature*)

Tight-binding nearest-neighbor hopping energy t_h for s-orbitals propagating k-state dispersion
$\hbar\omega = 2\ t_h\ (1 - \cos(kL))$

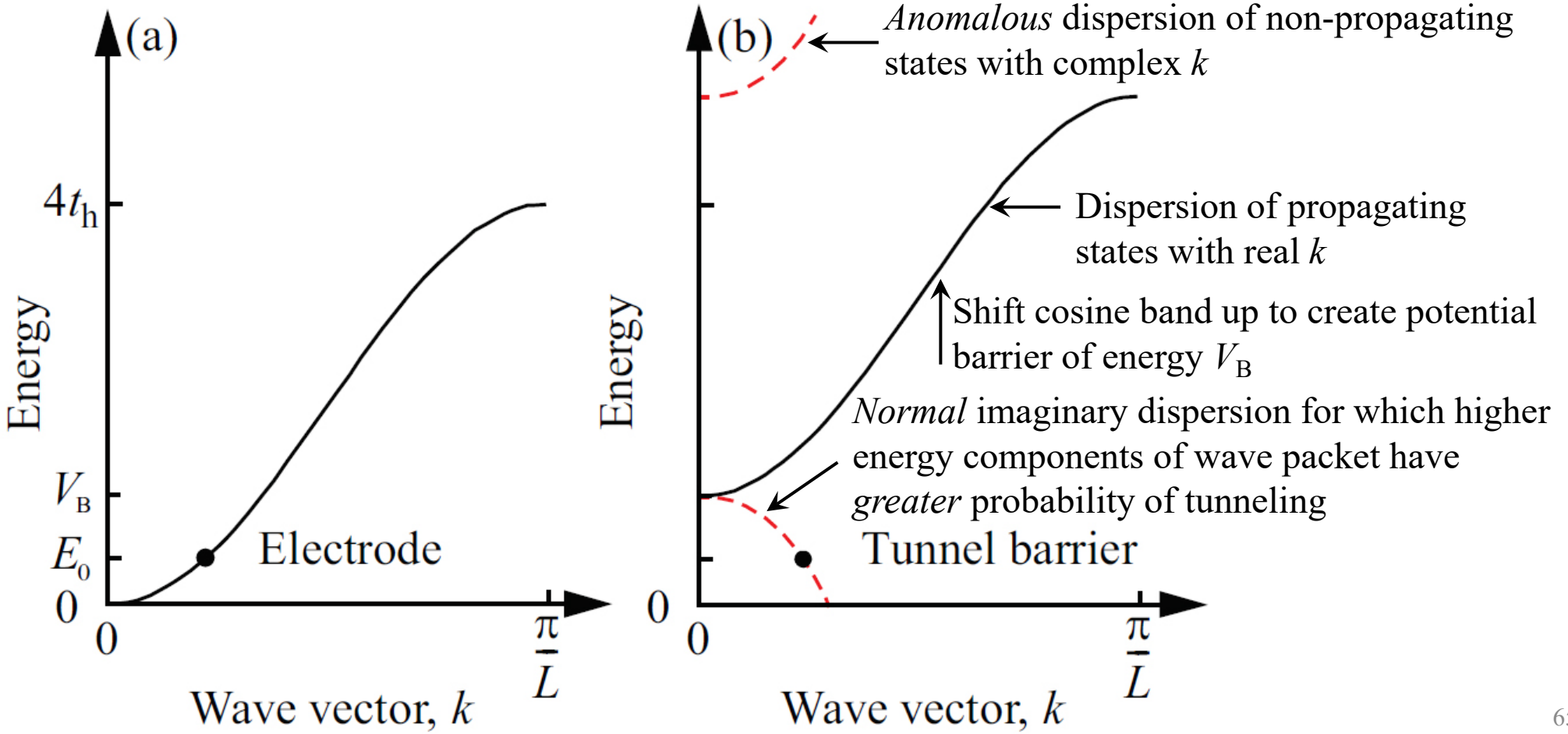

Single-electron pulse dynamics at a tunnel barrier

- (a) Electron wave packet propagating in a constant potential (upper sketch) and incident on a rectangular potential barrier of energy V_B (lower sketch). Measurement at position, x_R, far to the right of the potential barrier
- (b) Probability of measuring the electron at x_R as a function of time with and without a potential barrier. With *normal* imaginary dispersion, the peak in detection probability after tunneling occurs *before* the peak for an electron propagating in the absence of the potential barrier

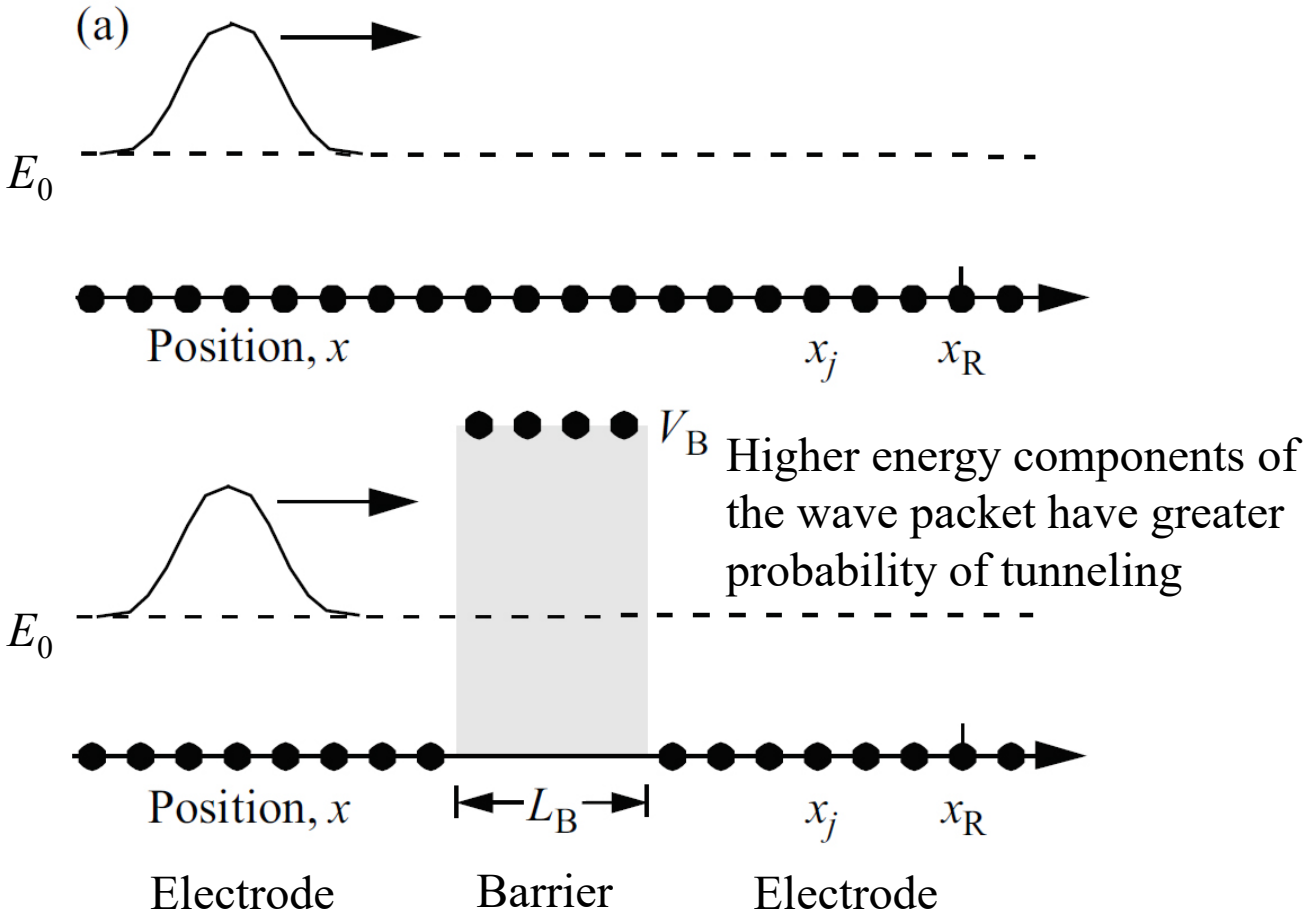

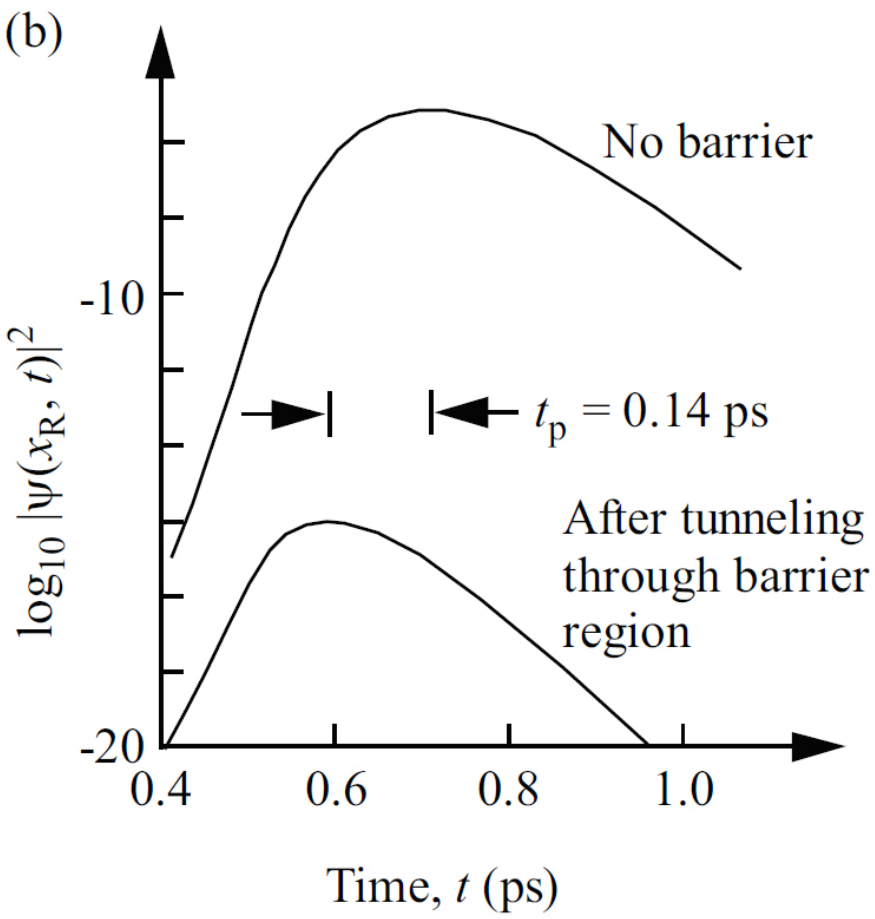

Single-electron pulse dynamics at a tunnel barrier

High-pass k-space filter in a tunnel barrier

- (a) Incident electron wave packet of energy E_0 in the electrode has distribution of k-space amplitudes with standard deviation σ_k about wave vector k_c. Because, with *normal* imaginary dispersion, higher energy components of the wave packet have greater probability of tunneling, the tunnel barrier of thickness L_B acts as a high-pass filter for wave vector amplitudes. The transmitted pulse is distorted relative to the incident pulse, contains *k*-states with amplitudes that peak at $k' > k_c$, and has a group velocity, υ_g, that is greater than that of the incident pulse. The transmitted pulse has a time-independent wave vector spectrum
- (b) Transmitted pulse group velocity, υ_g, depends on σ_k and L_B. Example: $E_0 = 0.15$ eV, $V_B = 0.35$ eV, and $m^* = 0.07 \times m_0$

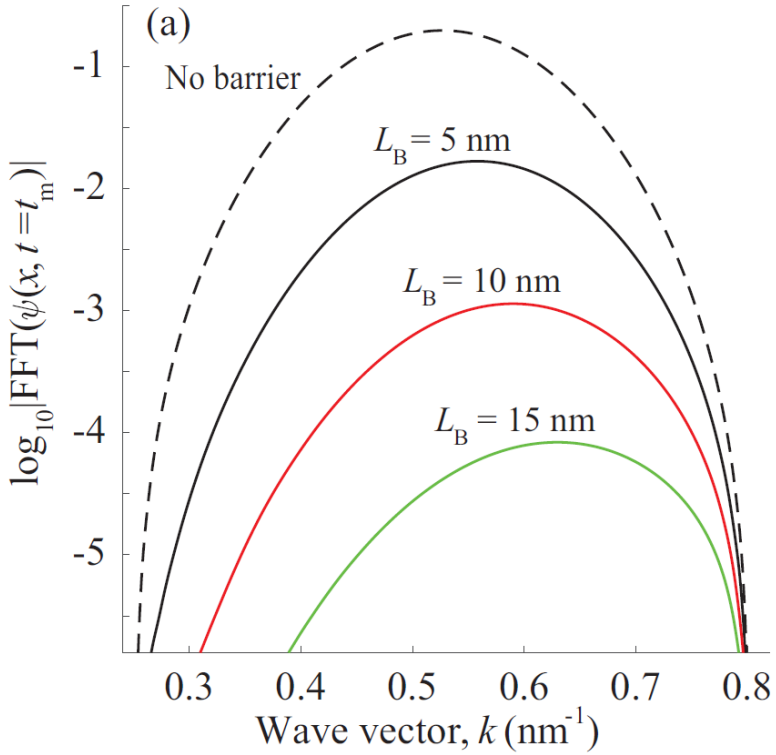

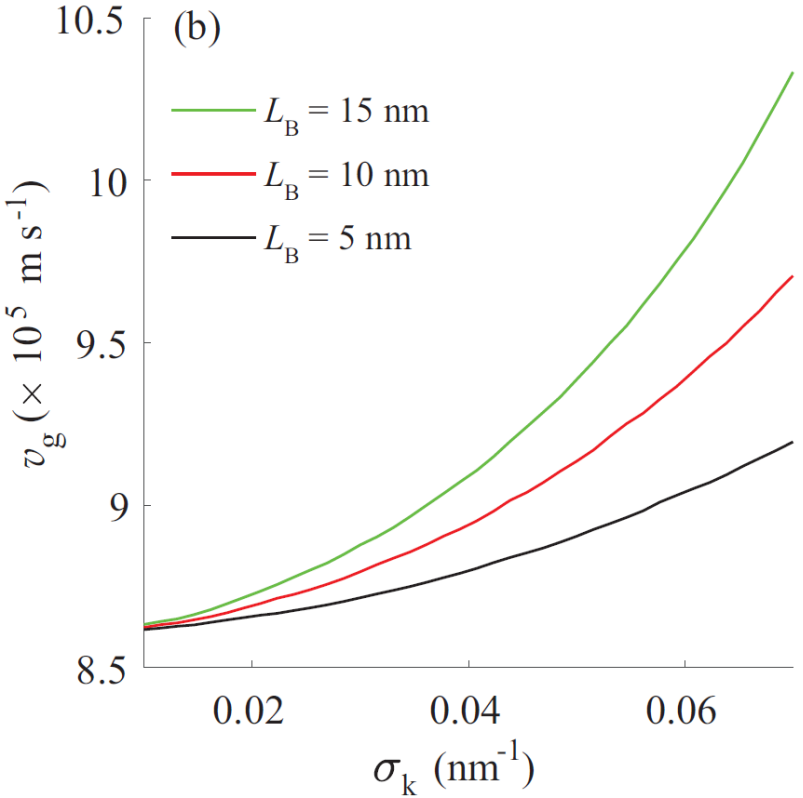

Space-time plot of *high-pass k*-space filter in a tunnel barrier

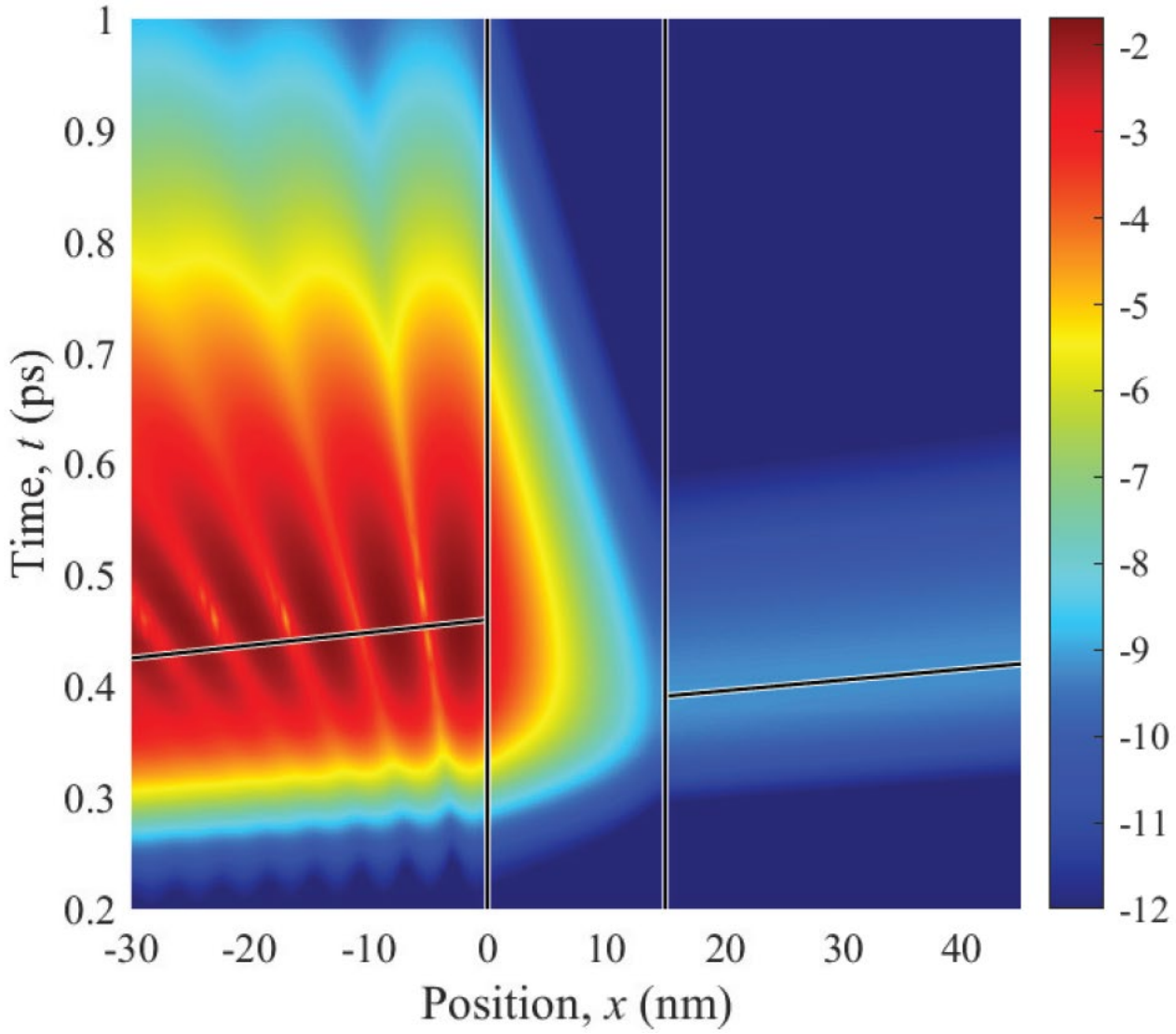

The transmitted pulse group velocity is *greater* than the incident pulse and the transmitted pulse emerges *before* the pulse in the absence of a barrier

Summary

- A coherent single-particle wave-packet incident on a classically impenetrable barrier can be reflected and interfere with itself and can be transmitted by tunneling
  - Tunneling acts as a filter in *k*-space (high-pass *k*-space filter with normal imaginary dispersion and a low-pass *k*-space filter with anomalous imaginary dispersion)
  - Complex *k*-space dispersion in a tunnel barrier controls the arrival time, shape, and group velocity of a transmitted single-electron single-peaked wave packet
- The tunnel-transmitted particle can move *faster* (high-pass *k*-space filter) or *slower* (low-pass *k*-space filter) than the incident particle
- The dispersion described by complex band structure due to the periodic potential of a bulk crystal can be used *as a guide* for component design (before solving the Schrödinger equation for the actual finite-sized nano-scale geometry under consideration)
  - Suggests a methodology and heuristics to expand design space and assist in the search for the optimal design
  - A resource to reduce complexity, control tunneling between quantum dot electron-spin qubits, increase the peak-to-valley ratio of a resonant tunnel diode (RTD), reduce subthreshold slope in a transistor (T-FET), etc.
- Super-luminal transmission of information is precluded because single-bit information detection requires a common bit-detection threshold. This results in the single-bit tunnel transmitted information in the pulse arriving after the pulse with no barrier present. *Collision lifetime* and the related *tunneling time* can also be defined by considering such information transport

"Wave packet tunneling and imaginary wave vector dispersion", W. Unglaub and A. F. J. Levi, *Physics Open* **17**, 100164 (2023).